Innovative Water Scrubber Packed with Sponge Carriers for Biogas Purification

スポンジ担体を用いた新規スクラバーによるバイオガスの精製

A dissertation by

SITI NOORAIN BINTI ROSLAN

in partial fulfillment of the requirements
for the degree of
Doctor of Engineering
in Civil and Environmental Engineering

Hiroshima University
Higashi-Hiroshima, Japan
April 2019

Promoter:	Professor Akiyoshi OHASHI Graduate School of Engineering, Hiroshima University
Committee:	Professor Akiyoshi OHASHI Graduate School of Engineering, Hiroshima Universiti Professor Yoshihisa KAWAHARA Graduate School of Engineering, Hiroshima Universiti Associate Professor Noriatsu OZAKI Graduate School of Engineering, Hiroshima Universiti Assistant Professor Tomonori KINDAICHI Graduate School of Engineering, Hiroshima Universiti Associate Professor Yoshiteru AOI Graduate School of Advances Sciences of Matter, Hiroshima University

ACKNOWLEDGEMENTS

In the name of Allah, the Most Gracious and the Most Merciful

Alhamdulillah, all praises to Allah for the strength and His blessing in completing this thesis. Special appreciation goes to my supervisor, Professor Akiyoshi Ohashi, for his supervision and constant support. His invaluable help of constructive comments and suggestions throughout the experimental and thesis works have contributed to the success of this research. Not forgotten, my appreciation to my co-supervisors, Professor Yoshihisa Kawahara, Associate Professor Noriatsu Ozaki, Associate Professor Yoshiteru Aoi and Assistant Professor Tomonori Kindaichi.

I would like to express my appreciation to all my laboratory members of Department of Environmental Preservation Engineering for their co-operations. Sincere thanks to all my friends especially Nafisah, Sharifah Nabiha, Sharifah Mariam, Ahmad Shoiful, Faris, Puji, Lusi, Rozyanti, Faridah and others for their kindness and moral support during my study. Thanks for friendship and memories.

Last but not least, my deepest gratitude goes to my beloved parents; Mr Roslan Karim and Mrs Siti Rokiah Ali and also to all my family members for their endless love, prayers and encouragement. To those who indirectly contributed in this research, your kindness means a lot to me. Thank you very much.

TABLE OF CONTENTS

CHAPTER 1

INTRODUCTION

TABLE OF CONTENTS

1.1 Background

Today, biogas technology is widely accepted as an alternative way to produce of energy that is clean and renewable (Yadvika et al., 2004; Tabatabaei et al., 2015). The increasing concerns about the impact of fossil fuel and the reduction of energy resources along with the fluctuation of crude oil price have made the biogas technology become more attractive (Farahnak et al., 2015; Hamzehkolaei et al., 2017). According to Scarlat et al. (2018), the utilization of biogas not only provides opportunities for energy production such as electricity, heat and fuel but also provides economic, environmental and climate benefits. Furthermore, the biogas production process through anaerobic digestion of organic waste such as municipal, agricultural, manure and sewage in bio-digester seems really promising in attaining a sustainable waste management (Qiang et al., 2012; Jedhe and Chendake, 2016; Goswami et al., 2016).

The biogas is usually composed of methane (CH_4; 50 – 70%), carbon dioxide (CO_2; 25 – 45%), water (H_2O; 2 – 7%), nitrogen (N_2; 2 – 5%), oxygen (O_2; 0 – 2%), hydrogen (H_2; $\leq$1%), ammonia (NH_3; 0 – 1%) and hydrogen sulphide (H_2S; 0 – 6000 ppm) (Akbulut, 2012). The composition of the biogas and its quality are varies significantly between different substrates depend on its chemical composition (Kougias and Angelidaki, 2018). Rasi et al. (2011), reported that the existence of trace compounds had limit the application of the biogas energy due to some negative effects on equipment used for biogas utilization such as corrosion, formation of abrasive of metal surface and deterioration of engine parts. Till now most of the energy produced from the biogas system is used for heat and electricity generation (Börjesson and Mattiasson, 2008; Bekkering et al., 2010; Angelidaki et al., 2018). The use of biogas as vehicle fuel or grid injection is only possible if the quality of the biogas is similar or more close to that of natural gas (Börjesson and Mattiasson, 2008; Rasi et al., 2011). That requirement had become one of the significant barriers to the deployment of biogas-based vehicle fuels in worldwide. All contaminants especially CO_2, H_2S and moisture are necessary to be removed or reduced as maximum as possible from the raw biogas for a wider variety of biogas uses.

Purification of raw biogas is usually performed to upgrade the biogas up to natural gas quality standard with CH_4 content of more than 90% (Ryckebosch et al., 2011). The purification process produced biomethane which not only has similar properties as the natural gas but also provides environmental benefit through the reduction of greenhouse gas emission of 2.596 tonCO_2 on a yearly basis (Koornneef et al., 2013). Currently, various of biogas upgrading technologies are available in market which is technically tested for their robustness and economic values. That includes cryogenic separation, membrane-based gas permeation, pressurized water scrubbing, amine scrubbing, physical and chemical separation and pressure swing adsorption (Niesner et al., 2013; Woon et al., 2016). Amongst all, the most common biogas upgrading technology applied is pressurized water scrubbing and pressure swing adsorption (Margareta et al., 2006). Nevertheless, according to Capodaglio et al. (2016), the overall use of biogas technology in practice is still not high and the utilization of the upgrading technology is generally dominated by large scale industries. For small scale plant, the biogas upgrading technology is not economically viable and only limited number of commercial upgrading technology is available. If the problem of high operational cost can be solved, it is undoubtedly that the biogas upgrading technology could be adopted widely.

A study reported by Rasi et al. (2014), suggest that pressurize water scrubbing is one of the simplest and most economical methods compared to membrane separation, pressure swing adsorption, chemical absorption and cryogenic separation. Till the moment, variety methods of enhancement of water scrubbing technology has been proposed to make the scrubbing system more versatile. Anyhow, most of previously studied had focused on the optimization of CH_4 concentration under high pressure condition due to the fact of water scarcity. Although, this considerably reduces the water used, yet distinctly has increased the energy and maintenance cost for the water scrubbing operation (Eze and Agbo, 2010). Despite that, the scrubbing process also leads to the emission of dissolved gases likes CH_4, CO_2 and H_2S with effluents. The released of CH_4 and CO_2 to the atmosphere will subsequently contributed in the increase of global warming, whilst H_2S gas give the effect of toxic and corrosive (Petersson and Wellinger, 2009). Therefore, there is a need to redesign and optimization of the existing water scrubbing process for more affordable and user-friendly system which can improve the quality of raw biogas and scrubbing effluent without harming the environment.

1.2 Objectives

The general objective of this thesis is to develop a biogas technology for CH_4 upgrading and its effluent treatment with an economic and environmentally benign approach. For this purpose, two different strategies are investigated:

a. Biogas purification at process level by imposing under atmospheric conditions in water scrubber reactor packed with sponge carrier.
b. End-of-pipe removal of dissolved CH_4, CO_2 and H_2S gas of scrubbing effluent by an integrated biological-physical process in single reactor.

The main aims of the section of this thesis dealing with process level enhancement of CH_4 content (strategy (a)) are:

1. to evaluate and describe the performance of a water scrubber packed with sponge carriers for biogas purification under atmospheric pressure condition.
2. to simulate the purification phenomenon and determine the operational conditions that yield highly purified gas that satisfying the quality requirements of city gas ($CH_4 \geq 90\%$, $CO_2 < 4\%$, $H_2S < 2$ ppm) by mathematical model.
3. to evaluate the performance of biological desulfurization of high hydrogen sulphide concentration from biogas.

The main objectives of the section of this thesis dealing with end-of-pipe removal of dissolved gasses (strategy (b)) are:

1. to evaluate the feasibility of the integration biological and physical stripping process while measuring the effect of hydraulic retention time (HRT) and air dosage in its performance.
2. to simulate and determine the optimum performance of biological oxidation and physical stripping in removing the CH_4 and recovering the effluent pH.

1.3 Thesis outlines

This thesis is organized as a compilation of research study, which are arranged in seven chapters. The description and links of the above objectives to the chapter of this thesis are as below;

Chapter 1 introduces the research background, purpose and outline of the thesis.

Chapter 2 was divided into two parts. First part discussing on the biogas composition, standard, utilization and treatment of methods. Second part focuses on the contains and treatment of effluent generated from biogas purification process.

Chapter 3 Elaborated on the development of mathematical model in Microsoft Excel, which involves the physical and biological process in treating the biogas and its effluent.

Chapter 4 was devoted to fulfill the first and second objectives of strategy (a) by studying the influence of liquid to gas flow ratio, pH, temperature, HRT, and initial H_2S concentration on the performance of water scrubbing process by experiment and simulation works.

Chapter 5 was devoted to fulfill the third objective of strategy (a) by studying the influence of initial H_2S concentration, liquid to gas flow ratio, and oxygen to H_2S concentration ratio on the performance of biological desulfurization of high H_2S from biogas.

Chapter 6 was devoted to fulfill the first and second objectives of strategy (b) by utilizing a reactor builds with air supplied at upper and bottom for the treatment of biogas purification effluent through biological oxidation and physical stripping process.

Chapter 7 summaries of the main finding obtained and recommendation for future study.

References

Akbulut, A., 2012. Techno-economic analysis of electricity and heat generation from farm-scale biogas plant: Cicekdagi case study. Energy, 44(1), 381 – 390.

Angelidaki, I., Treu, L., Tsapekos, P., Luo, G., Campanaro, S., Wenzel, H., Kougias, P.G., 2018. Biogas upgrading and utilization:Current status and perspectives. Biotechnology Advances, 36, 452 – 466.

Bekkering, J., Broekhuis, A.A., Gemert, W.J.T.V., Optimisation of a green gas supply chain-A review. Bioresour. Technol., 101, 450 – 456.

Börjesson, P., Mattiasson, B., 2008. Biogas as a resource-efficient vehicle fuel. Trends in Biotechnology, 26(1), 7 – 13.

Capodaglio, A.G., Callegari, A., Lopez, M.V., 2016. European framework for the diffusion of biogas uses: Emerging technologies, acceptance, incentive, strategies, and institutional-regulatory support. Sustanability, 8, 298.

Eze, J.I., Agbo, K.E., 2010. Maximizing the potentials of biogas through upgrading. Am. J. Sci. Ind. Res., 1, 604 – 609.

Farahnak, M., Gord, M.F., Dashtebayaz, M.D., Dashti, M., 2015. Optimal sizing of power generation unit capacity in ICE-driven CCHP systems for various residential building sizes. Appl. Energy, 158, 203 – 219.

Goswami, R., Chattopadhyay, P., Shome, A., Banerjee, S.N., Chakraborty, A.K., Mathew, A.K., Chaudhury, S., 2016. An overview of physico-chemical mechanisms of biogas production by microbial communities: a step towards sustainable waste management. 3 Biotech., 6(1), 72 – 84.

Hamzehkolaei, F.T., Amjad, N., 2017. A techno-economic assessment for replacement of conventional fossil fuel based technologies in animal farms with biogas fueled CHP units. Renewable Energy, 118, 602 – 614.

Jedhe, P.R., Chendake, Y.J., 2016. Biogas – renewable energy source: optimization of production and application. International Research Journal of Engineering and Technology, 3(6), 374 – 379.

Koornneef, J., Breevoort, P.V., Noothout, P., Hendriks, C., Luning, U., Camps, A., 2013. Global potential for biomethane production with carbon capture, transport and storage up to 2050. Energy Procedia, 37, 6043 – 6052.

Kougias, P.G., Angelidaki, I., 2018. Biogas and its opportunities – A review. Front. Environ. Sci. Eng., 12(3), 14.

Margareta, P., Owe, J., Arthur, W., 2006. Biogas upgrading to vehicle fuel standards and grid injection. IEA Bioenergy, December. [Online]. Available: http://task37.ieabioenergy.com/files/datenredaktion/download/publitask37/upgrading_report_final.pdf.

Niesner, J., Jecha, D., Stehlík, P., 2013. Biogas upgrading technologies: State of art review in European region. Chemical Engineering Transactions, 35, 517 – 522.

Petersson, A., Wellinger, A., 2009. Biogas upgrading technologies – developments and innovations, IEA Bioenergy-task 37 – Energy from biogas and landfill gas, IEA-International Energy Agency, Swedish Gas Centre, Malmoe, Sweden.

Qiang, H., Lang, D.L., Li, Y.Y., 2012. High-solid mesophilic methane fermentation of food waste with an emphasis on Iron, Cobalt and Nickel requirements. Bioresour. Technol., 103(1), 21 – 7.

Rasi, S., Läntelä, J., Rintala, J., 2011. Trace compounds affecting biogas energy utilization – A review. Energy Conversion and Management, 52, 3369 – 3375.

Rasi, S., Lantela, J., Rintala, J., 2014. Upgrading landfill gas using a high pressure water absorption process. Fuel, 115, 539 – 543.

Ryckebosch, E., Drouillon, M., Vervaeran, H., 2011. Techniques for transformation of biogas to biomethane. Biomass and Bioenergy, 35(5), 1633 – 1645.

Scarlat, N., Dallemand, J.F., Fahl, F., 2018. Biogas: Developments and perspectives in Europe. Renewable Energy, 129, 457 – 472.

Tabatabaei, M., Karimi, K., Kumar, R., Horvath, I.S., 2015. Editorial- Renewable energy and alternative fuel technologies. Biomed Research International.

Tim, P., Sandra, E., Richard, D., Alan, G., 2001. An evaluation of the policy and techno-economic factors affecting the potential for biogas upgrading for transport fuel use in the UK. Energy Policy, 39, 1806 – 1816.

Woon, K.S., Lo, I.M.C., Chiu, S.L.H., Yan, D.Y.S., 2016. Environmental assessment of food waste valorization in producing biogas for various types of energy use based on LCA approach. Waste Manag., 50, 290 – 299.

Yadvika., Santosh., Sreekrishnan, T.R., Kohli, S., Rana, V., 2004. Enhancement of biogas production from solid substrates using different techniques-a review. Bioresour. Technol., 95(1), 1 – 10.

CHAPTER 2

LITERATURE REVIEW

TABLE OF CONTENTS

PART A BIOGAS PURIFICATION TECHNOLOGIES

PART B TREATMENT OF BIOGAS PURIFICATION EFFLUENT

PART A: BIOGAS PURIFICATION TECHNOLOGIES

2.1 Quality and energy content of biogas

One of the most promising routes for the production of renewable gaseous fuel is biogas (Chandra et al., 2012). Biogas is a type of bioenergy that derived from the biological breakdown of biogenic material in the absence of oxygen known as anaerobic digestion process (Surendra et al., 2014; Sora and Yoo, 2014). The process releases a gas mixture primarily comprises of CH_4 and CO_2 with other several of trace compounds (Ryckebosh et al., 2011; Sun et al., 2015). The quality of the produced gas is determined by the amount of CH_4 and its impurities concentration level. In the biogas, the most common impurities present are H_2S, NH_3, N_2 and water vapor (Jansen, 2010).

Table 2.1: Composition of biogas based on different source
(Source: Rasi et al., 2007)

Component	Units	Organic waste	Sewage	Landfill
CH_4	% (vol)	60-70	55-65	45-55
CO_2	% (vol)	30-40	35-45	30-40
N_2	% (vol)	<1	<1	5-15
H_2S	ppm	10-2000	10-40	50-300

Generally, the production of CH_4 gas is highly depends on the substrate composition, fermentation technology and method of collection applied (Sun et al., 2015). **Table 2.1** shows the composition of biogas from different sources. The high content of CH_4 turn biogas into a combustible fuel with a deep blue flame while the CO_2 gas in addition is noncombustible gas (Starr et al., 2012). Also, the presence of the CO_2 gas together with the impurities in the biogas composition can give a negative effect during biogas utilization stage as described in **Table 2.2**. The primary energy carrier of biogas is CH_4 and normally, pure CH_4 gas has a heat heating value of 38 MJ Nm^{-3} (Gross et al., 2017). However, the heat heating value of raw biogas is in between 19 to 26 MJ Nm^{-3} or 6 kWh Nm^{-3} to 6.5 kWh Nm^{-3}, which is equivalent to 0.65 liters of crude oil (Deublein and Steinhauser, 2010; Toro et al., 2018). The difference in heat heating value of these two is largely due to the noncombustible part of biogas (Sohata et al., 2018). On the other hand, for 1 Nm^3 of biogas is equivalent to 1 liter of diesel and gasoline fuel, respectively (Onofre et al., 2015). However, in relation to natural gas, 1.2 liter of petrol or diesel is corresponding to 1 Nm^3 of natural gas (Awe et al., 2017). Amongst all fossil fuel natural gas is the cleanest fuel that content CH_4 within ranges of 75 to

98% (Liang et al., 2012; Divyang et al., 2016). **Table 2.3** shows the comparison between the typical properties of raw biogas with natural gas.

Table 2.2: Typical biogas contaminants effects.
(Source: Weiland, 2009; Munoz et al., 2015)

Contaminant	Typical compound composition (%)	Risk
Water vapor	5-10%^{a}	Corrosion of pipeline gas storage tanks, compressor and engine technologies, deterioration of lubrication oils
CO_2	30-47%^{a}	Corrosion of the equipment
N_2	0-3%^{a}	NO_X flue gas emission
H_2S	0-10 ppm^a	Corrosion of pipelines gas storage tanks, compressors and engine technologies, SO_X flue gas emission
NH_3	0-100 ppm^a	Generation of corrosive products during combustion
O_2	0-1%^{a}	Explosion hazards
Siloxanes	0-41 mg m^{-3a}	Risk of causing abrasion, overheating and malfunctioning in combustion engines and valves
Volatile organic compound	0-4500 mg m^{-3b}	Risk for human health threat
Molds and bacteria	-	Risk for human health threat, equipment damage
Halogenated hydrocarbons	20-200ppm(V$^{)b}$	Generation of corrosive products during combustion
Heavy metals	-	Risk for human health threat

^{a}:for biogas produced from sewage sludge, livestock manure or agricultural biowaste; ^{b}:for biogas recovered from conventional landfills

Table 2.3: Comparison between typical properties and composition of raw biogas with natural gas (Source: Ryckebosh et al. 2011)

Parameter	Units	Raw biogas	Natural gas
Lower heating value	MJ Nm^{-3}	23	39
CH_4	% (mol)	60 – 70	85 – 92
CO_2	% (mol)	30 – 40	0.2 – 1.5
H_2S	ppm	0 – 4000	1.1 – 5.9
O_2	% (mol)	0	-
N_2	% (mol)	0.2	0.3
H_2	% (mol)	0	-
H_2O	% (mol)	1 – 5	-
NH_3	ppm	100	-
Heavy hydrocarbon	% (mol)	0	9

2.2 Biogas utilization and standard requirements

Biogas can be applied for a variety of end uses which included household and industrial purposes. However, the final use of the biogas is determined by its composition and generally its uses is not readily suited for all energy application. This is primarily due to its low level of heating value and impurities content (Sarker et al., 2018). **Figure 2.1** shows the possible use of biogas as energy source.

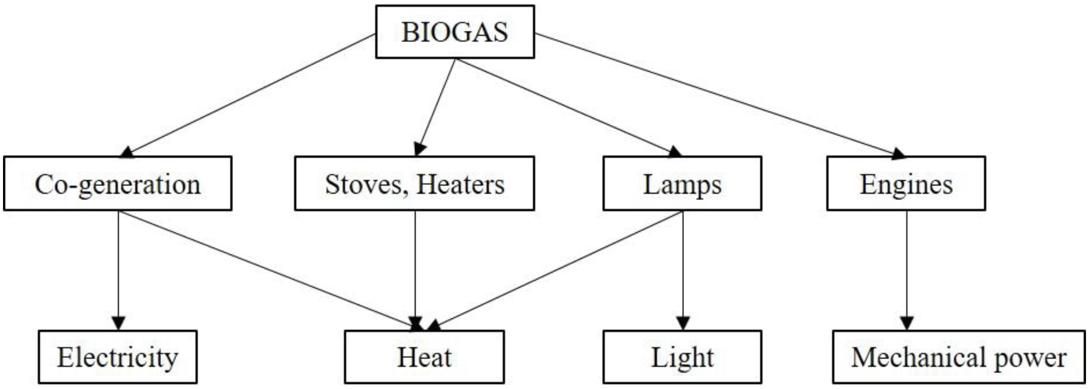

Figure 2.1: Possible uses of biogas as energy (source: Quin and Myns, 1993)

In some of developing countries like China, India and Vietnam the heat energy produced from the combustion of biogas can be directly used for application such as cooking, water heating and lighting (Okonkwo et al., 2018). Yet, in industrial countries region, high tolerance of biogas quality is mostly needed for the combustion of biogas especially for engines, boilers, vehicle and fuel cell applications (Sun et al., 2015; Zafar, 2018). Due to that the quality of the CH_4 content of the biogas is usually been increased or brought nearer to specifications like natural gas through upgradation process and the final gas product is call biomethane (Kougias et al., 2017; Bauer et al., 2013; Cozma et al., 2012; Mateescu et al., 2008; Petersson and Wellinger 2009). Biomethane is more environmentally beneficial than either biodiesel or first-generation of bioethanol by emitting less hydrocarbons, nitrogen oxide and carbon monoxide (Patterson et al., 2008; Murphy and Power, 2009; Zhao et al., 2010).

Patterson et al. (2011) reported that generally there is no quality standard for energy fuel derived from biogas. However, national standard and specification of biogas utilization for grid injection and vehicle fuel have been developed in several countries as in **Table 2.4**. The standard is intentionally to prevent damage of the equipment from corrosion, fouling and harmful environmental emission.

Table 2.4: Vehicle and grid injection standard requirements in several countries.
(Source: Bauer et al., 2013; Munoz et al., 2015; Svensson, 2014; Petersson et al., 2009)

Compound	Unit	Germany	Sweden	France	California	Switzerland
Wobbe index$_{\text{upper}}$	MJ Nm^{-3}	46.1-56.5	44.7-46.4	48.2-56.5	47.6-51.6	47.9-56.5
Wobbe index$_{\text{lower}}$	MJ Nm^{-3}	37.8-46.8	43.9-47.3	42.5-46.8		*Unlimited
CH_4	% (vol)	-	≥ 97	≥ 86	-	≥ 96
CO_2	% (vol)	≤ 6 dry	≤ 3	$\geq 2.5^a$	3	≤ 4
H_2	% (vol)	≤ 5	≤ 0.5	≤ 6	-	≤ 4
O_2	% (vol)	≤ 3	≤ 1	≤ 0.01	< 0.2	≤ 0.5
$CO_2 + O_2 + N_2$	-	-	≤ 5	-	-	-
H_2S	ppm	< 5	< 15.2	≤ 5	88	≤ 5
Total sulfur	ppm	< 30	< 23	< 30	265	< 30
Mercaptans	ppm	≤ 15	-	≤ 6	106	≤ 5
NH_3	ppm	≤ 20	≤ 20	≤ 3	≤ 0.001 mol %	≤ 20
Siloxanes (Si)	mg m^{-3}				0.1 or free	
Halogenated compounds	mg m^{-3}	≤ 1	≤ 1	$\leq 1^b$ $< 10^c$	≤ 0.1 ppm	≤ 1
Water dew point	˚C	Ground Temp	$\leq -5^d$ ≤ -9 at 200 bar	≤ -5 at P_{max}		-8 at P_{max}

^{a}: France allows flexibility in O_2 and CO_2 under certain conditions;^{b}: Chlorine compounds;^{c}: Fluorine compounds;^{d}: Ambient temperature;*: Switzerland allowed unlimited gas injection.

2.3 Purification technologies

Energy content of biogas is in direct proportion with CH_4 concentration, therefore apart from CH_4, all the other gasses contained in biogas are categorized as undesirable and is identified as biogas contaminant (Angelidaki et al., 2018). Removal of those contaminants are important in order to have a high quality of energy in a more productive and economic way. In addition, according to Appels et al. (2008), biogas is upgraded to reach a sufficient gas appliances quality especially for engines, boilers, fuel cells and vehicle purposes, to increase the heating value of the raw biogas and finally to standardize the biogas quality.

Various biogas upgrading technologies has been developed mainly based on the factors which related to the nature of its operation such as (Awe et al., 2017);

i. physical, chemical and biological,
ii. their efficiency and operational conditions,
iii. investment and maintenance costs

It should be note that there are two different type of biogas purification treatments applied in removing the biogas contaminants or pollutants. The first treatment is targeting at removing of harmful and toxic compounds particularly H_2S gas. Next treatment method is aims to intensify the low heat heating value of the biogas either by removing or converting the CO_2 gas (Kougias et al., 2017). Ali et al. (2013), has suggested that selection of right purification technology is very important in order to prevent from any damaging consequences which may result with higher total cost or even ruin the system. Commonly, the selections of purification technologies should depend on scale, actual specification and individual requirement of biogas facilities (Hjuler and Aryal, 2017).

Table 2.5: Comparison of different physical and chemical technologies for biogas purification. (Source: Angelidaki et al., 2018)

Items	**Cryogenic**	**PSA**	**Water scrubbing**	**Chemical absorption**	**Membrane separation**
Consumption for raw biogas (kWh m^{-3})	0.76	0.23-0.3	0.25-0.3	0.05-0.15	0.18-0.2
Consumption for clean biogas (kWh m^{-3})	-	0.29-1	0.3-0.9	0.05-0.25	0.14-0.26
Heat consumption (kWh m^{-3})	-	None	None	0.5-0.75	None
Head demand (˚C)	-196	-	-	100-180	-
Cost	High	Medium	Medium	High	High
CH_4 losses (%)	2	<4	<2	<0.1	<0.6
CH_4 recovery (%)	97-98	96-98	96-98	96-99	96-98
Pre-purification	Yes	Yes	Recommended	Yes	Recommended
H_2S co-removal	Yes	Possible	Yes	Contaminant	Possible
N_2 & O_2 co-removal	Yes	Possible	No	No	Partial
Operation pressure (bar)	80	3-10	4-10	Atmospheric	5-8
Pressure at outlet (bar)	8-10	4-5	7-10	4-5	4-6

The following are six different types of biogas upgrade technologies which currently have a high market value;

i. Water scrubbing and/or physical absorption
ii. Pressure swing adsorption
iii. Chemical absorption
iv. Membrane separation
v. Biological
vi. Cryogenic technology

Table 2.5 and **2.6** compares the performance of the upgrade technologies. Notice that among the technologies water scrubbing was found to be one of the simplest and most economical method that provides simultaneous removal of CO_2 and H_2S gas. Some technologies such as biological and cryogenic technology are categorized underdeveloped and most available information about it are based on laboratory scale or pilot test (Sun et al., 2015). Comprehensive review corresponding to the performance of water scrubbing technology is provided in the next subtopic.

Table 2.6: Advantages and disadvantages of biogas purification technologies
(Source: Andriani et al., 2014)

Technology	Advantages	Disadvantages
Water scrubbing	• Simple process, remove both CO_2 and H_2S using water as a solvent • More than 97% CH_4 upgradation • Low CH_4 loss (<2%) from the system	• Highly energy intensive system to press gas and to pump water • Slow process due to physical solubility of water • Corrosion problem due to H_2S • Clogging problem due to bacterial growth • Small amount of O_2 left
Chemical absorption	• High CH_4 purities (>95%) and low CH_4 loss (<0.1%) • Faster process compared to water scrubber • Chemical solvent is easier to regenerated	• Energy intensive because steam has to be supplied to regenerate the chemicals • Corrosion problem due to H_2S • Further chemical waste treatment is necessary
Pressure swing adsorption	• Capital cost share moderate • Relatively quicker start up and installation • High CH_4 purities (95-98%)	• Higher capital cost (affected by number of column) • Incomplete scrubbing (other treatment are needed) • High CH_4 loss might be possible due to malfunctioning of valves
Membrane separation	• Fast installation and startup • Flexible production output • Purity and flowrate can vary • Low energy required • High CH_4 purities (>96%) • Low CH_4 loss	• Low membrane selectivity • Consume relatively more electricity per unit of gas production • Often yields lower CH_4 concentration though high purity is possible
Biological	• Low energy requirements • No unwanted end products • Enrichment of CH_4 (>99%) • Low cost process	• Additional nutrients are required for bacterial growth • Small amount of O_2 and N_2 are left in treated biogas
Cryogenic	• High CH_4 purities (90-98%)	• Lot of devices are required such as

technology	• Relative pure CO_2 can be separated for further utilization • Liquid CH_4 reduces gas volume, thus can be packaged in the tube and can be easily disturbed • Low CH_4 loss	compressor, heat exchanger and cooler • High operating and maintenance cost

2.3.1 Water scrubbing technology

Water scrubbing technology is used extensively to treat water soluble inorganic gaseous pollutant in a wet scrubber based on absorption principle. For wet scrubbing, packed scrubbers are the most commonly used devised (**Figure 2.2**).

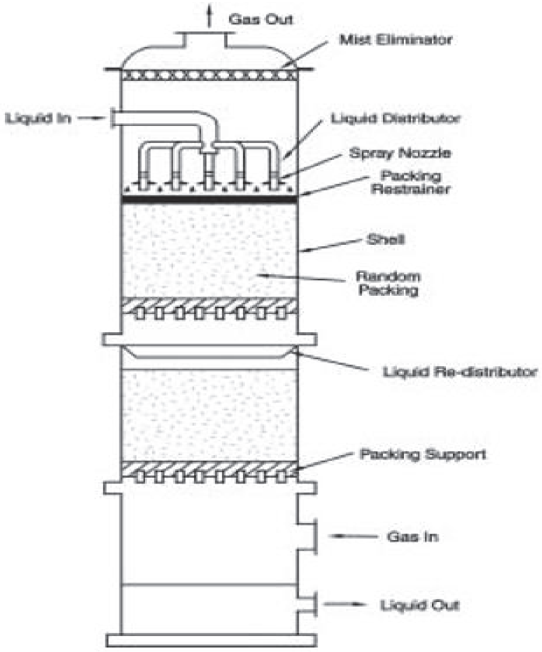

Figure 2.2: Packed scrubber tower for gas absorption (Source: Barbour et al., 1995)

In the scrubbing system, the biogas and water are pumped from the bottom and upper of the column respectively, and packing materials are install for the gas and water to interact, then the unwanted gases are removed by the water (Ryckebosch et al., 2011). A simple expression of mass transfer of gas molecules (gas phase) to the scrubbing liquid (liquid phase) is given below;

$$Q_G(P_i - P_o) = Q_L(C_O - C_i) \tag{2.1}$$

Where;

Q_G = molar flow rate of carrier gas, mol s^{-1}

P_i = inlet gas mol ratio of pollutant to unpolluted carrier gas

P_o = outlet gas mol ratio of pollutant to unpolluted carrier gas
Q_L = molar flow rate of scrubbing liquid, mol s^{-1}
C_i = inlet liquid mol ratio of pollutant to unpolluted scrubbing liquid
C_o = outlet liquid mol ratio of pollutant to unpolluted scrubbing liquid

From Eqn. 2.1 it indicates that the total quantity of pollutant dissolved in scrubbing liquid is equivalent to the total quantity of pollutant loss in the gas phase. The important operating variables that affect mass transfer efficiency are gas velocity, liquid flow rate, packing size, packing height and solubility of the gaseous pollutant. The solubility of the pollutant in the liquid is the driving force for the absorption of pollutants between phases and it can be predict using Henry's Law equation as below;

$$p = HC^* \tag{2.2}$$

Where;
p = partial pressure of pollutant at equilibrium, atm
H =Henry's law constant, atm L mol^{-1}
C^* = concentration of the pollutant in a liquid that equilibrium with partial pressure, mol L^{-1}

The net rate of the pollutant transfer between the liquid and gas phases are expressed using the two-film theory as follows;

$$N = K_L a(C^* - C) \tag{2.3}$$

Where;
N = rate of gas pollutant transfer, mol L^{-1} d^{-1}
$K_L a$ =overall mass transfer coefficient, h^{-1}
C = dissolved concentration of gas pollutant, mol L^{-1}

$K_L a$ is describing the overall driving force for the liquid phase through an interfacial area of a contact in finite section. **Table 2.7** shows several of $K_L a$ value recorded from different type of packing material. The design of the wet scrubber system usually focus on the estimation of two primary performance parameters which are the efficiency of removal and the pressure drop. The pressure drop dictates the power requirements and the size of auxiliary equipment such as fans and pumps for the system. There are several general types of wet scrubbers as shown in **Table 2.8**, with a summary of their performance and ranges of operation. The performance of the absorption process may also be influence by factors such as temperature and pressure of the gas stream, construction material of the scrubber, selection of scrubbing liquid, liquid viscosity and liquid-gas ratios (Vendruscolo et al., 2012). Ryckebosch et al. (2011) reported that, gas pressure of 1000 to 2000 kPa is usually needed to enhance the solubility of gas in scrubbing liquid.

2.3.1.1 Packing materials

Mass transfer between gas and liquid phases is also enhanced by the installation of a packing material or absorber. Packing materials with large wetted surface area can offer greater removal efficiency, handle higher rates of liquid, and relatively have lower water consumption requirements. However, the presence of packing material may also give some negative effects to the system such as high pressure drops, high clogging and fouling potential, and comprehensive maintenance (McInnes et al., 1990).

According to Tan et al. (2012), increased in surface area can increased the mass transfer performance. Study reported by Uemura et al. (2016), suggested that polyurethane foam (PUF) material as a packing carrier offering excellent water distribution and O_2 mass transfer. Furthermore, PUF have been regarded as the media that, yielding high removal efficiencies in the treatment of volatile organic compound and sulfur reduce compound while exhibiting low clogging and pressure drop. **Figure 2.3** shows the characteristics and structure of PUF material.

- Insoluble
- Non-biodegradable
- In-expensive
- Highly mechanically stable
- Large void volume more than 98%
- High surface area
- Reusable

Figure 2.3: The structure of PUF material and its characteristics
Source: Uemura et al., 2016

Table 2.7: Process conditions and K_La values

Parameter	Unit	Reference				
		Biard et al., (2017)	Almenglo et al., (2016)	Dorado et al., (2009)	Kim and Deshusses (2008)	Evren et al., (1999)
K_La	h^{-1}	5.58	32.4-34.4	43.19	30-35	58
Gas retention time	min	0.0037	2-10	0.583	0.005-0.24	0.12
Height/Diameter	-	7.83	1.7	14.26	2.67	15
Packing material	-	Hiflow ring	PUF*	PUF*	PUF*	PUF*
Pressure	MPa	0.1	-	0.12	-	-
Liquid velocity	mh^{-1}	69.32	10	2	0.1-12	84
Temperature	˚C	20	22.6	23	20	20

*: polyurethane foam

Table 2.8: Wet scrubber types, performance and ranges of operation
(Source: Calvert and Englund, 1984)

Type	Efficiency	Cut diameter, µm	Pressure drop, ΔP	Liquid consumption for $1000m^3$ of gas	Gas velocity
Packed bed	99%	1.5	Cross flow:80200 Pa/m depth Counter flow:160-1250 Pa/m depth	Cross flow:0.133-0.53 m^3 Counter flow:1.35-2.7 m^3	12m/s
Plate	90-98%	1	250-1000 Pa	0.4-0.8m^3	3m/s
Preformed spray	70-80%	2	100-200 Pa/m depth	0.4-2.7m^3	15-45cm/s
Centrifugal	87%	4-5	500-1500 Pa	0.27-0.67m^3	Cyclone inlet velocity 15-25m/s
Venturi	99%	-	1450-17500	0.27-1.33m^3	Through venturi throat 60-120m/s
Moving bed	99%	-	750-1250 Pa per stage	-	-
Orifice type	90-95%	-	750-2500 Pa	-	-

Principally, there are two different types of packing materials that are available; random packing (Pall ring, Raschig rings, IMTP) and structured packing (Flexipa, Mellapak, Gempak, BX). Some examples of available random and structured packings are shown in **Table 2.9**. Every packing material have specific characteristics with regards to surface area, weight, corrosion resistance, pressure drop and cost. According to Arachchige and Melaaen (2012), the surface area and void fraction are the two main criteria that always become preference for the selection of the packing. **Table 2.9** is showing the characteristics comparison between random and structured packing. The selection of packing material for an industrial application however depend on several factor such as the nature of the contaminants, geometric mode of contact, size of the absorber, cost, low pressure drops, corrosion resistance, large specific area, structural strength, weight, design flexibility and arrangement (MacDonald,1977).Generally, most of the packings used are made from ceramic, metal or plastic which build with engineered shapes that intended to maximize surface-to-volume ratio and minimize pressure drop (Perry and Chilton, 1984).

Table 2.9: Comparison of random and structured packing
(Source: Arachchige and Melaaen, 2012; Udara and Morteen, 2012)

Random	Structured
• Flow channels do not have a fixed shape. • It can have a nominal size from ½” to 4” and is normally dumped randomly into a column. • Made of ceramic, metal or plastic. • Easy transport and storage. • Cheaper than structured packing.	• It is manufactured in modular form to permit stacking in an ordered array. • The height of each module cab be varied from 6 to 12 inches. • Having higher surface area than random packing • Provides better performance and are costly. • Transportation is difficult without damaging the shape.
	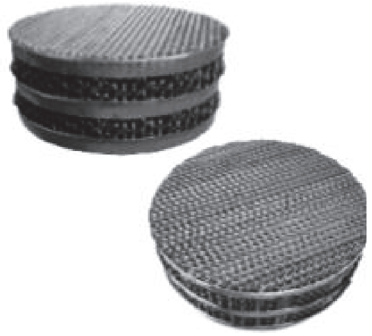

2.3.1.2 Energy demand

An energy requirement for biogas upgrading is one of the key factors in assessing their performance and for attaining the sustainability of biogas. In the water scrubbing process the energy requirement depends on plant configurations and plants operating parameter such as temperature and pressure (Budzianowski et al., 2017). For an efficient contaminants' removal, pressure around 9 to 12bar is used to pressurize the water and accelerate the mass transfer between gas-liquid phases. Cozma et al. (2013) reported that the equipment for biogas compression and the circulation pump for water processing are the main energy consumer in water scrubbing system. Approximately about 0.11kWh/Nm^3 of energy is required for compression of upgraded biogas (Patterson et al., 2011; Budzianowski et al., 2017). Through compression, gas with higher energy density is produced, thus enable the upgraded biogas to be applied for transportation or gas grid injection. In water scrubbing system, the minimum works of compression are roughly proportional to the temperature. Low compression energy is applied under low operating temperature. Therefore, the energy and performance of water scrubbing technology are superior in moderate and colder climates (Budzianowski et al., 2017). **Table 2.10** presents the data of energy demand from several biogas upgrading technologies.

Table 2.10: Energy demand of biogas upgrading technologies
(Source: Persson et al., 2007; Benjaminsson et al., 2006)

Technology	Energy demand (kWh/Nm^3 of upgraded biogas)
PSA	0.5-0.6
Water scrubbing	0.3
Chemical amine scrubbing	0.15
Membrane separation	0.27
Cryogenic	0.42

Generally, a total energy demand of 171.5kWh is required for the production of 309.36Nm^3/h of upgraded biogas by water scrubbing technology (Cozma et al., 2013). To be specific, the energy requirement for upgraded biogas or biomethane production from biogas is about 0.32kWh/Nm^3 raw biogas and the energy amounts are become increased with the installation of flash tank and water regeneration in water scrubbing system. However, the benefit from using the flash tank is limited CH_4 slip captured from the stripper into stripping air (Budzianowski et al., 2017). Taking this into consideration, energy reduction is seeming feasible in plants without flash and water regeneration.

2.3.1.3 Economic consideration

The most important factor for economic consideration is the total plant cost that included the investment, operating and maintenance cost. All of these costs are largely depend on the scale of the upgrading plant (Petersson and Wellinger, 2009). Urban (2009) found that the economics for larger plants had much lower specific costs compared to the small biogas upgrading plants. According to Rehnlund and Rahm (2007) for large scale plants (200-300Nm^3/h) the upgrading costs are around 0.01-0.16€kW/h and small plants (<100Nm^3/h) upgrading costs are 0.03-0.04€kW/h. The larger plants are favor for higher quality gas, lower CH_4 losses, higher plant efficiency and higher profitability. The economic comparison between different method of upgrading technologies are shown in **Table 2.11**. Among all the upgrading technologies water scrubbing offered the cheapest compared to the others. Persson (2003) also reported that lower of investment cost is the primary reason for industries to choose water scrubbing as their biogas treatment method. However, the implementation of water scrubbing technology for small scale is very limited. This is due to the cost for quality and quantity control together with gas transportation that makes it too expensive for small scale application. The water scrubbing technology can be made economically viable for small scale by reducing the electricity and water cost.

Table 2.11: Economics estimation of several biogas upgrading technologies
(Source: Hullu et al., 2008)

Technology	Investment cost (€/yr)	Maintenance cost (€/yr)	Cost per Nm^3/biogas upgraded (€)
PSA	680,000	187,250	0.25
Water scrubbing	265,000	110,000	0.13
Chemical amine scrubbing	353,000-179,500	134,00-179,500	0.17-0.28
Membrane separation	233,000-749,000	81,750-126,000	0.12-0.22
Cryogenic	908,500	397,500	0.44

PART B: TREATMENT OF BIOGAS PURIFICATION EFFLUENT

2.4 Effluent composition

The operation of biogas upgradation results in direct emission of greenhouse gases such as CH_4 and CO_2 from its effluent. H_2S is also emitted during the process that come from dissolved H_2S gas in the effluent which subsequently create bad odors.

2.4.1 Dissolved methane (CH_4)

There is no study yet been investigated on the removal of dissolved CH_4 of biogas purification effluent. However, several peer reviewed had reported on the dissolved CH_4 removal and recovery of anaerobic treatment effluent by using methods such as biological oxidation, aeration, air stripping and membrane-based recovery. Crone et al. (2016) reported that for the treatment of dissolved CH_4 from up-flow anaerobic sludge blanket (UASB), biological treatment by downflow hanging sponge (DHS) is more suitable compared to membrane-based method due to high removal of residual dissolved CH_4, suspended solid and COD thus eliminating the need for post treatment. **Table 2.12** shows the performance of dissolved CH_4 removal from municipal wastewater by biological oxidation treatment.

2.4.2 Dissolved carbon dioxide (CO_2)

In wastewater treatment plant the CO_2 production is attributed to two main sources; biological treatment process and electricity consumption (Campos et al., 2016). Dissolved CO_2 needs to be removed in order to make the effluent of biogas upgradation system become reusable. Reducing the concentration of CO_2 leads to a rise in pH and a reduction of aggressive CO_2 which can disintegrate concreate pipe. Aeration and gas stripping are normally applied for gas separation from liquid solution. According to Hu et al. (2011), the gas to liquid (G/L) flow ratio has the most significant influence on the CO_2 removal efficiency. The efficiency increased with the increase of (G/L) and ratio of 5 to 8 is considered to be the best for the CO_2 removal from aquaculture water.

2.4.3 Dissolved hydrogen sulfide (H_2S)

The presence of high concentration of H_2S gas in biogas upgradation effluent can caused corrosion problem on concreate, steel and water transport system (Krayzelova et al., 2014). Removal of sulfide (S^{2-}) from the effluent can be carried out either by physical, chemical or biological processes. However, although physical and chemical are rapid and efficient processes due to their high operational cost (Appels et al., 2008) and production of secondary pollutants it is become unfavorable (Ho et al., 2013). However, for biological processes, the operational of H_2S metabolization is in an efficient, inexpensive way (Ho et al., 2013) with lower or no need for chemical addition (Buisman et al., 1989; Syed et al., 2006; Krayzelova et al., 2014). Nevertheless, the accumulation of sulfate (SO_4^{2-}) reduce from the oxidation of sulfite (SO_3^{2-}) has caused drop in pH (Lee et al., 2006; Gonzalez-Sanchez et al., 2008; Jiang et al., 2009; Ho et al., 2013). Among biological method microaeration has been gaining attention over the past years for desulfurization. This process is based on the controlled dosing of a limited amount of air or oxygen into the reactor to ensure the oxidation of S^{-2} into elemental sulfur (S_o). **Table 2.13** shows the performance of different biological sulfide oxidizing systems.

Table 2.12: Biological treatment performance of dissolved methane

Reference	Scale	Source of dissolved CH_4	Dissolved CH_4 loading rate (kg/m^3day)	HRT (h)	Air supply (L/dy)	CH_4 removal efficiency (%)	CH_4 removal (kg/m^3day)	CH_4 recovery (%)	Remarks
Hatamoto et al. (2010)	Lab-scale	Artificial wastewater effluent contains dissolved CH_4 and NH_3	0.21 0.92	2 0.5	2.5 2.5	95 60	0.2 0.55	- -	-CH_4 oxidation occurred preferentially over NH_3 oxidation -type I methanotrophs were the dominant CH_4 oxidizers
Hatamoto et al. (2011)	Lab-scale	Artificial wastewater effluent contains dissolved CH_4, NH_3 and sulfide	0.14 0.22	2 1	3.24 3.24	93 45	0.13 0.1	- -	-sulfide oxidation occurred prior to methane oxidation - maximum oxidation capacity of the DHS is approximately 2.5 kg-O_2 m^{-3} day^{-1}
Matsuura et al. (2010)	Pilot-scale (for 131day) at temperature 21-28˚C	UASB effluent	0.002-0.003	2	200	>99	0.0019-0.003	76.8%	-Adjustment of air supplied is required to maintain the recovered CH_4 concentration above 30%
Matsuura et al. (2015)	Pilot-scale (for 1 year) at temperature 10-28˚C	UASB effluent	0.002-0.003	2	200	>99	0.0019-0.003	57- 88%	-ratio of air to wastewater flow is the most important parameter to control the CH_4 emission

Table 2.13: Performance of different biological sulfide oxidizing systems

Reference	**System**	**Scale**	**Sulfide in wastewater/gas/others**	**Sulfide loading rate (kg/m^3 day)**	**Sulfide inlet conc. (mg/L)**	**Sulfide removal efficiency (%)**	**Sulfur recovery (%)**
Henshaw et al., (1998)	Phototrophic	Lab-scale	wastewater	0.004	20-30	100	100
Khanna et al., (1996)	Phototrophic	Lab-scale	wastewater	0.43	2.5	-	70
Kobayashi et al., (1983)	Phototrophic	Lab-scale	wastewater	0.87-1.1	1.0	95	-
Buisman et al., (1993)	Chemotrophic	Pilot-scale	paper mill effluent	6	60-240	70	60-90
Krishnakumar et al., (2005)	Chemotrophic	Lab-scale	Synthetic wastewater	7.5-30	240	90-100	65-90

References

Adriani, D., Wresta, A., Atmaja, T.D., Saepudin, A., 2014. A review on optimization production and upgrading biogas through CO2 removal using various techniques. Appl. Biochem. Biotechnol., 172.

Almenglo, F., Bezerra, T., Lafuente, J., Gabriel, D., Ramírez, M., Cantero, D., 2016. Effect of gas-liquid flow pattern and microbial diversity analysis of a pilot-scale biotrickling filter for anaoxic biogas desulfurization. Chemosphere 157, 215 – 223.

Angelidaki, I., Treu, L., Tsapekos, P., Luo, G., Campanaro, S., Wenzel, H., Kougias, P.G., 2018. Biogas upgrading and utilization:Current status and perspectives. Biotechnology Advances, 36, 452 – 466.

Appels, L., Baeyens, J., Degre, V.J., Dewil, R., 2008. Principles and potential of the anaerobic digestion of waste-activated sludge. Prog Energy Combust Sci., 34(6), 755 – 781.

Arachchige, U.S.P.R., Melaaen, M.C., 2012. Selection of packing material for gas absorption. European Journal of Scientific Research, 117 – 126.

Awe, O.W., Zhao, Y., Nzihou, A., Minh, D.P., Lyczko, N., 2017. A review of biogas utilization, purification and upgrading technologies. Waste and Biomass Valorization, 8(2), 267 – 283.

Barbour, W., Oommen, R., Shareef, G.S., Vatavuk, W.M., 1995. Wet scrubbers for acid gas. Office of Research and Development, U.S. Environmental Protection Agency, Research Triangle Par,, North Carolina, Publication No. EPA/452/B-02-001.

Bauer, F., Persson, T., Hulteberg, C., Tamm, D., 2013. Biogas upgrading: technology overview, comparison and perspectives for the future. Biofuels Bioprod. Biorefin., 7, 499 – 511.

Biard.P.F., Couvert.A., Renner.C., 2017. Intensification of volatile organic compound absorption in a compact wet scrubber at co-current flow. Chemosphere 173, 612 – 621.

Buisman, C., Post, R., Ijspeert, P., Geraats, G., Lettinga, G., 1989. Biotechnological process for sulphide removal with sulphur reclamation. Acta Biotechnol., 9(3), 255 – 267.

Buisman, C.J.N., Bloembergen, J.R., Paalvast, C., 1993. Biological sulphur recovery from paper mill effluent. TAAPI proceedings, 841.

Calvert, S., Englund, H., 1984. Handbook of air pollution technology. John Wiley & Sons, New York.

Campos, J.L., Valenzuela, H.D., Pedrouso, A., Val del Rio, A., Belmonte, M., Corral, M.A., 2016. Greenhouse gases emission from wastewater treatment plants: minimization, treatment and prevention. Journal of Chemistry.

Chandra, R., Vijay, V.K., Subbarao, P.M.V., Khura, T.K., 2012. Production of methane from anaerobic digestion of jatropha and pongamia oil cakes. Appl. Energy, 93.

Cozma, P., Wukovits, W., Friedl, A., Gavrilescu, M., 2012. Biogas upgrading using water scrubbing technology. Bull Polytech Inst. Jassy. Sect. Chem. Eng. Tome., 59(62), 58 – 73.

Cozma, P., Ghinea, C., Mamaliga, I., Wukovits, W., Friedl, A., Gavrilescu, M., 2013. Environmental impact assessment of high-pressure water scrubbing biogas upgrading technology. CLEAN-Soil, Air, Water, 41(9), 917 – 927.

Crone, B.C., Garland, J.L., Sorial, G.A., Vane, L.M., 2016. Significance of dissolved methane in effluents of anaerobically treated low strength wastewater and potential for recovery as an energy product: a review. Water Research, 104, 520 – 531.

Deublein, D., Steinhauser, A., 2010. Biogas from waste and renewable resources: An introduction. Wiley.

Divyang, S.R., Hemant, N.J., Pradeep, A., 2016. Purification of biogas using chemical scrubbing and application of purified biogas as fuel for automotive engines. Res. J. Recent. Sci., 5, 1-7.

Dorado, A.D., Rodríguez, G., Ribera, G., Bonsfills, A., Gabriel, D., Lafuente, J., Gamisans, X., 2009. Evaluation of mass transfer coefficients in biotrickling filters: Experimental determination and comparison to correlations. Chemical Engineering and Technology, 32(12), 1941 – 1950.

Evren, V., Cağatay, T., Özdural, A.R., 1999. Carbon dioxide-air mixtures: Mass transfer in recycling packed-bed absorption columns operating under high liquid flow rates. Separation and Purification Technology, 17, 89 – 96.

González-Sánchez, A., Revah, S., Deshusses, M.A., 2008. Alkaline biofiltration of H2S odors. Environ. Sci. Technol. 42, 7398 – 7404.

Gross, T., Zahnd, A., Adhikari, S., Kaphre, A., Sharma, S., Baral, B., Kumar, S., Hugi, C., 2017. Potential of biogas production to reduce firewood consumption in remote high-elevation Himalayan communities in Nepal. Renew. Energy Environ. Sustain., 2 (8).

Hatamoto, M., Yamamoto, H., Kindaichi, T., Ozaki, N., Ohashi A., 2010. Biological oxidation of dissolved methane in effluents from anaerobic reactors using a down-flow hanging sponge reactor. Water research, 44(5), 1409 – 1418.

Hatamoto, M., Miyauchi, T., Kindaichi, T., Ozaki, N., Ohashi, A., 2011. Dissolved methane oxidation and competition for oxygen in down-flow hanging sponge reactor for post-treatment of anaerobic wastewater treatment. Bioresource Technology, 102(22), 10299 – 10304.

Henshaw, P.F., Bewtra, J.K., Biswas, N., 1998. Hydrogen sulphide conversion to elemental sulphur in a suspended growth continuous stirred tank reactor using Chlobium Limicola. Water Resource, 32(6), 1769 – 1778.

Hjuler, K., Aryal, N., 2017. Review of biogas upgrading. Project report Danish Gas Technology center. http//www.dgc.eu/sites/default/files/filarkiv/documents/R1704_FutureGas_Biogas_Upgradin g .pdf.

Ho, K.L., Chung, Y.C., Lin, Y.H., Tseng, C.P., 2013. Elimination of high concentration hydrogen sulfide and biogas purification by chemical-biological process. Chemosphere, 92, 1396 – 1401.

Hullu, D.J., Maassen, J.L.W., Meel, V., Shazad, S., Vaessen, J.M.P., 2008. Comparing different biogas upgrading techniques. Eindhoven University of Technology. http://students.chem.tue.nl/ifp24/BiogasPublic.pdf.

Jansen, J.C., 2010. Anaerobic digestion: technology. Solid waste technology & management, 2 volume set. John Wiley & Sons Ltd., 607 – 612.

Jiang, X., Yan, R., Tay, J.H., 2009. Simultaneous autotrophic biodegradation of H_2S and NH_3 in a biotrickling filter. Chemosphere 75, 1350 – 1355.

Khanna, P., Rajkumar, B., Jyothikumar, N., 1996. Microbial recovery of sulphur from thiosulphate bearing wastewater with phototrophic and sulphate reducing bacteria. Current Microbiol., 32(1), 33 – 37.

Kim, S., Deshusses, M.A., 2008. Determination of mass transfer coefficients for packing materials used in biofilters and biotrickling filters for air pollution control.1. Experimental results. Chemical engineering science, 63, 841 – 855.

Kobayashi, H.A., Stenstrom, M., Mah, R.A., 1983. Use of photosynthetic bacteria for H_2S removal from anaerobic waste treatment effluent. Water Resource, 17(8), 579 – 587.

Kougias, P.G., Treu, L., Benavente, D.P., Boe, K., Campanaro, S., Angelidaki, I., 2017. Ex-situ biogas upgrading and enhancement in different reactor systems. Bioresour. Technol., 225, 429 – 437.

Krayzelova, L., Bartacek, J., Kolesarova, N., Jenicek, P., 2014. Microaeration for hydrogen sulfide removal in UASB reactor. Bioresour Technol., 172, 297 – 302.

Krishnakumar, B., Majumdar, S., Manilal, V.B., Haridas, A., 2005. Treatment of sulphide containing wastewater with sulphur recovery in a novel reverse fluidized loop reactor (RFLR). Water Resource, 39(4), 639 – 647.

Lee, E.Y., Lee, N.Y., Cho, K.S., Ryu, H.W., 2006. Removal of hydrogen sulfide by sulfate-resistant *Acidithiobacillus thiooxidans* AZ11. J Biosci Bioeng., 101(4), 309 – 314.

Liang, F.Y., Ryvak, M., Sayeed, S., Zhao, N., 2012. The role of natural gas as a primary fuel in the near future, including comparisons of acquisition, transmission and waste handling costs of as with competitive alternatives. Chemistry Central Journal, 6 (1).

MacDonald, J.W., 1977. Packed wet scrubbers, In P.N. Cheremisinoff and R.A. Young (Eds.), Air Pollution Control and Design Handbook. Part 2. New York: Marcel Dekker.

Mateesu, C., Baran, G., Babutanu, C.A., 2008. Opportunities and barriers for development of biogas technologies in Romania. Environ. Eng. Manag. J., 7, 603 – 607.

Matsuura, N., Hatamoto, M., Sumino, H., Syutsubo, K., Yamaguchi, T., Ohashi, A., 2010. Closed DHS system to prevent dissolved methane emissions as greenhouse gas in anaerobic wastewater treatment by its recovery and biological oxidation. Water Science & Technology, 2407 – 2415.

Matsuura, N., Hatamoto, M., Sumino, H., Syutsubo, K., Yamaguchi, T., Ohashi, A., 2015. Recovery and biological oxidation of dissolved methane in effluent from UASB treatment of municipal sewage using a two-stage closed downflow hanging sponge system. Journal of Environmental Management, 151, 200 – 209.

McInnes, R., Jameson, K., Austin, D., 1990. Scrubbing Toxic Inorganics. Chemical Engineering, 116 – 121.

Munoz, R., Meier, L., Diaz, I., Jeison, D., 2015. A review on the state-of-the-art of physical/chemical and biological technologies for biogas upgrading. Rev. Environ. Sci. Biotechnol., 14 (4), 727 – 759.

Murphy, J.D., Power, N., 2009. Technical and economic analysis of biogas production in Ireland utilizing three different crop rotations. Applied Energy, 86, 25 – 36.

Okonkwo, U.C., Onokpite, E., Onokwai, A.O., 2018. Comparative study of the optimal ratio of biogas production from various organic wastes and weeds for digester/restarted digester. Journal of King Saud University – Engineering Sciences, 30 (2), 123 – 129.

Onofre, S.B., Abatti, D., Refosco, D., Tessaro, A.A., Onofre, J.A.B., Tessaro, A.B., 2015. Energy potential of poultry litter for the production of biogas. African Journal of Agricultural Research, 10 (31), 3062 – 3066.

Patterson, T., Dinsdale, R.M., Esteves, S.R., 2008. Review of energy balances and emissions associated with biomass based transport fuels relevant to the United Kingdom context. Energy and Fuels, 22, 3506 – 3512.

Patterson, T., Esteves, S., Dinsdale, R., Guwy, A., 2011. An evaluation of the policy and techno-economic factors affecting the potential for biogas upgrading for transport fuel in the UK. Enery Policy, 39, 1806 – 1816.

Perry, R.H., Chilton, C.H., 1984. Chemical Engineers Handbook (Sixth edition), McGraw-Hill Book Company, New York.

Persson, M., 2003. Evaluation of upgrading techniques for biogas, Report Swedish Gas Center, Malmoe, Sweden.

Petersson, A., Wellinger, A., 2009. Biogas upgrading technologies – developments and innovations, IEA Bioenergy-task 37 – Energy from biogas and landfill gas, IEA-International Energy Agency, Swedish Gas Centre, Malmoe, Sweden.

Quin, N.J., Myns., 1993. Bio-methanization-A developing technology association (BORDA).

Udara, S.P.R.A., Morteen, C.M., 2012. Selection of packing material for gas absorption. European Journal of Scientific Research, 87(1), 117 – 126.

Uemura, S., Okubo, T., Maeno, K., Takahashi, M., Kubota, K., Harada, H., 2016. Evaluation of water distribution and oxygen mass transfer in sponge support media for a down-flow hanging sponge reactor. Int. J. Environ. Res., 10(2), 265 – 272.

Rehnlund, B., Rahm, L., 2007. Report on technological applicability of existing biogas upgrading processes. BiogasMax project. Stockholm, Sweden.

Ryckebosh, E., Drouillon, M., Vervaeren, H., 2011. Technique for transformation of biogas to biomethane. Biomass Bioenergy, 35, 1633 – 1645.

Sahota, S., Shah, G., Ghosh, P., Kapoor, R., Sengupta, S., Singh, P., Vijay, V., Sahay, A., Vijay, V., Thakur, I., 2018. Review of trends in biogas upgradation technologies and future perspectives. Bioresource Technology Report, 1, 79 – 88.

Sarker, S., Lamb, J.J., Hjelme, D.R., Lien, K.M., 2018. Overview of recent progress towards in-situ biogas upgradation techniques- A review. Fuel, 226, 686 – 697.

Sora, Y., Yoo, K.Y., 2014. Greenhouse gas emissions and cost analyses for the treatment options of food waste and human excrement. Journal of Environment Protection, 5 (7), 597 – 607.

Starr, K., Gabarrell, X., Villalba, G., Talens, L., Lombardi, L., 2012. Life cycle assessment of biogas upgrading technologies. Waste Manage., 32, 991 – 999.

Sun, Q., Li, H., Yan, J., Liu, L., Yu, Z., Yu, X., 2015. Selection of appropriate biogas upgrading technology- A review of biogas cleaning, upgrading and utilization. Renewable and Sustainable Energy Reviews, 51, 521 – 532.

Surendra, K.C., Takara, D., Hashimoto, A.G., Khanal, S.K., 2014. Biogas as a sustainable energy source for developing countries: Opportunities and challenges. Renewable and Sustainable Energy Reviews, 31, 846 – 859.

Syed, M., Soreanu, G., Falletta, P., Be´land, M., 2006. Removal of hydrogen sulfide from gas streams using biological processes—a review. Can Biosyst Eng., 48, 2.1 – 2.14.

Svensson, M., 2014. Biomethane standards: Gas quality standardization of biomethane, going from national to international level. In: European workshop Biomethane, Brussels. Green Gas Grids.

Toro, J.C.S., Pérez, Y.C., Alzate, C.A.C., 2018. Evaluation of biogas and syngas as energy vectors for heat and power generation using lignocellulosic biomass as raw material. Electronic Journal of Biotechnology, 33, 52 – 62.

Vendruscolo, F., Rossi, M.J., Schmidell, W., Ninow, L., 2012. Determination of oxygen solubility in liquid media. ISRN Chemical Engineering.

Vijay, V.K., 2012. Book on biogas production and slurry management. Narosa Publishing House, 56.

Weiland, P., 2009. Biogas production: current state and perspectives. Applied Microbiology and Biotechnology, 85 (4), 849 – 860.

Wylock, C.E., Budzianowski, W.M., 2017. Performance evaluation of biogas upgrading by pressurized water scrubbing via modelling and simulation. Chemical Engineering Science, 170, 639 – 652.

Zafar, S., 2018. Trends in utilization of biogas. Bioenergy Consult. www.bioenergyconsult.com.

Zhao, Q., Leohardt, E., MacConnell, C., Frear, C., Chen, S., 2010. Purification technologies for biogas generated by anaerobic digestion. Compressed Biomethane, CSANR Research Report, 1 – 24. http://www.build-a-biogas-plant.com/PDF/BiogasPurificationTech2010.PDF

CHAPTER 3

MODEL DEVELOPMENT

TABLE OF CONTENTS

3.1 Introduction

A mathematical model describing biogas treatment using physical and biological process is performed using Microsoft Excel and validate by experimental data. The model is used to predict the treatment efficiency of biogas purification (by physical process) and its effluent treatments (by physical and biological process). In the model the mass transfer and concentration for each species in the gas and liquid phases at each finite different along the column were calculated separately. For both physical and biological models, the parameters in **Table 3.1** and the following assumptions are used;

i. The system operates at steady state conditions.
ii. The column is divided into 20 iteration, n=20.
iii. The transport of the gas components (CH_4, CO_2, H_2S, O_2 and N_2), air and liquid occurred in the axial direction; they were assumed to be homogeneous and completely mixed.
iv. The liquid flow is constant for a given distance (dz) and given time (t).
v. The input air contains of 21% O_2, 79% N_2, and 0.04% CO_2.
vi. The dissolved N_2 does not undergo any biological or chemical reaction in the reactor.
vii. The maximum biological consumption rate (R*) of CH_4 and H_2S for biological process model are determined based on input and output of experimental data.

Table 3.1: Model parameters

A. General parameter	
Column height, (m)	1.2
Sponge volume, Vsponge, (L)	0.42
Gas volume, Va, (L)	1.87
B. Parameter for physical model (biogas purification)	
Gas flow rate, Q_G, ($L\ d^{-1}$)	10.18-60.48
Liquid flow rate, Q_L, ($L\ d^{-1}$)	30.53-120.96
Operational temperature, T, (˚C)	5-30
Operational pressure, P, (atm)	1
Input biogas, CH_4: CO_2: H_2S, (%)	60-67:32-40:0-3
Time, Δt, (s)	0.3
Input pH	7-8
C. Parameter for physical combine with biological model (effluent treatment)	
Gas flow rate, Q_G, ($L\ d^{-1}$)	2.02
Liquid flow rate, Q_L, ($L\ d^{-1}$)	5.04-50.4
Operational temperature, T, (˚C)	25

Operational pressure, P, (atm)	1
Input dissolved gas, CH_4: CO_2: H_2S, (mg L^{-1})	11.2:44:12
Time, Δt, (s)	0.3
Input pH	5.64
Max. consumption rate CH_4, R* (mol L^{-1} d^{-1})	0.02
Max. consumption rate H_2S, R* (mol L^{-1} d^{-1})	0.0008
Monod constant of O2 gas, Kc_{o2}, (mol L^{-1})	2μ

3.2 Physical model

In the simulation process, a multicomponent absorption of biogas (CH_4, CO_2, H_2S, N_2 and O_2) in scrubbing water was governed by Henry's law as in equation 2.2 and the Henry's constants applied are as in **Table 3.2**. The scrubbing water was reacted as an inert component for the transfer of biogas components in the liquid phase. The dissolution of CO_2 and H_2S in water are higher compared to CH_4, N_2 and O_2 (Tippayawong and Thanompongchart, 2010).

Table 3.2: Henry's constant (*E*) values of selected gases in water at different temperatures.
(Source: Foust et al., 1960)

Gases /	$E \times 10^4$ (atm/mole fraction)					
Temperature (°C)	5	10	15	20	25	30
CH_4	2.61	2.97	3.37	3.76	4.13	4.49
CO_2	0.088	0.104	0.123	0.142	0.164	0.186
H_2S	0.0318	0.0367	0.0425	0.0483	0.0546	0.0609
O_2	2.91	3.27	3.64	4.01	4.38	4.75
N_2	5.99	6.68	7.36	8.04	8.64	9.24

NOTE: In this study, Henry's constant (H_j) is in units of atm L mol^{-1}. Therefore, the unit conversion can be calculated using the following relation equation:

$H_j = \frac{x_w}{E}$, where x_w is the water solution concentration at a specified temperature condition.

Sample calculation of O_2 at 25 °C: At 25 °C, the H_2O solution concentration is 55.626 mol/L; therefore, $H_j@_{25^\circ C}$ (atm L mol^{-1}) = 55.626 / (43800) = 0.00127.

By assuming that the biogas and scrubbing water are of plug-flow in the column, a conceptual schematic of the mass transfer model is shown in **Figure 3.1**, and the following mass balances in an infinitesimal distance dz at position i are established for the gas components.

$$\left(Q_{G_i} P_{j,i} - Q_{G_{i+1}} P_{j,i+1}\right) / \frac{22.4T}{273.1} = Q_L\left(C_{j,i+1} - C_{j,i}\right) = -N_{j,i} \Delta V_s, \quad (3.1)$$

$$\sum_i Q_{G_i} P_{j,i} - \sum_i Q_{G_{i+1}} P_{j,i+1} = \Delta V_s \sum_j N_{j,i} \cdot \frac{22.4T}{273.15}, \text{ for } j = CH_4, CO_2, H_2S, N_2, \text{ and } O_2, \quad (3.2)$$

where N_j is the molar flux of the pollutant transfer between the liquid and gas phases, can be calculated from the overall mass transfer coefficient (K_La) and the concentration driving force as shown by equation 2.3.

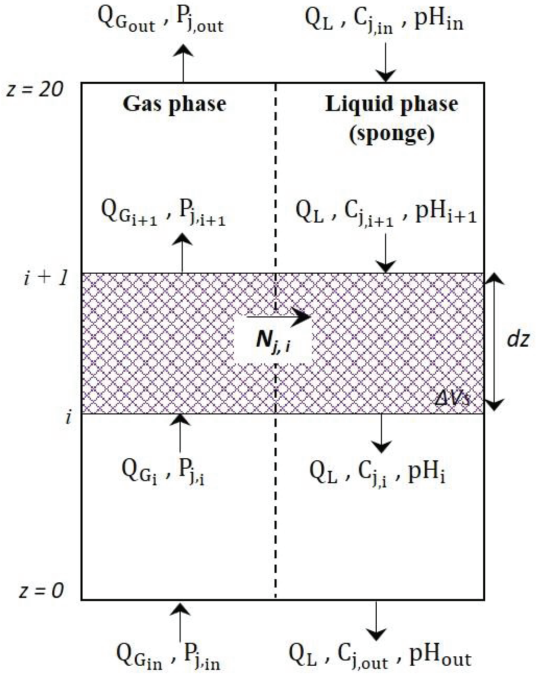

Figure 3.1: Differential element of absorption column. With z is the position along the column and dz is the height of the finite element, the gaseous and liquid flow rates are shown by Q_G and Q_L, respectively, the concentrations for i component (CH_4, CO_2, H_2S, O_2, N_2) in gas and liquid are shown by P and C, respectively.

The CO_2 and H_2S that dissolved in the water are dissociated into ions (Eqns. 3.3 & 3.4), and the concentrations of dissociated ionic compounds are depend on pH.

$$CO_2(aq) + H_2O \leftrightarrow [H_2CO_3^-(aq)] \xrightarrow{[K_1]} [HCO_3^-] + [H^+] \xrightarrow{[K_2]} [CO_3^{2-}] + [H^+] \quad (3.3)$$

$$H_2S + H_2O \leftrightarrow [H_2S(aq)] \xrightarrow{[K_1]} [HS^-] + [H^+] \xrightarrow{[K_2]} [S^{2-}] + [H^+] \quad (3.4)$$

Where in the reaction between dissolved CO_2 and H_2S gas with H_2O show the production of bicarbonate (HCO_3^-), carbonate (CO_3^{2-}), bisulfide (HS^-) and sulfide (S^{2-}) ions. Whilst, K_1 and K_2 are the dissociation constant of CO_2 and H_2S (**Table 3.3**).

The pH is calculated using the charge balance of ions in water as represented as follows:

$$[H^+] + [Alk] - \left[\frac{K_w}{H^+}\right] - 2[CO_3^{2-}] - [HCO_3^-] - [HS^-] - 2[S^{2-}] = 0 \tag{3.5}$$

$$[H^+] = \left[\frac{K_w}{H^+}\right] + 2[CO_3^{2-}] + [HCO_3^-] + [HS^-] + 2[S^{2-}] - [Alk] \tag{3.6}$$

$$[H^+] = \left[\frac{K_w}{H^+}\right] + 2[CO_3^{2-}] + [HCO_3^-] + [HS^-] + 2[S^{2-}] - [Alk] \tag{3.7}$$

$$[pH] = -log[H^+] \tag{3.8}$$

Table 3.3: Dissociation constants (*K*) of several components at different temperatures. (Source: Stumm and Morgan, 1981; Frank 1986)

Component		Temperature (°C)					
		5	10	15	20	25	30
H_2O	K_W	1.862×10^{-15}	2.951×10^{-15}	4.467×10^{-15}	6.761×10^{-15}	1×10^{-14}	1.148×10^{-14}
CO_2	K_1	3.02×10^{-7}	3.47×10^{-7}	3.80×10^{-7}	4.17×10^{-7}	4.47×10^{-7}	3.42 × 10-7
	K_2	2.75×10^{-11}	3.24×10^{-11}	3.72×10^{-11}	4.17×10^{-11}	4.67×10^{-11}	3.52×10^{-11}
H_2S	K_1		1.29×10^{-7}			1×10^{-7}	
	K_2		1×10^{-19}			1×10^{-19}	

Where, Alk is alkalinity, and K_w is dissociation constant of water (**Table 3.3**). In other words, the dissociated ionic concentrations are determined using H^+ concentration with the dissociation constants of CO_2 and H_2S.

3.3 Biological model

For the biological oxidation process, the mass transfer of CH_4, H_2S, CO_2, O_2, and N_2 gas components in the three different phases (gas, liquid, and biofilm) with a biological reaction in the biofilm, are shown in the schematic in **Figure 3.2**. A multiple-substrate Monod kinetic expression was used to describe the influence of CH_4, H_2S, and O_2 substrates on the cell growth as follows:

$$R_j = R_j^* \cdot \left(C_j/\left(K_{C_j} + C_j\right)\right) \cdot \left(C_{O_2}/\left(K_{C_{O_2}} + C_{O_2}\right)\right) \text{, for j= } CH_4 \text{ and } H_2S \tag{3.9}$$

where R_j (mol L^{-1} d^{-1}) is the biological substrate consumption rate of cells. R^*_j (mol L^{-1} d^{-1}) is the maximum biological consumption rate constant of substrate *j*. C_j (mol L^{-1}) is the substrate concentration of *j*, and Kc_j (mol L^{-1}) is the Monod constant for substrate *j*. Further, C_{O2} (mol L^{-1}) and K_{CO2} (mol L^{-1}) are the concentration and Monod constant of the O_2 substrate, respectively. With the assumption that the dissolved O_2 concentration is low in the liquid with $K_{CO2} > C_{O2}$; the effects of the other substrates (CH_4 and H_2S) on cell growth were considered negligible by assuming that $Kc_j<C_j$; therefore, the specific substrate consumption rate of cells becomes;

$$R_j = R_j^* \cdot \left(C_{O_2}/\left(K_{C_{O_2}} + C_{O_2}\right)\right). \tag{3.10}$$

The R^*_j values used were taken from the experimental data measured during the optimal removal of CH_4 and H_2S. K_{CO2} value of 2 µmol L^{-1} was applied, according to Robinson and Tiedje (1983).

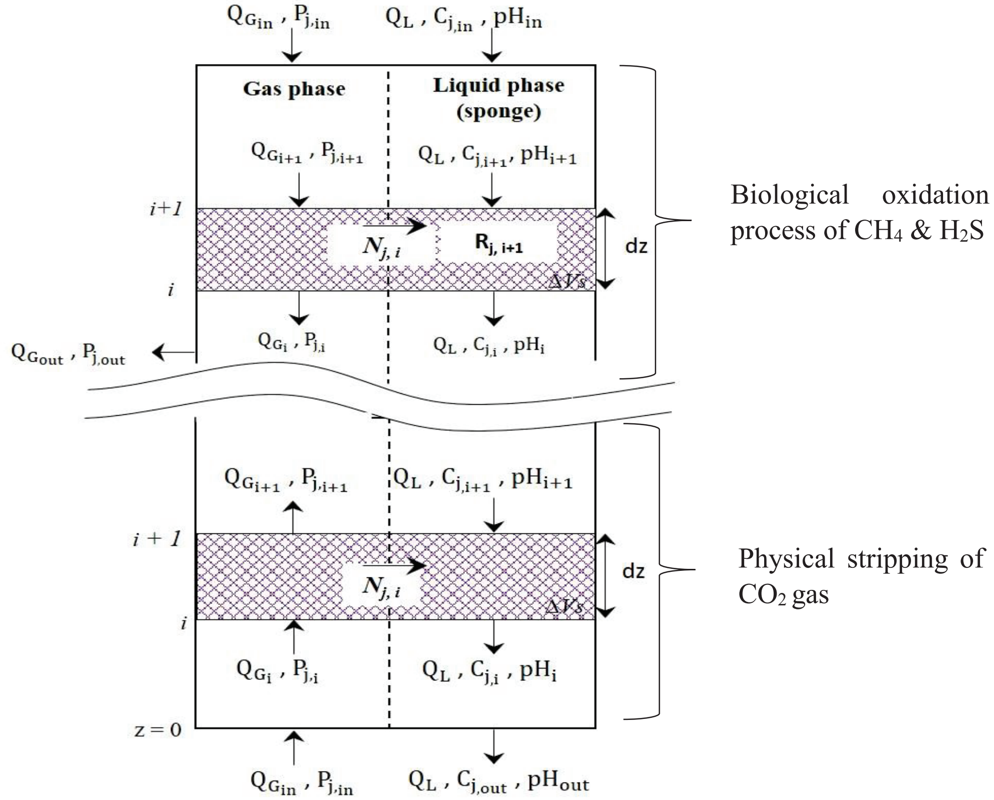

Figure 3.2: Differential element of integrated biological and physical process in a reactor column. With z is the position along the column and dz is the height of the finite element, the gaseous and liquid flow rates are shown by Q_G and Q_L, respectively, the concentrations for i component (CH_4, CO_2, H_2S, O_2, N_2) in gas and liquid are shown by P and C, respectively.

The following equations describe the overall mass balance over an infinitesimal distance d*z* at position *i* at the top and bottom of the reactor column:

At position *i* at the top of the reactor:

$$R_{j,i+1}\left(Q_{G_{i+1}}P_{j,i+1} - Q_{G_i}P_{j,i}\right)/\frac{22.4T}{273.1} = Q_L\left(C_{j,i+1} - C_{j,i}\right) + R_{j,i+1}\Delta V_S = N_{j,i}\Delta V_S \tag{3.11}$$

At position *i* at the bottom of the reactor:

$$\left(Q_{G_i}P_{j,i} - Q_{G_{i+1}}P_{j,i+1}\right)/\frac{22.4T}{273.1} = Q_L\left(C_{j,i+1} - C_{j,i}\right) = -N_{j,i}\Delta V_{S,} \tag{3.12}$$

Here, gas j corresponds to CH_4, CO_2, H_2S, O_2, and N_2. However, in the gas phase during t=0, at the inlet positions, $P_{j,\text{in}}$ represents the partial pressure of gas j corresponding O_2, N_2, and CO_2 only.

3.4 Simulation procedure

Figure 3.3 showing the Excel forms of the develop simulation and the procedure for each concentration calculations in the column is as follows:

a. The initial concentrations of component j in the gas phase, $P_{j,i}$, and liquid phase, $C_{j,i}$, in the column are assumed for $i = 0$ to n and at $t = 0$, where $j = CH_4, CO_2, H_2S, N_2$, and O_2 (**Figure 3.4**).

b. $P'_{j,i}$ and $C'_{j,i}$ at $t = \Delta t$ are calculated based on the Henry's law, molar flux equations and material balance (**Figures 3.5 & 3.6**).

c. $P_{j,i}$ is replaced with $P'_{j,i}$, and $C_{j,i}$ is replaced with $C'_{j,i}$.

d. Steps (b) and (c) are repeated.

e. Steady state is achieved when $P'_{j,i} = P_{j,i}$ and $C'_{j,i} = C_{j,i}$

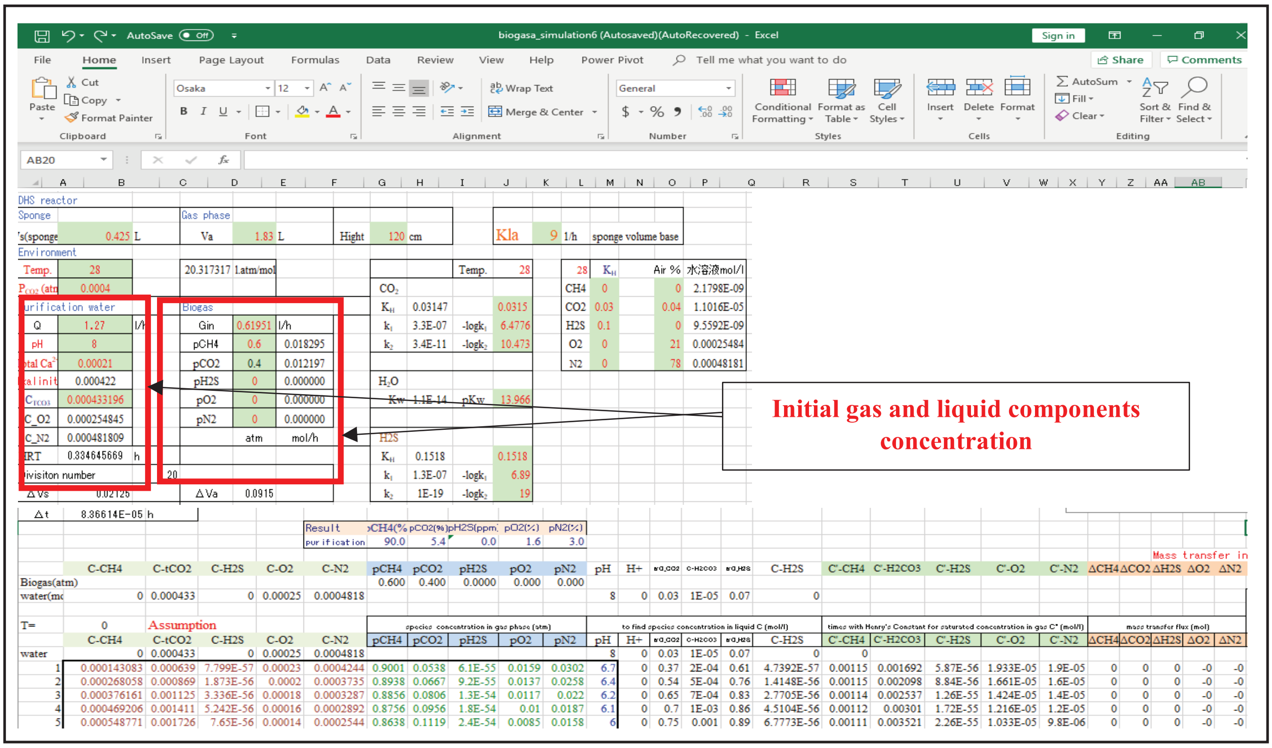

DHS reactor

Sponge

's(sponge 0.425 L

Gas phase

Va 1.83 L

Hight 120 cm

Kla 9 1/h sponge volume base

Environment

Temp. 28

P_{CO_2} (atn 0.0004

20.317317 1.atm/mol

urification water		
Q	1.27	l/h
pH	8	
otal Ca^{2+}	0.00021	
alinit	0.000422	
C_{TCO3}	0.000433196	
C_O2	0.000254845	
C_N2	0.000481809	
IRT	0.334645669	h
ivisiton number		
ΔVs	0.02125	
Δt	8.36614E-05	h

Biogas		
Gin	0.61951	l/h
pCH4	0.6	0.018295
pCO2	0.4	0.012197
pH2S	0	0.000000
pO2	0	0.000000
pN2	0	0.000000
	atm	mol/h
20		
ΔVa	0.0915	

		Temp.	28
CO_2			
K_H	0.03147		0.0315
k_1	3.3E-07	$-\log k_1$	6.4776
k_2	3.4E-11	$-\log k_2$	10.473
H_2O			
Kw	1.1E-14	pKw	13.966
H2S			
K_H	0.1518		0.1518
k_1	1.3E-07	$-\log k_1$	6.89
k_2	1E-19	$-\log k_2$	19

28	K_H		Air %	水溶液mol/l
CH4	0		0	2.1798E-09
CO2	0.03		0.04	1.1016E-05
H2S	0.1		0	9.5592E-09
O2	0		21	0.00025484
N2	0		78	0.00048181

Initial gas and liquid components concentration

Result	pCH4(%	pCO2(%)	pH2S(ppm	pO2(%)	pN2(%)
purification	90.0	5.4	0.0	1.6	3.0

Mass transfer in

	C-CH4	C-tCO2	C-H2S	C-O2	C-N2	pCH4	pCO2	pH2S	pO2	pN2	pH	H+	αa,CO2	C-H2CO3	αa,H2S	C-H2S	C'-CH4	C'-H2CO3	C'-H2S	C'-O2	C'-N2	ΔCH4	ΔCO2	ΔH2S	ΔO2	ΔN2
Biogas(atm)						0.600	0.400	0.0000	0.000	0.000																
water(mc	0	0.000433	0	0.00025	0.0004818						8	0	0.03	1E-05	0.07	0										

T=	0	Assumption				species concentration in gas phase (atm)					to find species concentration in liquid C (mol/l)						times with Henry's Constant for saturated concentration in gas C* (mol/l)					mass transfer flux (mol)				
	C-CH4	C-tCO2	C-H2S	C-O2	C-N2	pCH4	pCO2	pH2S	pO2	pN2	pH	H+	αa,CO2	C-H2CO3	αa,H2S	C-H2S	C'-CH4	C'-H2CO3	C'-H2S	C'-O2	C'-N2	ΔCH4	ΔCO2	ΔH2S	ΔO2	ΔN2
water	0	0.000433	0	0.00025	0.0004818						8	0	0.03	1E-05	0.07	0	0									
1	0.000143083	0.000639	7.799E-57	0.00023	0.0004244	0.9001	0.0538	6.1E-55	0.0159	0.0302	6.7	0	0.37	2E-04	0.61	4.7392E-57	0.00115	0.001692	5.87E-56	1.933E-05	1.9E-05	0	0	0	-0	-0
2	0.000268058	0.000869	1.873E-56	0.0002	0.0003735	0.8938	0.0667	9.2E-55	0.0137	0.0258	6.4	0	0.54	5E-04	0.76	1.4148E-56	0.00115	0.002098	8.84E-56	1.661E-05	1.6E-05	0	0	0	-0	-0
3	0.000376161	0.001125	3.336E-56	0.00018	0.0003287	0.8856	0.0806	1.3E-54	0.0117	0.022	6.2	0	0.65	7E-04	0.83	2.7705E-56	0.00114	0.002537	1.26E-55	1.424E-05	1.4E-05	0	0	0	-0	-0
4	0.000469206	0.001411	5.242E-56	0.00016	0.0002892	0.8756	0.0956	1.8E-54	0.01	0.0187	6.1	0	0.7	1E-03	0.86	4.5104E-56	0.00112	0.00301	1.72E-55	1.216E-05	1.2E-05	0	0	0	-0	-0
5	0.000548771	0.001726	7.65E-56	0.00014	0.0002544	0.8638	0.1119	2.4E-54	0.0085	0.0158	6	0	0.75	0.001	0.89	6.7773E-56	0.00111	0.003521	2.26E-55	1.033E-05	9.8E-06	0	0	0	-0	-0

Figure 3.3: Example of simulation in Excel spreadsheet

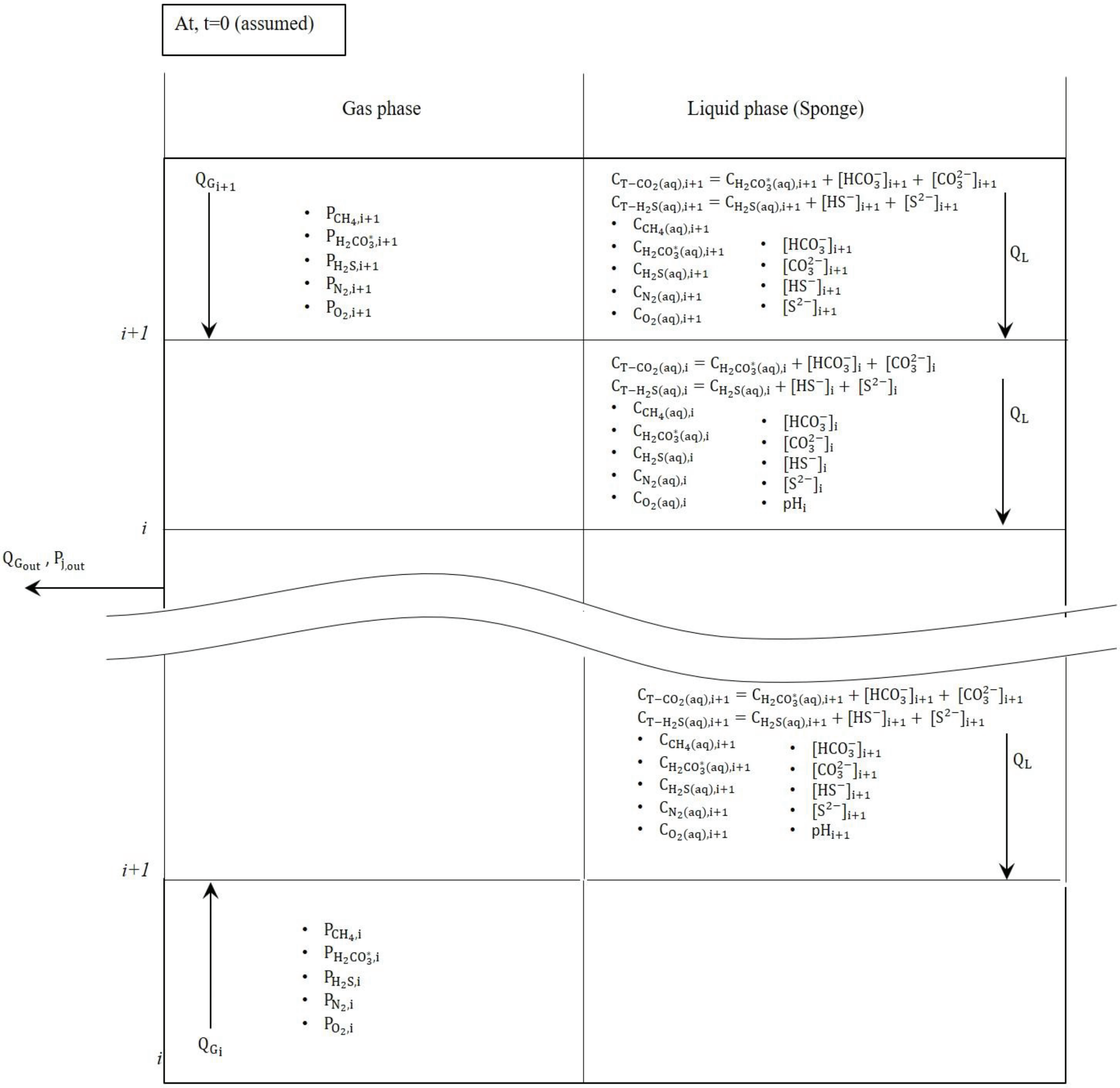

Figure 3.4: Schematic of differential element of the system at t=0

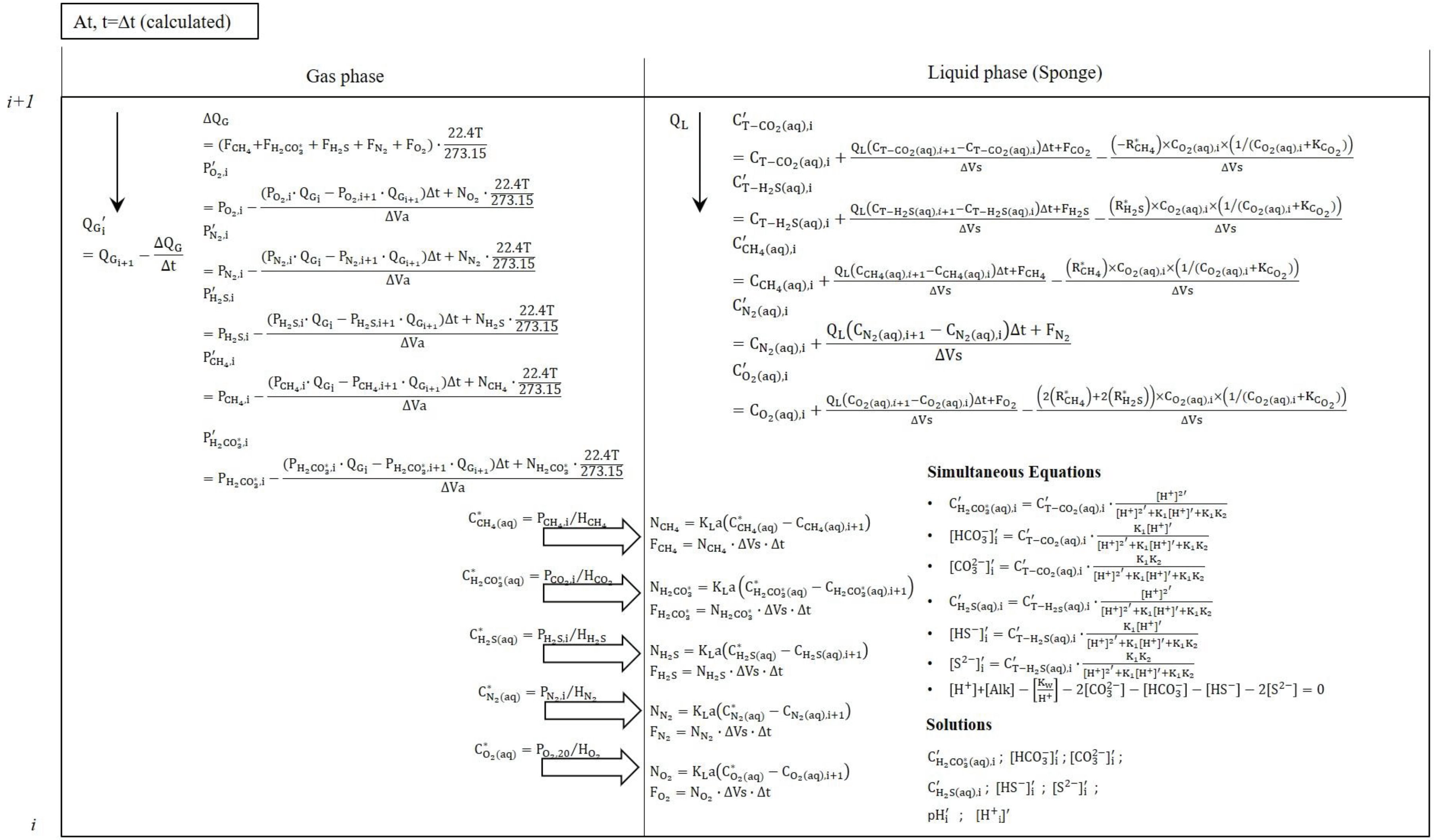

$$Q_{G_i}' = Q_{G_{i+1}} - \frac{\Delta Q_G}{\Delta t}$$

$$\Delta Q_G = (F_{CH_4} + F_{H_2CO_3^*} + F_{H_2S} + F_{N_2} + F_{O_2}) \cdot \frac{22.4T}{273.15}$$

$$P_{O_2,i}' = P_{O_2,i} - \frac{(P_{O_2,i} \cdot Q_{G_i} - P_{O_2,i+1} \cdot Q_{G_{i+1}})\Delta t + N_{O_2} \cdot \frac{22.4T}{273.15}}{\Delta Va}$$

$$P_{N_2,i}' = P_{N_2,i} - \frac{(P_{N_2,i} \cdot Q_{G_i} - P_{N_2,i+1} \cdot Q_{G_{i+1}})\Delta t + N_{N_2} \cdot \frac{22.4T}{273.15}}{\Delta Va}$$

$$P_{H_2S,i}' = P_{H_2S,i} - \frac{(P_{H_2S,i} \cdot Q_{G_i} - P_{H_2S,i+1} \cdot Q_{G_{i+1}})\Delta t + N_{H_2S} \cdot \frac{22.4T}{273.15}}{\Delta Va}$$

$$P_{CH_4,i}' = P_{CH_4,i} - \frac{(P_{CH_4,i} \cdot Q_{G_i} - P_{CH_4,i+1} \cdot Q_{G_{i+1}})\Delta t + N_{CH_4} \cdot \frac{22.4T}{273.15}}{\Delta Va}$$

$$P_{H_2CO_3^*,i}' = P_{H_2CO_3^*,i} - \frac{(P_{H_2CO_3^*,i} \cdot Q_{G_i} - P_{H_2CO_3^*,i+1} \cdot Q_{G_{i+1}})\Delta t + N_{H_2CO_3^*} \cdot \frac{22.4T}{273.15}}{\Delta Va}$$

$$C_{T-CO_2(aq),i}' = C_{T-CO_2(aq),i} + \frac{Q_L(C_{T-CO_2(aq),i+1} - C_{T-CO_2(aq),i})\Delta t + F_{CO_2}}{\Delta Vs} - \frac{(-R_{CH_4}^*) \times C_{O_2(aq),i} \times (1/(C_{O_2(aq),i} + K_{C_{O_2}}))}{\Delta Vs}$$

$$C_{T-H_2S(aq),i}' = C_{T-H_2S(aq),i} + \frac{Q_L(C_{T-H_2S(aq),i+1} - C_{T-H_2S(aq),i})\Delta t + F_{H_2S}}{\Delta Vs} - \frac{(R_{H_2S}^*) \times C_{O_2(aq),i} \times (1/(C_{O_2(aq),i} + K_{C_{O_2}}))}{\Delta Vs}$$

$$C_{CH_4(aq),i}' = C_{CH_4(aq),i} + \frac{Q_L(C_{CH_4(aq),i+1} - C_{CH_4(aq),i})\Delta t + F_{CH_4}}{\Delta Vs} - \frac{(R_{CH_4}^*) \times C_{O_2(aq),i} \times (1/(C_{O_2(aq),i} + K_{C_{O_2}}))}{\Delta Vs}$$

$$C_{N_2(aq),i}' = C_{N_2(aq),i} + \frac{Q_L(C_{N_2(aq),i+1} - C_{N_2(aq),i})\Delta t + F_{N_2}}{\Delta Vs}$$

$$C_{O_2(aq),i}' = C_{O_2(aq),i} + \frac{Q_L(C_{O_2(aq),i+1} - C_{O_2(aq),i})\Delta t + F_{O_2}}{\Delta Vs} - \frac{(2(R_{CH_4}^*) + 2(R_{H_2S}^*)) \times C_{O_2(aq),i} \times (1/(C_{O_2(aq),i} + K_{C_{O_2}}))}{\Delta Vs}$$

$$C_{CH_4(aq)}^* = P_{CH_4,i}/H_{CH_4}$$

$$N_{CH_4} = K_La(C_{CH_4(aq)}^* - C_{CH_4(aq),i+1})$$
$$F_{CH_4} = N_{CH_4} \cdot \Delta Vs \cdot \Delta t$$

$$C_{H_2CO_3^*(aq)}^* = P_{CO_2,i}/H_{CO_2}$$

$$N_{H_2CO_3^*} = K_La(C_{H_2CO_3^*(aq)}^* - C_{H_2CO_3^*(aq),i+1})$$
$$F_{H_2CO_3^*} = N_{H_2CO_3^*} \cdot \Delta Vs \cdot \Delta t$$

$$C_{H_2S(aq)}^* = P_{H_2S,i}/H_{H_2S}$$

$$N_{H_2S} = K_La(C_{H_2S(aq)}^* - C_{H_2S(aq),i+1})$$
$$F_{H_2S} = N_{H_2S} \cdot \Delta Vs \cdot \Delta t$$

$$C_{N_2(aq)}^* = P_{N_2,i}/H_{N_2}$$

$$N_{N_2} = K_La(C_{N_2(aq)}^* - C_{N_2(aq),i+1})$$
$$F_{N_2} = N_{N_2} \cdot \Delta Vs \cdot \Delta t$$

$$C_{O_2(aq)}^* = P_{O_2,20}/H_{O_2}$$

$$N_{O_2} = K_La(C_{O_2(aq)}^* - C_{O_2(aq),i+1})$$
$$F_{O_2} = N_{O_2} \cdot \Delta Vs \cdot \Delta t$$

Simultaneous Equations

- $C_{H_2CO_3^*(aq),i}' = C_{T-CO_2(aq),i}' \cdot \frac{[H^+]^{2'}}{[H^+]^{2'} + K_1[H^+]' + K_1K_2}$
- $[HCO_3^-]_i' = C_{T-CO_2(aq),i}' \cdot \frac{K_1[H^+]'}{[H^+]^{2'} + K_1[H^+]' + K_1K_2}$
- $[CO_3^{2-}]_i' = C_{T-CO_2(aq),i}' \cdot \frac{K_1K_2}{[H^+]^{2'} + K_1[H^+]' + K_1K_2}$
- $C_{H_2S(aq),i}' = C_{T-H_2S(aq),i}' \cdot \frac{[H^+]^{2'}}{[H^+]^{2'} + K_1[H^+]' + K_1K_2}$
- $[HS^-]_i' = C_{T-H_2S(aq),i}' \cdot \frac{K_1[H^+]'}{[H^+]^{2'} + K_1[H^+]' + K_1K_2}$
- $[S^{2-}]_i' = C_{T-H_2S(aq),i}' \cdot \frac{K_1K_2}{[H^+]^{2'} + K_1[H^+]' + K_1K_2}$
- $[H^+] + [Alk] - \left[\frac{K_w}{H^+}\right] - 2[CO_3^{2-}] - [HCO_3^-] - [HS^-] - 2[S^{2-}] = 0$

Solutions

$C_{H_2CO_3^*(aq),i}'$; $[HCO_3^-]_i'$; $[CO_3^{2-}]_i'$;

$C_{H_2S(aq),i}'$; $[HS^-]_i'$; $[S^{2-}]_i'$;

pH_i' ; $[H^+{}_i]'$

Figure 3.5: Schematic of differential element of an absorption and biodegradation process at t=Δt and position i of upper side.

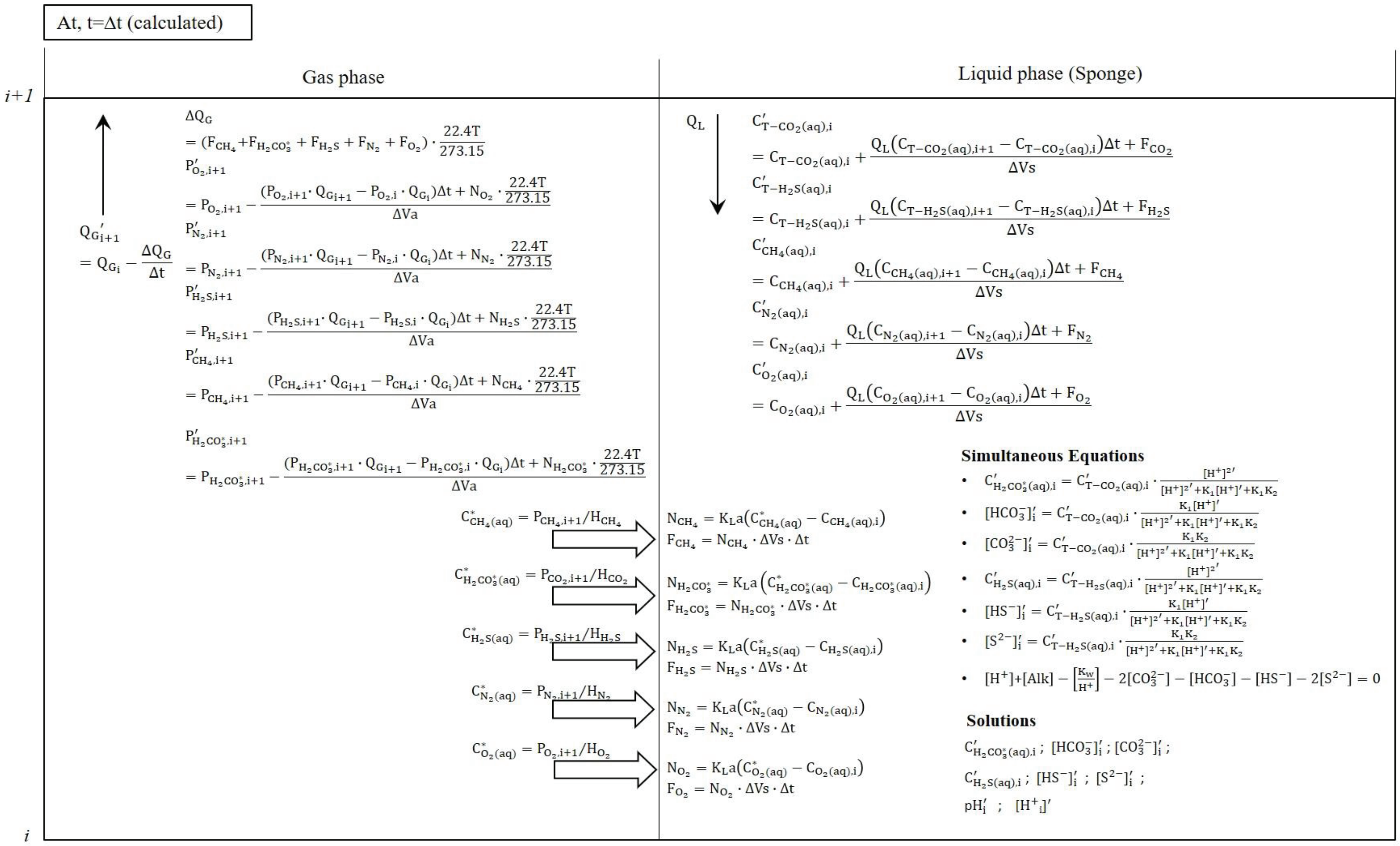

$$\Delta Q_G = (F_{CH_4} + F_{H_2CO_3^*} + F_{H_2S} + F_{N_2} + F_{O_2}) \cdot \frac{22.4T}{273.15}$$

$$Q'_{G_{i+1}} = Q_{G_i} - \frac{\Delta Q_G}{\Delta t}$$

$$P'_{O_2,i+1} = P_{O_2,i+1} - \frac{(P_{O_2,i+1} \cdot Q_{G_{i+1}} - P_{O_2,i} \cdot Q_{G_i})\Delta t + N_{O_2} \cdot \frac{22.4T}{273.15}}{\Delta Va}$$

$$P'_{N_2,i+1} = P_{N_2,i+1} - \frac{(P_{N_2,i+1} \cdot Q_{G_{i+1}} - P_{N_2,i} \cdot Q_{G_i})\Delta t + N_{N_2} \cdot \frac{22.4T}{273.15}}{\Delta Va}$$

$$P'_{H_2S,i+1} = P_{H_2S,i+1} - \frac{(P_{H_2S,i+1} \cdot Q_{G_{i+1}} - P_{H_2S,i} \cdot Q_{G_i})\Delta t + N_{H_2S} \cdot \frac{22.4T}{273.15}}{\Delta Va}$$

$$P'_{CH_4,i+1} = P_{CH_4,i+1} - \frac{(P_{CH_4,i+1} \cdot Q_{G_{i+1}} - P_{CH_4,i} \cdot Q_{G_i})\Delta t + N_{CH_4} \cdot \frac{22.4T}{273.15}}{\Delta Va}$$

$$P'_{H_2CO_3^*,i+1} = P_{H_2CO_3^*,i+1} - \frac{(P_{H_2CO_3^*,i+1} \cdot Q_{G_{i+1}} - P_{H_2CO_3^*,i} \cdot Q_{G_i})\Delta t + N_{H_2CO_3^*} \cdot \frac{22.4T}{273.15}}{\Delta Va}$$

$$C'_{T-CO_2(aq),i} = C_{T-CO_2(aq),i} + \frac{Q_L(C_{T-CO_2(aq),i+1} - C_{T-CO_2(aq),i})\Delta t + F_{CO_2}}{\Delta Vs}$$

$$C'_{T-H_2S(aq),i} = C_{T-H_2S(aq),i} + \frac{Q_L(C_{T-H_2S(aq),i+1} - C_{T-H_2S(aq),i})\Delta t + F_{H_2S}}{\Delta Vs}$$

$$C'_{CH_4(aq),i} = C_{CH_4(aq),i} + \frac{Q_L(C_{CH_4(aq),i+1} - C_{CH_4(aq),i})\Delta t + F_{CH_4}}{\Delta Vs}$$

$$C'_{N_2(aq),i} = C_{N_2(aq),i} + \frac{Q_L(C_{N_2(aq),i+1} - C_{N_2(aq),i})\Delta t + F_{N_2}}{\Delta Vs}$$

$$C'_{O_2(aq),i} = C_{O_2(aq),i} + \frac{Q_L(C_{O_2(aq),i+1} - C_{O_2(aq),i})\Delta t + F_{O_2}}{\Delta Vs}$$

$$C^*_{CH_4(aq)} = P_{CH_4,i+1}/H_{CH_4}$$

$$N_{CH_4} = K_La(C^*_{CH_4(aq)} - C_{CH_4(aq),i})$$
$$F_{CH_4} = N_{CH_4} \cdot \Delta Vs \cdot \Delta t$$

$$C^*_{H_2CO_3^*(aq)} = P_{CO_2,i+1}/H_{CO_2}$$

$$N_{H_2CO_3^*} = K_La\left(C^*_{H_2CO_3^*(aq)} - C_{H_2CO_3^*(aq),i}\right)$$
$$F_{H_2CO_3^*} = N_{H_2CO_3^*} \cdot \Delta Vs \cdot \Delta t$$

$$C^*_{H_2S(aq)} = P_{H_2S,i+1}/H_{H_2S}$$

$$N_{H_2S} = K_La(C^*_{H_2S(aq)} - C_{H_2S(aq),i})$$
$$F_{H_2S} = N_{H_2S} \cdot \Delta Vs \cdot \Delta t$$

$$C^*_{N_2(aq)} = P_{N_2,i+1}/H_{N_2}$$

$$N_{N_2} = K_La(C^*_{N_2(aq)} - C_{N_2(aq),i})$$
$$F_{N_2} = N_{N_2} \cdot \Delta Vs \cdot \Delta t$$

$$C^*_{O_2(aq)} = P_{O_2,i+1}/H_{O_2}$$

$$N_{O_2} = K_La(C^*_{O_2(aq)} - C_{O_2(aq),i})$$
$$F_{O_2} = N_{O_2} \cdot \Delta Vs \cdot \Delta t$$

Simultaneous Equations

- $C'_{H_2CO_3^*(aq),i} = C'_{T-CO_2(aq),i} \cdot \frac{[H^+]^{2'}}{[H^+]^{2'} + K_1[H^+]' + K_1K_2}$
- $[HCO_3^-]'_i = C'_{T-CO_2(aq),i} \cdot \frac{K_1[H^+]'}{[H^+]^{2'} + K_1[H^+]' + K_1K_2}$
- $[CO_3^{2-}]'_i = C'_{T-CO_2(aq),i} \cdot \frac{K_1K_2}{[H^+]^{2'} + K_1[H^+]' + K_1K_2}$
- $C'_{H_2S(aq),i} = C'_{T-H_2S(aq),i} \cdot \frac{[H^+]^{2'}}{[H^+]^{2'} + K_1[H^+]' + K_1K_2}$
- $[HS^-]'_i = C'_{T-H_2S(aq),i} \cdot \frac{K_1[H^+]'}{[H^+]^{2'} + K_1[H^+]' + K_1K_2}$
- $[S^{2-}]'_i = C'_{T-H_2S(aq),i} \cdot \frac{K_1K_2}{[H^+]^{2'} + K_1[H^+]' + K_1K_2}$
- $[H^+] + [Alk] - \left[\frac{K_w}{H^+}\right] - 2[CO_3^{2-}] - [HCO_3^-] - [HS^-] - 2[S^{2-}] = 0$

Solutions

$C'_{H_2CO_3^*(aq),i}$; $[HCO_3^-]'_i$; $[CO_3^{2-}]'_i$;
$C'_{H_2S(aq),i}$; $[HS^-]'_i$; $[S^{2-}]'_i$;
pH'_i ; $[H^+_i]'$

Figure 3.6: Schematic of differential element of physical stripping process at t=Δt and position i of bottom side.

References:

Foust, A.S., Wenzel, L.A., Clump, C.W., Maus, L., Anderson, L. 1960. Principle of Unit Operations, John Wiley &Sons, New York.

Frank, J.M., 1986. The thermodynamics and kinetics of the hydrogen sulfide system in natural waters. Marine Chemistry 18, 121-147.

Robinson, J.A., Tiedje, J.M., 1983. Nonlinear estimation of Monod growth kinetic parameters from a single substrate depletion curve. Appl. Environ. Microbiol. 45, 1453.

Stumm, W., Morgan, J.J. 1981. An introduction emphasizing chemical equilibrium in natural waters. 2nd edition, John Wiley & Sons, New York, p. 127.

Tippayawong, N., Thanompongchart, P., 2010. Biogas quality upgrade by simultaneous removal of CO_2 and H_2S in a packed column reactor. Energy 35, 4531-4535.

CHAPTER 4

BIOGAS PURIFICATION PERFORMANCE OF NEW WATER SCRUBBER PACKED WITH SPONGE CARRIERS

TABLE OF CONTENTS

4.1 Introduction

Biogas can be biologically produced in anaerobic digestion processes for treating wastewater or solid organic waste such as animal manure, sewage sludge, agricultural residue, and food scraps (Bauer et al., 2013). Generally, biogas is composed of 50−75% (CH_4), 25−50% (CO_2), 0−10% (N_2), 0−3% (H_2S), 0−1% (H_2), and traces of other gases (Goswami et al., 2016). The main component, CH_4, is very valuable as a clean and renewable energy source, which renders biogas a potential candidate to replace fossil fuels.

Biogas is similar to natural gas in most physical and chemical properties. The main differences between these two gases are the CH_4 content and their applications. Natural gas normally consists of 75−98% CH_4 and has higher burning energy; for instance, a lower heating value of 38.6 MJ Nm^{-3} is generated from 94% CH_4 content (Agarwal et al., 2014). In contrast, a lower heating value of biogas in the range of approximately 15−30 MJ Nm^{-3} results from much lower CH_4 content (Tippayawong and Thanompongchart, 2010), and this value is far less than that of natural gas owing to the CO_2 content. The large amount of noncombustible CO_2 gas present in biogas reduces not only its calorific value, but also the flame velocity and flammability limit (Wylock and Budzianowski, 2017). Therefore, biogas application is restricted to vehicle engines and city gas. In addition, if biogas is used as a transport vehicle fuel, CO_2 gas occupies additional space in the storage cylinder tanks, generating additional energy consumption for biogas compression and indirect increase in operational cost (Shah et al., 2016).

Apart from the issue of CO_2, even the small amount of H_2S present in biogas is problematic as H_2S is one of the most harmful environmental pollutants and causes severe corrosion of equipment such as pipes, engines, pumps, compressors, gas storage tanks, and valves (Ryckebosch et al., 2011). Moreover, sulfur dioxide (SO_2) is formed by H_2S combustion, and this gas is considered more dangerous than H_2S. The product of the reaction between SO_2 and water vapor in the atmosphere induces smog formation and acid rain problems (Wichitpan et al., 2012).

Various countries have different standards and recommendations for upgrading biogas to vehicle fuel. For example, the Swiss regulations for biogas use in vehicle engines or as city gas state that the standard CO_2 and H_2S concentrations must be lower than 6% and 5 mg m^{-3}, respectively (Margareta et al., 2006). Nagaoka City, Japan, has purified biogas produced by the municipal sewage treatment plant for use as city gas, satisfying the quality requirements that the heat value must be more than 35.56 MJ Nm^{-3} (equivalent to

90% CH_4 content) and the CO_2 and H_2S concentrations must be less than 4% and 2 ppm, respectively (Tatsuo and Shojiro, 2012). Thus, it is essential to remove CO_2 and H_2S from biogas to attain a feasible energy source.

There are several methods of biogas purification: physicochemical absorption, pressure swing adsorption (PSA), membrane separation, cryogenic separation, and/or use of biological technologies (Paolo et al., 2017). As these purification methods have individual characteristics, the appropriate technology should be selected by considering the purification efficiency, operational conditions, investment, and maintenance cost (Olumide et al., 2017). PSA and wet scrubbing with water (water scrubbing) are popular. The PSA process consists of several steps to separate CH_4 and CO_2 from biogas under pressure according to the molecular characteristics of the gases and their affinity to the adsorbent material; however, this process is complex compared to water scrubbing (Rafael et al., 2016). Indeed, the most difficult aspect of PSA operation is controlling the high temperature and pressure, which has limited the application of this method on a wider scale (Shang et al., 2012).

In contrast, water scrubbing at high pressure is the most commercially feasible technology for biogas purification owing to its simplicity and performance reliability (Karim and Fatima, 2018). However, according to Cozma et al. (2013), the disadvantage of this technology is its higher electricity cost (0.34 kWh m^{-3} raw biogas). Therefore, water scrubbing performed at near atmospheric pressure has been proposed, which requires a lower specific electricity of 0.24 kWh m^{-3} for raw biogas (Budzianowski et al., 2017). However, water scrubbing at atmospheric pressure is limited to very small installations and is not usually offered by commercial vendors because a higher liquid-to-biogas flow ratio is required (Budzianowski et al., 2017). Moreover, high purification performance is difficult to achieve. Geng et al. (2015) and Walozi et al. (2016) reported that they achieved maximum purified CH_4 concentrations of only 77 and 80%, respectively under atmospheric pressure conditions using the water scrubbing method.

Packing carriers are usually installed in water scrubbers to enhance the mass transfer efficiency between the gas and liquid phases (Tan et al., 2012). The most commonly used packing carriers are pall ring, intallox metal, berl saddles, tellerette, tri-packs and rasching ring (Yasin et al., 2018). The packing carrier configuration is selected considering the porosity, specific surface area, and water holding capacity, which are directly related to the mass transfer efficiency (Dorado et al., 2009). However, even if packing carriers with high efficiency were used, improved purification performance under low-pressure conditions cannot be expected, as discussed above. General packing carriers provide minimal water retention, yielding a very short actual hydraulic retention time (HRT), which in turn results in a short contact time for water and biogas and a short absorption time. Therefore, the present authors surmised that high purification performance would be possible for a water scrubber even at low pressures if the HRT was increased. Sponge has very high water retention characteristic. Thus, high biogas purification performance was predicted for a water scrubber with a sponge material as the packing carrier owing to the expected increase in the HRT.

In this chapter, a new water scrubber packed with sponge carriers is proposed. To evaluate the performance of the proposed water scrubber, biogas purification experiments were conducted under atmospheric conditions. In addition, a mathematical model to simulate the purification phenomenon was constructed, and simulation experiments were conducted to determine the water scrubber operational conditions that yield highly purified gas satisfying the quality requirements of city gas ($CH_4 \geq 90\%$, $CO_2 < 4\%$, $H_2S < 2$ ppm in Nagaoka).

4.2 Material and methods

4.2.1 Experimental setup

A column with a height of 1.2 m and working volume of 2.3 L was used as a lab-scale water scrubber in this study. A string of 23 carriers, which were connected to each other in series, was hung in the column (**Figure 4.1**). Each carrier consisted of polyurethane sponge (volume: 18.5 cm^3) and a plastic frame (framed sponge). An artificial biogas made in a gas bag was provided to the scrubber from the lower end, at atmospheric pressure. The purified gas was collected from the top. The scrubbing water supplied from the top was down-flowed through and onto the sponges in contact with the biogas, and was discharged from the bottom, primarily with absorbed CO_2.

The artificial biogas was composed of CH_4 (60−67%), CO_2 (32−40%), and H_2S (0−3.0%). The scrubbing water was made by adding sodium bicarbonate ($NaHCO_3$) to tap water to set the alkalinity to approximately 0.411−0.769 meq L^{-1}. The scrubbing water pH was adjusted by adding hydrochloric acid (HCl).

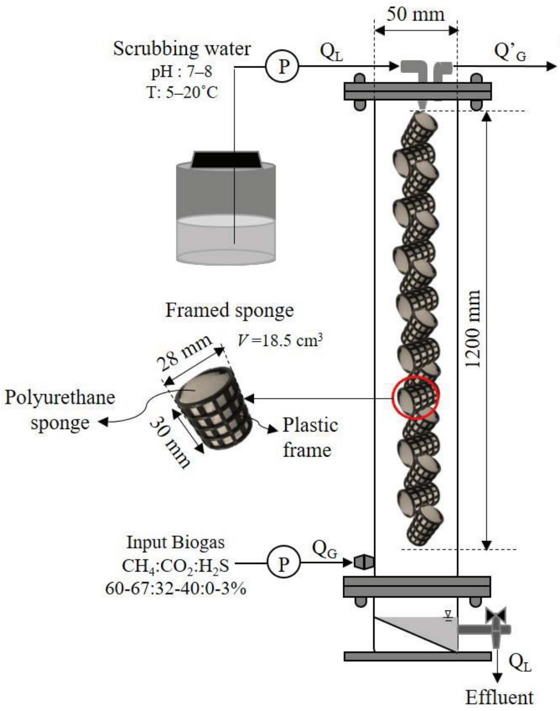

Figure 4.1: Schematic diagram of water scrubber packed with framed sponge

4.2.2 Operational conditions

Biogas purification experiments were conducted under various conditions for 16 runs (Runs 1 to 16, **Table 4.1**). For all runs, the ratio of the liquid flow rate Q_L $(\mathrm{L\,d^{-1}})$ to the biogas flow rate Q_G $(\mathrm{L\,d^{-1}})$, namely Q_L/Q_G, was varied as detailed in **Table 4.1**, and the effects were investigated. Runs 1 and 2 were conducted to investigate the effects of the pH at a constant Q_L of 21.2 ml min^{-1} (corresponding to 20 min HRT based on the sponge volume) and 20 °C. Runs 3 and 4 were conducted at 5 and 30 °C, respectively, to investigate the influence of temperature compared to Run 1. Runs 5 to 7 were conducted at three different HRTs of 5, 10, and 15 min, respectively. The H_2S removal performance was investigated in Runs 8 and 9 by changing the gases that make up the artificial biogas. To evaluate and verify the mass transfer coefficient (K_La) inherent in the used water scrubber, Runs 10 to 16 were separately conducted under various operational conditions (**Table 4.1**).

4.2.3 Sampling and analyses

The biogas purification performance should attain a steady state after several HRTs or gas retention times (GRTs) from the start of operation because the flow used in the scrubber is

Table 4.1: Experimental conditions.

Run	Input biogas (%) (CH_4:CO_2:H_2S:N_2)	Q_L (ml min^{-1})	*HRT (min)	pH	Temperature (˚C)	Q_L/Q_G	Objectives
1	60:40:0:0	21.2	20	8	20	0.5,1,1.5,2.5,3	Effect of pH
2		21.2	20	7	20	0.5,1,1.5,2.5,3	
3		21.2	20	8	5	0.5,1,1.5,2.5,3	Effect of temperature
4		21.2	20	8	30	0.5,1,1.5,2.5,3	
5		84.0	5	8	20	0.5,1,1.5	Effect of HRT
6		42.0	10	8	20	0.5,1,1.5	
7		28.0	15	8	20	0.5,1,1.5	
8	60:39.5:0.5:0	21.2	20	8	20	1,3	Effect of H_2S
9	60:37.5:2.5:0	21.2	20	8	20	1,3	
10	67:32:0:1	21.2	20	8	20	0.5,1,1.5	K_La evaluation
11		28.0	15	8	20	0.5,1,1.5	
12		42.0	10	8	20	0.5,1,1.5	
13		84.0	5	8	20	0.5,1,1.5	
14	67:33:0:0	21.2	20	8	10	0.3,0.5,0.7,0.9,1,1.1,1.3,1.5	K_La verification
15	60:39.5:0.5:0	21.2	20	8	20	1,3	
16	60:37:3:0	21.2	20	8	10	1,3	

*HRT is based on sponge volume.

almost a plug flow. Therefore, the effluent gas and water were sampled and analyzed at 6, 8 and 24 h after adjustment to achieve each operational mode listed in **Table 4.1**. The study confirmed that the performance attained a steady state by 24 h as expected. The purification gas was collected into a gasbag (Smart Bag PA, GL SCIENCE/CEK 3008-97720) and the CH_4, CO_2, O_2, and N_2 concentrations were measured using a gas chromatograph equipped with a thermal conductivity detector (GC-TCD, Shimadzu GC-8A). Kitagawa detector tubes (Tube Nos. 120SM, 120SB, and 120SH) were used to measure the H_2S gas concentration. The measurements were conducted in triplicate. Some of the raw measurement data are shown in the supplementary material section. The effluent pH was measured.

4.3 Mathematical model concept

In this study, a mathematical model was constructed to describe the gasification and absorption phenomena in the water scrubber and simulate the biogas purification performance. The CH_4 and CO_2 in the biogas are absorbed into the scrubbing water of the liquid phase as dissolved gas, whereas dissolved gases in the scrubbing water such as N_2 and O_2 are gasified into the gas phase and mixed with the purified gas. Each mass transfer at the liquid–gas interface is governed by Fick's law; however, the transfer phenomenon is very complex. Therefore, physical model was developed as discussed in Chapter 3. The biogas concentration profiles are shown in **Figure 4.2** as a sample of simulation result.

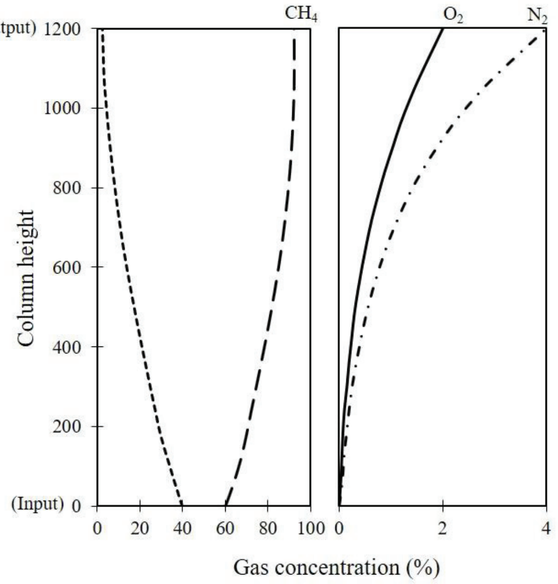

Operational conditions:
pH =8
T=20˚C
$Q_L/QG = 2$
HRT = 20 min
Input CO_2:CH_4:H_2S (%) = 40:60:0

Figure 4.2: Simulated biogas purification performance according to column height for specific operational conditions.

4.4 Results

4.4.1 Purification performance

Before conducting the purification experiment, the exact amount of biogas that can be treated by a scrubbing column containing sponge carriers with capacities of 0.42 L, and the required amount of scrubbing water to obtain purified gas of 90% CH_4 were still unknown. Therefore, at the beginning of the experiment (Run 1), scrubbing water of pH 8 was supplied randomly at Q_L of 21.2 ml min^{-1} (corresponding to water loading rate R_L of 332 L m^{-3} h^{-1}, based on the sponge volume) at approximately 20 °C. Artificial biogas composed of 60% CH_4 and 40% CO_2 was first fed at Q_G of 42.3 ml min^{-1} (corresponding to biogas loading rate R_G of 166 L m^{-3} h^{-1}, based on the sponge volume). Under this operational condition, which corresponds to Q_L/Q_G of 0.5 (= 21.2/42.3), 75.2% CH_4 was observed in the purified gas. Unfortunately, the target CH_4 concentration was not achieved (**Figure 4.3a**). Then, we gradually reduced Q_G. Hence, the purified CH_4 content was increased to 85.1 and 91.3% at Q_G of 21.2 and 14.1 ml min^{-1}, respectively (corresponding to Q_L/Q_G of 1.0 and 1.5, respectively). However, the purified CH_4 concentration decreased slightly to 90.5% at Q_L/Q_G of 3.0, suggesting that a much higher Q_L/Q_G ratio slightly degrades the purification performance. Note that this is the first time biogas of 60% CH_4 was concentrated to ≥90% (v/v) using water scrubbing technology under normal pressure conditions. In Run 2, water of pH 7 was supplied under the same conditions as in Run 1 (except for the pH difference). Surprisingly, the respective CH_4 concentrations in the purified gas were very close to those obtained in Run 1. Thus, almost identical purification performance was observed even when water of different pH values was used (**Figure 4.3a**). Therefore, it was found that the Q_L/Q_G ratio is one of the crucial factors that affect biogas purification performance compared to the scrubbing water pH value.

To investigate the effect of temperature on biogas purification, Runs 3 and 4 were conducted at 5 and 30 °C respectively, with the operational conditions being the same as in Run 1 (except for the temperature changes). The tendency for the CH_4 concentration of the purified gas to increase with increased Q_L/Q_G was similar to that at 20 °C for Run 1 (**Figure 4.3b**). However, the effluent CH_4 concentrations differed significantly. A CH_4 concentration ≥90% (v/v) was obtained at a lower Q_L/Q_G of 1.0 in Run 3, compared to the result for Run 1. This difference in the purification performance indicates that the purification water Q_L required to obtain a highly purified gas is strongly dependent on temperature.

In Runs 1 to 4 described above, the experiments were conducted at a constant Q_L of 21.2 ml min^{-1}, corresponding to 20-min HRT based on the sponge volume. The HRT should influence the purification performance. Then, Runs 5−7 were conducted at various HRTs of 5, 10, and 15 min, respectively. Interestingly, the results exhibited very little difference in CH_4 concentration for the respective HRTs at the same Q_L/Q_G (**Figure 4.3c**). Thus, the purification performance was found to be mainly governed by the Q_L/Q_G ratio at the same temperature regardless of the HRT. This means that it is only necessary for Q_L to be changed proportional to the change in the Q_G provided to the scrubbing column in order to obtain the same performance.

The effect of H_2S on the purification performance was investigated in Runs 8 and 9, where the provided artificial biogases with approximately 60% CH_4 contained H_2S at concentrations of 0.5 and 2.5%, respectively. This differed from Run 1, which had 0% H_2S. The CH_4 concentrations in the purified gas were almost the same regardless of the input H_2S concentration (**Figure 4.3d**). Thus, it was found that the H_2S in the biogas had a very small impact on the CH_4 concentration, even at a high H_2S concentration. On the other hand, the H_2S removal was influenced by the provided H_2S concentration. H_2S concentrations of 400 and 700 ppm in the purified gas were detected for the cases of 0.5 and 2.5% influent H_2S, respectively, under Q_L/Q_G of 1.0 (data not shown). However, as the Q_L/Q_G was increased to 2.5, H_2S was sufficiently removed within the scrubbing column. That is, the H_2S concentration in the purified gas was below the detection limit (ppm), even though a very high H_2S of 2.5% was provided (data not shown). Therefore, the described experimental results indicate that the artificial biogas was successfully purified using the water scrubbing column to produce ≥90% (v/v) CH_4 gas with simultaneous H_2S removal under operation with appropriate Q_L/Q_G ratios, even under atmospheric pressure conditions.

4.4.2 Mass transfer coefficient determination and validation

The experiment discussed above demonstrate that biogas purification is possible using the proposed water scrubber. However, the operational conditions suitable for attaining high performance were not revealed. It is difficult to determine appropriate water scrubber operational conditions from insufficient experimental data. Therefore, the study attempted to determine these conditions using a mathematical model to simulate the water scrubbing phenomenon. In the model, the only unknown parameter is the overall K_La, which is generally strongly dependent on the packing material configuration in the scrubbing column.

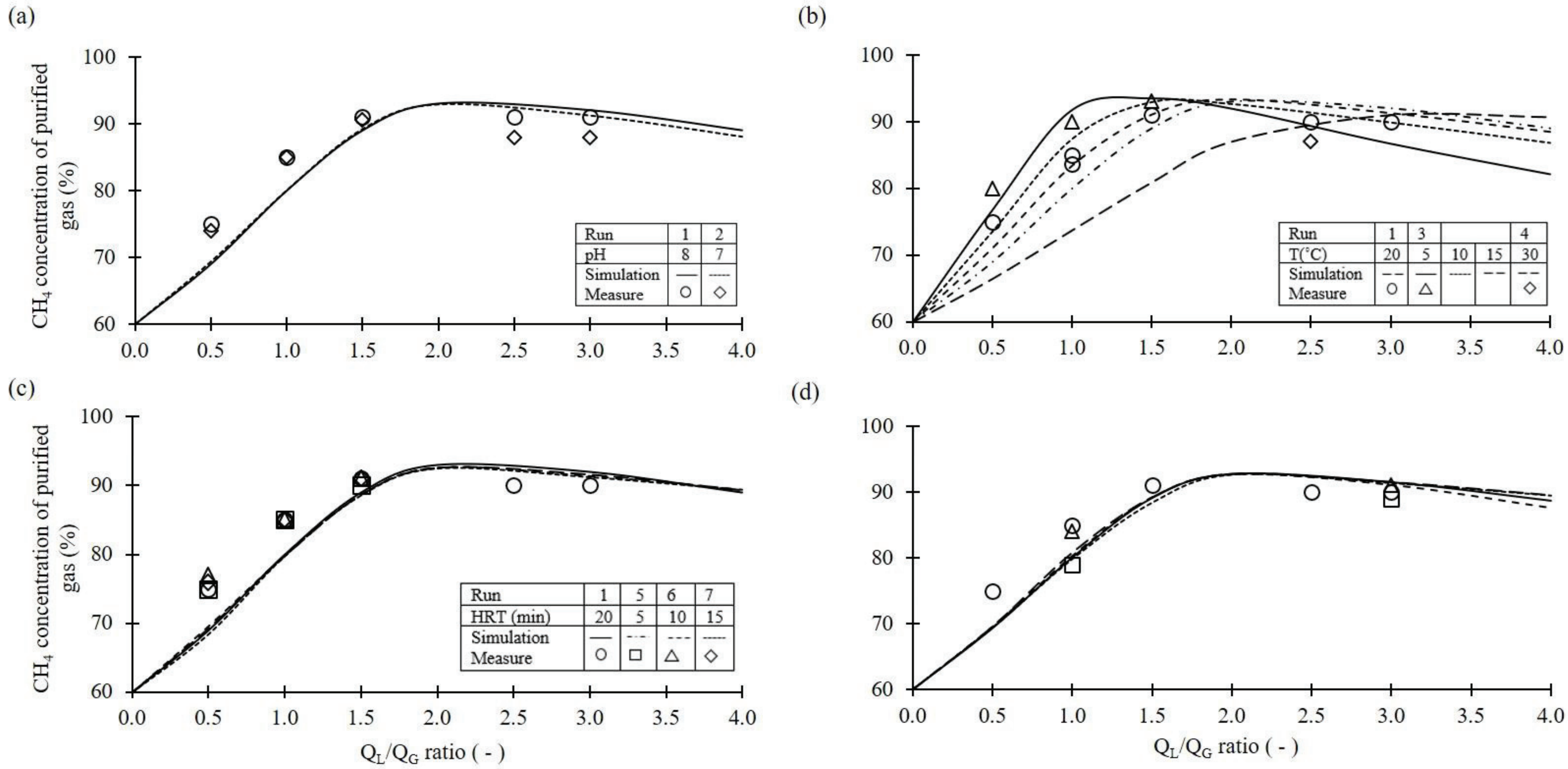

Figure 4.3: Measured (symbols) and simulated (lines) CH_4 concentrations of purified gas at different Q_L/Q_G ratios in Run 1-9. Effects of (a) pH (b) temperature (c) HRT and (d) input H_2S concentration.

Therefore, the first attempted was to estimate the $K_L a$ value. For an effective model, the observed performance should be coincident with the simulated results; here, it was found the $K_L a$ that yielded a simulated purified-gas CH_4 concentration corresponding to the measured concentration through trial and error. Runs 10−13 (**Table 4.1**) were specifically conducted to determine $K_L a$ for a wide range of liquid velocities (υ_L). As shown in **Figure 4.4**, the determined $K_L a$ values (based on the sponge volume, not the column volume) were inconstant, and tended to linearly increase with increasing υ_L. This observed trend was also reported in a previous study (Sherwood and Holloway, 1939). In addition, the evaluated $K_L a$ values of 8.5–34.2 L h^{-1} for the tested υ_L of 0.09–0.36 m h^{-1} were in the same order as those reported in previous studies, even though different packing materials such as Raschig rings (Evren et al., 1999), Hiflow rings (Biard et al., 2017), and polyurethane sponges (Almenglo et al., 2016; Dorado et al., 2009; Kim et al., 2008) were used. The determined $K_L a$ (h^{-1}) was expressed as a function of υ_L ($\mathrm{m\ h}^{-1}$) as follows:

$K_L a = 95.0 \upsilon_L$.

(4.1)

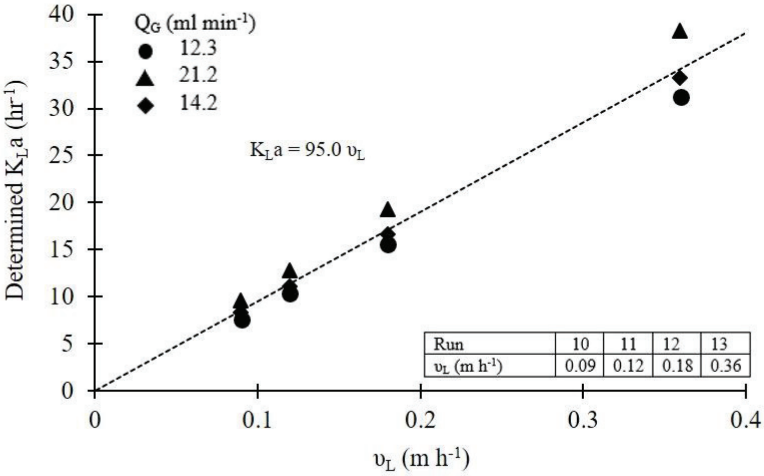

Figure 4.4: Determined $K_L a$ at different water-scrubber liquid velocities (υL).

To check the validity of the simulation performed based on the constructed model and using the determined $K_L a$, the simulated performance was compared with experimental data. **Figure 4.5** shows a graph of the simulated purified gas concentrations versus the measured results for Runs 14−16; the data were plotted almost on a straight line, which indicates that the simulated values were almost coincident with the measured values. Further, the simulations were in agreement with the measured results not only for CH_4, but also for the other gas compositions, namely, CO_2, O_2, N_2, and H_2S. In terms of the effect of the Q_L/Q_G ratio on biogas purification, the measured concentrations and effect were well simulated (**Figures 4.3a–d**). This good agreement between simulation and measurement indicates that the constructed model and determined K_La are acceptable for simulating the purification phenomena. Note that, although K_La should be dependent on the temperature, we neglected its influence in the simulation owing to its minimal value. Further, the simulated data agreed well with measurement data even under different temperature conditions (**Figure 4.5**).

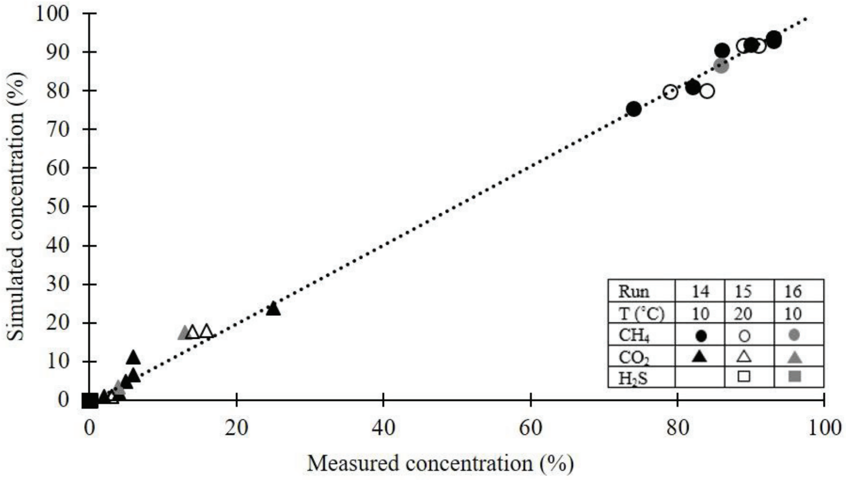

Figure 4.5: Relationship between measured and simulated concentrations using determined K_La of purified biogas.

4.4.3 Simulation performance

4.4.3.1 Appropriate Q_L/Q_G ratio

The biogas purification performance was significantly affected by temperature and the Q_L/Q_G ratio, as mentioned above. Temperature is an uncontrollable parameter; however, the Q_L/Q_G ratio can be controlled. Numerical simulations using the proposed mathematical model were used to assess the appropriate Q_L/Q_G. The range of predicted Q_L/Q_G ratios for achieving purified gas with ≥90% (v/v) CH_4 concentration at any temperature is shown in **Figure 4.6**, where the two lines correspond to 90% CH_4. The area bounded by the lines corresponding to the minimum and maximum Q_L/Q_G ratios (hatching) indicates $CH_4 \geq$ 90% (v/v). For example, if the scrubber is operated in the range of 1.0–3.0 Q_L/Q_G at 20 °C and HRT is 20 min, the CH_4 concentration of the purified gas exceeds 90%. Thus, the appropriate Q_L/Q_G ratio must be increased with increasing temperature to achieve the target purification (**Figure 4.6**).

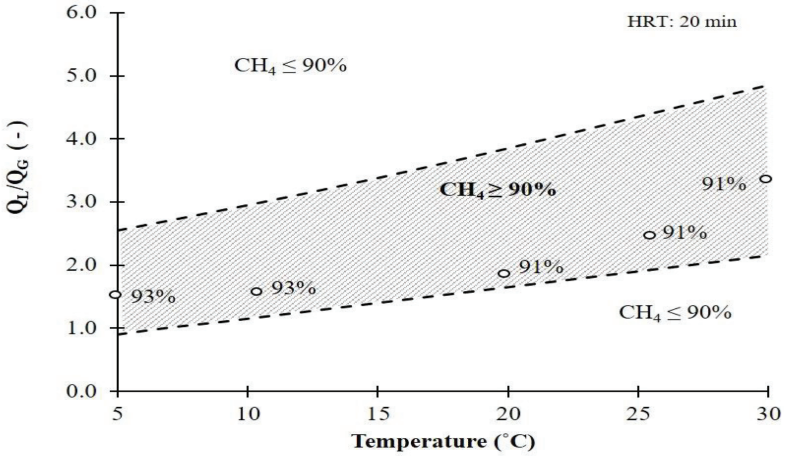

Figure 4.6: Temperature and Q_L/Q_G operational conditions to obtain purified gas with minimum 90% CH_4 content at 20 min HRT. The two lines correspond to 90% CH_4. The circles indicate the measured CH_4 concentrations.

The GRT was thought to strongly influence the biogas purification performance. However, simulations show that although Q_L/Q_G it is a crucial factor, the effect of GRT is not significant. That is, the Q_L/Q_G ratio required to achieve 90% CH_4 concentration is almost constant even if GRT is changed (**Figure 4.7**). Although the minimum Q_L/Q_G should increase with decreasing GRT, the necessary increment is minimal for a wide range of GRTs (10–60 min) at any temperature. Even if the scrubber is operated for a short GRT of 10 min, good performance can be achieved by increasing Q_L. Thus, the numerical simulations performed in this study were very useful for determining the appropriate operational conditions of the water scrubber.

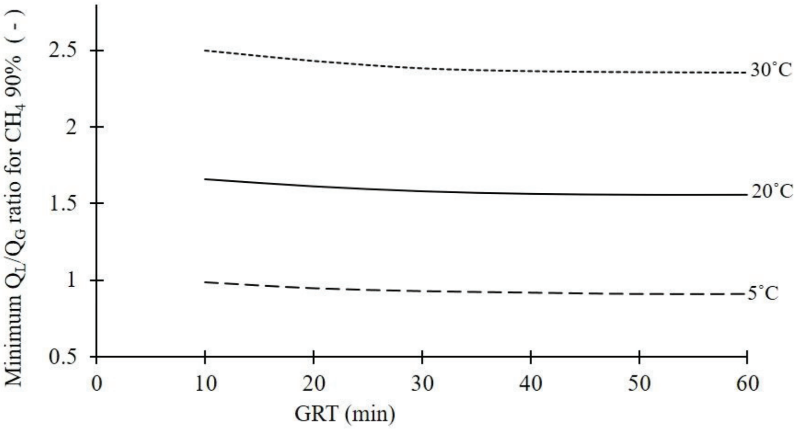

Figure 4.7: Relationship between GRT and minimum Q_L/Q_G ratio for CH_4 90% in simulation at different temperatures.

4.4.3.2 Column height

In this study, a column height of 1.2 m was used. However, I am not certain that this is the optimum height for biogas purification. Theoretically, a higher column yields higher purification performance. The effect of column height on performance was investigated through simulation using the mathematical model. As predicted, the simulation results show that the CH_4 concentration of the purified gas increased with increasing column height (**Figure 4.8**). Surprisingly, a very small column height of approximately 0.6 m is sufficient under operation with Q_L/Q_G of 2.5 and Q_G of 8.5 ml min^{-1} at 20 °C. In other words, the simulation indicates that the purification is not enhanced even if a higher column (>0.6 m) is used. For a lower Q_L/Q_G of 1.5, a higher column is required; however, a column height of only 1.3 m is sufficient and the CH_4 concentration of the purified gas increases (**Figure 4.8**).

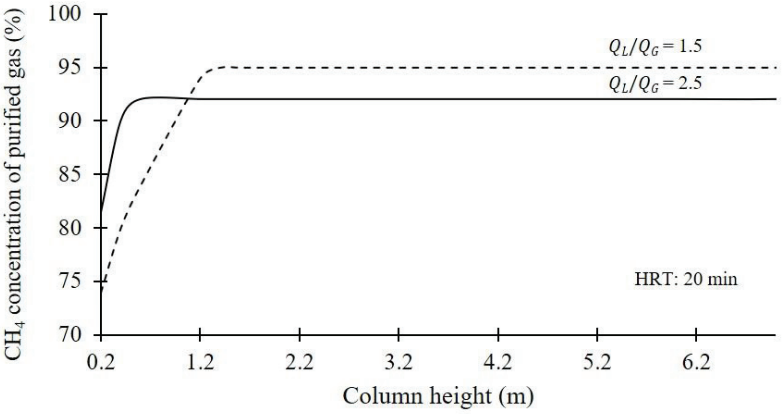

Figure 4.8: Effect of column height on biogas purification at 20˚C.

Fortunately, the column with a height of 1.2 m used in this study is appropriate for the purification experiment. There is a negative relation between the column height required to achieve 90% CH_4 and the implemented Q_L/Q_G ratio (**Figure 4.9**). This indicates that increasing the column height while decreasing Q_L/Q_G is necessary to obtain the same purification performance. In terms the influence of temperature, the column height should increase with increasing temperature for any Q_L/Q_G. In addition, **Figure 4.9** suggests that, under conditions with excessively low Q_L/Q_G, good purification is impossible even if a very tall column is used.

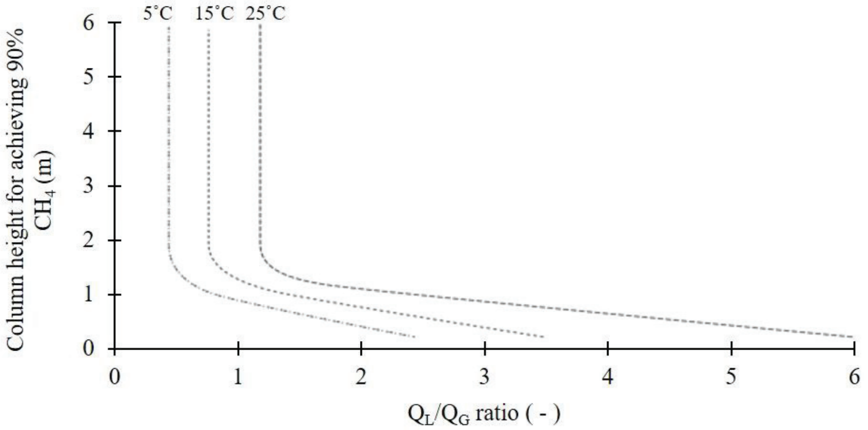

Figure 4.9: Column height required to achieve 90% CH_4 in purified gas at 20-min HRT.

4.5 Discussion

In this study, artificial biogas purification through water scrubbing was successfully performed using a column packed with original carriers, that is, sponge with plastic-ringed frames (framed sponge), even under atmospheric pressure. The purification performance was excellent compared with previous reports (Geng et al., 2015; Walozi et al., 2016), with purified gas with more than 90% CH_4 successfully produced, even for a very short column. The experiment differs completely from other studies involving packed carriers. The framed sponge has a water retention characteristic, which facilitates longer actual HRT. Note that the interphase mass transfer performance of the water scrubber should be affected by the actual HRT owing to its relation to the time in contact with the gas and liquid. That is, the interphase mass transfer performance is expected to increase with increased actual HRT. To investigate the manner in which the water retention of the framed sponge affects the purification performance, simulations were conducted under different water retention conditions, which can be established by virtually changing the sponge volume in the ringed frame in an actual experiment. For constant $K_L a$, the calculated CH_4 concentration of the purification gas clearly declined with decreased sponge volume (**Figure 4.10**). This means shortening of the actual HRT, suggesting that the carrier water retention is very important. For a ringed-frame with 50% sponge volume, only 85.8% CH_4 concentration was achieved at a Q_L/Q_G of 2. However, the CH_4 concentration was improved to 90% by increasing Q_L/Q_G under the operational conditions shown in **Figure 4.11**. However, improved purification performance cannot be expected for a framed sponge of 10% sponge volume, even if Q_L/Q_G is increased significantly (Fig. 10). Previously, Läntelä et al. (2012) reported that purified gas with 88.1% CH_4 was achieved in a purification experiment using a pall ring as packed carrier for $K_L a$ value almost identical to that used in the present study. However, in a study reported by William et al. (2014), good purification was not achieved even though a pall ring was used with a reactor height of less than 3 m. These packed carriers should have low water retention capability, yielding a brief period of time in contact with the gas and liquid because of the short actual HRT. If framed-sponge carriers were used in the experiments (Läntelä et al., 2012; William et al., 2014), excellent purification performance similar to my results could be expected under suitable operational conditions.

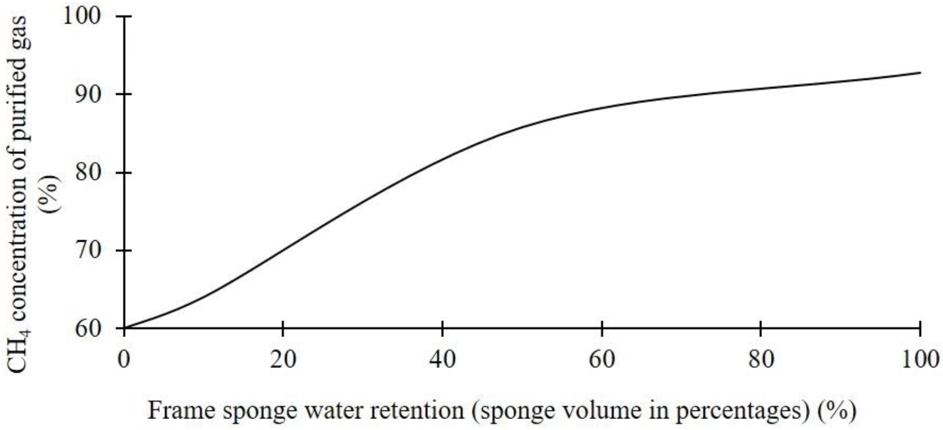

Figure 4.10: Effect of framed-sponge water retention (assumed sponge volume in percentage) on biogas purification at 20˚C and HRT 20 min.

Before conducting the experiment, t the scrubbing water pH is predicted to have some effect on the purification performance because the amount of dissolved CO_2 is dependent on the pH. However, both the experiment and simulation results indicate that the pH has minimal impact on the purification. The scrubbing water pH should decrease along with the down-flow in the scrubbing column through absorption of the CO_2 of the provided biogas. When all the CO_2 is absorbed, that is, for 100% CO_2 removal, the decrease in the pH should stop. However, no limitless pH drop occurred. As the dissolved CO_2 concentration achieved equilibrium with the provided biogas at the bottom of scrubber, the pH became constant. This corresponds to a minimum pH for the effluent, which depends on the alkalinity and biogas CO_2 concentration. Assuming 100% CO_2 removal efficiency, the pH in the effluent can be estimated based on the CO_2 balance. The pH calculation is described in the Chapter 3. For the operation at Q_L/Q_G ratio of 2, the pH in the effluent became 5.30 and 5.01 for influent pH values of 8.00 and 5.32, respectively, with 100% CO_2 removal. This simulation result indicates that, even if scrubbing water samples in a very wide pH range (e.g., spanning a range >5.32) are supplied, complete CO_2 removal is possible. When Q_L/Q_G is increased to 3, a wide applicable pH range (spanning >5.19) is attained. Thus, the pH has minimal impact on the purification performance because water has high CO_2 absorption capacity for a wide range of pH values. At a low Q_L/Q_G of 1, the effluent pH reaches a minimum value of 5.01 for any influent pH (<8), meaning that 100% CO_2 removal is not attained. Therefore, the Q_L/Q_G ratio is of notable significance in biogas purification without considering the scrubbing water pH.

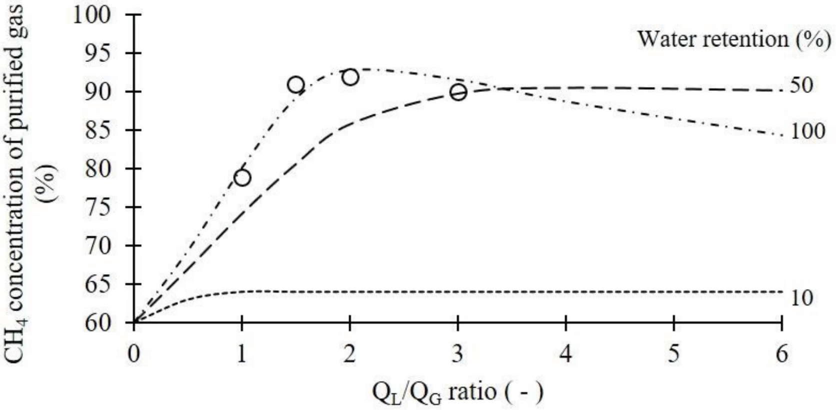

Figure 4.11: Effect of Q_L/Q_G ratio on CH_4 concentration of purified gas for different framed sponge water retentions (10, 50 and 100%) at 20˚C and HRT 20 min. The lines and circles correspond to simulation and experiment data, respectively.

As discussed above, it was confirmed that there is theoretical relationship between the Q_L/Q_G ratio and CO_2 gas removal. Previously, Rasi et al. (2008) also reported that a higher Q_L/Q_G yields greater CO_2 removal. In **Figure 4.12**, 100% CO_2 removal is theoretically attained for Q_L/Q_G ratios of 2 and 3 and scrubbing water of pH 8. This performance shows that purified gas with 100% CH_4 can be produced. However, different results were observed in experiment (**Figure 4.3a**). The gas purified at Q_L/Q_G of 2.5 did not consist of 100% CH_4; rather, 90.5% CH_4 was detected. Moreover, as Q_L/Q_G was increased to 3, the CH_4 concentration declined. Water contains 6–8 and 10–20 mg L^{-1} of dissolved O_2 and N_2 at normal temperatures and equilibrium conditions, respectively (Díaz and Breitburg, 2009). This dissolved O_2 and N_2 should be gasified in the scrubbing column, so that the purified gas does not contain O_2 and N_2. In fact, O_2 and N_2 were detected in our experiments; **Table 4.2** lists sample measured values for the purified gas obtained in Run 10.

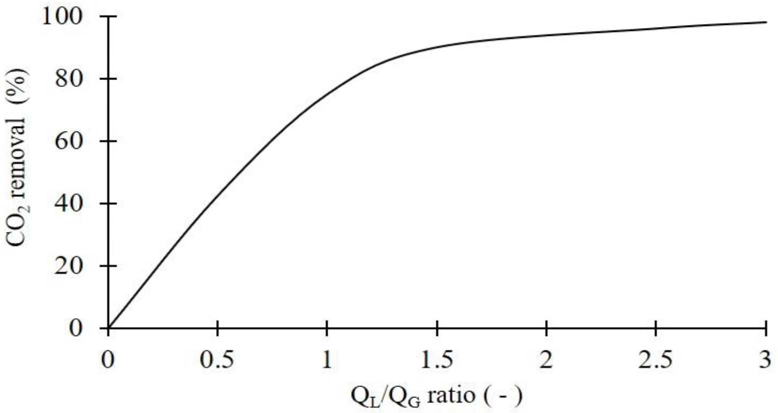

Figure 4.12: Effect of Q_L/Q_G ratio on CO_2 removal simulated for biogas with 40% CO_2 at 20 ˚C, pH 8 and 20 min HRT.

Table 4.2: Operational conditions and performance for experimental conditions of Run 10.

Input biogas (%) (CH_4:CO_2:H_2S:N_2)	pH_{in}	P (atm)	T (°C)	K_La (h^{-1})	Q_L/Q_G	Purified gas (%)				
						CH_4	CO_2	H_2S	N_2	O_2
67:32:0:1	8	1	20	8.5	0.5	75	22	0	2	1
					1	85	10	0	3	2
					1.5	91	4	0	3	2

A simulation was conducted under the conditions shown in **Figure 4.13** to elucidate the manner in which Q_L/Q_G affects the purified gas composition. As expected, the CO_2 concentration in the produced gas decreased steadily with increasing Q_L/Q_G, corresponding to a large amount of water supply. Eventually, no residual CO_2 was attained at Q_L/Q_G of approximately 3. In contrast, increased Q_L/Q_G induced increments in the O_2 and N_2 concentrations due to gasification of the dissolved gases.

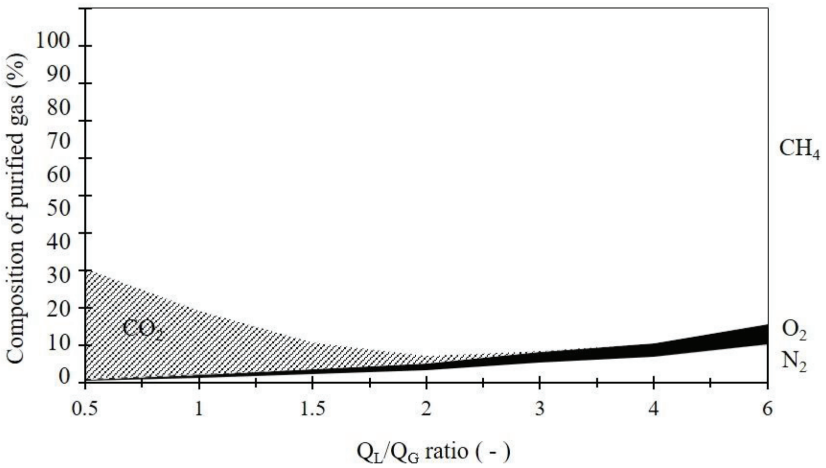

Figure 4.13: Composition of purified gas simulated for biogas for 60% CH_4 biogas operated at 20 ˚C, pH 8 and 20 min HRT.

Therefore, although the CH_4 concentration initially increases with increasing Q_L/Q_G, it subsequently decreases. It is impossible to produce a perfectly purified gas. However, the simulation revealed that there is an optimum Q_L/Q_G ratio for biogas purification using a water scrubber, which can be determined using the mathematical model proposed in this study.

4.6 Conclusion

The study experimentally demonstrated that a water scrubber can purify biogas to have a methane concentration exceeding 90% without imposing external pressure. The developed mathematical model and numerical simulations indicate that framed-sponge carriers are effective in biogas purification and essential for high performance because the use of a sponge with high water retention increases the HRT.

The Q_L/Q_G ratio was found to be the most crucial factor determining the purification performance. Excessively high Q_L/Q_G values deteriorate the performance because the dissolved nitrogen and oxygen in the scrubbing water are incorporated into the recovered purified gas, which decreases the methane concentration. Although the proposed water scrubber can be applied to a wide range of pH and temperature values, it should be operated at an appropriate Q_L/Q_G ratio depending on the temperature.

References

Agarwal, A.K., Pandey, A., Gupta, A.K., Aggarwal, S.K., Kushari, A., 2014. Novel combustion concepts for sustainable energy development. Springer India.

Almenglo, F., Bezerra, T., Lafuente, J., Gabriel, D., Ramírez, M., Cantero, D., 2016. Effect of gas-liquid flow pattern and microbial diversity analysis of a pilot-scale biotrickling filter for anaoxic biogas desulfurization. Chemosphere 157, 215-223.

Bauer, F., Hulteberg, C., Persson, T., Tamm D., 2013. Biogas upgrading: Review of commercial technologies. SGC Rapport 270 [Online]. Available: http://vav.griffel.net/filer/C_SGC2013-270.pdf.

Biard, P.F., Couvert, A., Renner, C., 2017. Intensification of volatile organic compound absorption in a compact wet scrubber at co-current flow. Chemosphere 173, 612-621.

Budzianowski, W.M., Wylock, C.E., Marciniak, P.A., 2017. Power requirements of biogas upgrading by water scrubbing and biomethane compression: Comparative analysis of various plant configurations. Energy Conversion and Management 141, 2-19.

Coughlin, R.W., 1969. Carbon as adsorbent and catalyst. Industrial & Engineering Chemistry Product Research and Development 8(1), 12-23.

Cozma, P., Ghinea, C., Mâmâligâ, I., Wukovits, W., Friedl, A., Gavrilescu, M., 2013. Environmental impact assessment of high pressure water scrubbing biogas upgrading technology. Clean-Soil Air Water 41(9), 917-927.

Díaz, R.J., Breitburg, D.L., 2009. The hypoxic environment. Hypoxia, Fish Physiology 27, 1-25.

Dorado, A.D., Rodríguez, G., Ribera, G., Bonsfills, A., Gabriel, D., Lafuente, J., Gamisans, X., 2009. Evaluation of mass transfer coefficients in biotrickling filters: Experimental determination and comparison to correlations. Chemical Engineering and Technology 32(12), 1941-1950.

Evren, V., Cağatay, T., Özdural, A.R., 1999. Carbon dioxide-air mixtures: Mass transfer in recycling packed-bed absorption columns operating under high liquid flow rates. Separation and Purification Technology 17, 89-96.

Frank, J.M., 1986. The thermodynamics and kinetics of the hydrogen sulfide system in natural waters. Marine Chemistry 18, 121-147.

Geng, H., Chen, Q., Zhao, G., 2015. The experiment study of biogas atomization upgrading with water scrubbing at atmospheric pressure. Proceedings of the International Conference on Industrial Technology and Management Science (ITMS), 34.

Goswami, R., Chattopadhyay, P., Shome, A., Banerjee, S.N., Chakraborty, A.K., Mathew, A.K., Chaudhury, S., 2016. An overview of physico-chemical mechanisms of biogas production by microbial communities: a step towards sustainable waste management. Biotech 6, 72-84.

Karim, G., Fatima, Z.B.F., 2018. Power to methane: a state of the art review. Renewable and Sustainable Energy Reviews 81, 433-446.

Kim, S., Deshusses, M.A., 2008. Determination of mass transfer coefficients for packing materials used in biofilters and biotrickling filters for air pollution control: 1. Experimental results. Chemical Engineering Science 63, 841-855.

Läntelä, J., Rasi, S., Lehtinen, J., Rintala, J., 2012. Landfill gas upgrading with pilot-scale water scrubber. Applied Energy 92, 307-314.

Margareta, P., Owe, J., Arthur W., 2006. Biogas upgrading to vehicle fuel standards and gas grid injection. IEA Bioenergy, December. [Online]. Available: http://task37.ieabioenergy.com/files/daten-redaktion/download/publi task37/upgrading_report_final.pdf.

Olumide, W.A., Yaqian, Z., Ange, N., Doan, P.M., Nathalie, L., 2017. A review of biogas utilisation, purification and upgrading technologies. Waste and Biomass Valorization 8, 267-283.

Paolo, R., Andrea, L., Pierluigi, L., 2017. Energy and economic analysis of a water scrubbing based biogas upgrading process for biomethane injection into the gas grid or use as transportation fuel. Renewable Energy 102, 417-432.

Rafael, M.S., Geovane, R.F., Hugo, R.P., Jailton, F.N., Ana, P.S.M., Antonio, E.B.T., Diana, C.S.A., Moises, B-N., 2017. Carbon dioxide capture by pressure swing adsorption. Energy Procedia 114, 2182-2192.

Rasi, S., Läntelä, J., Veijanen, A., Rintala, J., 2008. Landfill gas upgrading with countercurrent water wash. Waste Management 28, 1528-1534.

Ryckebosch, E., Drouillon, M., Vervaeren, H., 2011. Techniques for transformation of biogas to biomethane. Biomass Bioenergy 35(5), 1633-1645.

Shah, D.R., Nagarsheth, H.J., Acharya, P., 2016. Purification of biogas using chemical scrubbing and application of purified biogas as fuel for automotive engines. Research Journal of Recent. Sciences 5, 1-7.

Shang, G., Shen, G., Wang, T., Chen, Q., 2012. Effectiveness and mechanism of hydrogen sulphide adsorption by camphor-derived biochars. Journal of the Air and Waste Management Association 62, 873-879.

Sherwood, T.K., Holloway, F.A.L., 1940. Performance of packed towers-liquid film data for several packings. Transactions of the American Institute of Chemical Engineers 36, 1-2.

Stumm, W., Morgan, J.J., 1981. An introduction emphasizing chemical equilibrium in natural waters, 2nd edition. John Wiley & Sons, New York.

Tan, L.S., Shariff, A.M., Lau, K.K., Bustam, M.A., 2012. Factor affecting CO_2 absorption efficiency in packed column: A review. Journal of Industrial and Engineering Chemistry 18, 1874-1883.

Tatsuo, K., Shojiro, O., 2012. Upgrading biogas to bio-methane: Green natural gas - Technology and cost. 25th World Gas Conference, Kuala Lumpur 5th June 2012. Retrieved from conference slide presentation.

Thomas, B.L., 2002. Fundamentals of aquacultural engineering. Second printing (2002). Kluwer Academic Publishers.

Tippayawong, N., Thanompongchart, P., 2010. Biogas quality upgrade by simultaneous removal of CO_2 and H_2S in a packed column reactor. Energy 35, 4531-4535.

Walozi, R., Nabuuma, B., Sebiti, A., 2016. Application of low pressure water scrubbing technique for increasing methane content in biogas. Universal Journal of Agricultural Research 4(2), 60-65.

Wichitpan, R., Somnuk, B., Suttichai, A., Navadol, L., Ratana, J., 2012. Simultaneous absorption of CO_2 and H_2S from biogas by capillary membrane contactor. Journal of Membrane Science 392, 38-47.

William, J.N., Mark, W., Rimika, K., Sonia, H., 2014. Modelling the water scrubbing process and energy requirements for CO_2 capture to upgrade biogas to biomethane. Industrial and Engineering Chemistry Research 53(32), 12783-12792.

Wylock, C.E., Budzianowski, W.M., 2017. Performance evaluation of biogas upgrading by pressurized water scrubbing via modelling and simulation. Chemical Engineering Science 170, 639-652.

Yasin, P., Ramesh, A., Ramana, M.V., Rahul, V., 2018. CVR J. of Sci. and Technol. 14, 86 – 90.

CHAPTER 5

BIOLOGICAL DESULFURIZATION OF HIGH H_2S FROM BIOGAS

TABLE OF CONTENTS

5.1 Introduction

Hydrogen sulphide (H_2S) is one of the atmospheric pollutants that categorize under harmful and toxic gas, which it is not only corrode the metal pipes and equipment but also could threatens the human health (Maas and Marie, 1987). Biogas generally containing (55-80%) of CH_4, (20-45%) of CO_2, (0-10%) of N_2, (200-18000 mg/m3) of H_2S and other impurities (Pourzolfaghar et al., 2014). The concentration of H_2S is far higher than the provisions of European environmental standards (not exceed 20 mg/m^3) (Dai et al., 2008).

The traditional desulfurization technologies for biogas was included dry desulfurization (membrane separation, molecular sieve, PSA, fixed bed adsorption method, Claus oxidation process), wet desulfurization (chemical absorption, physical absorption, physical and chemical absorption, wet oxidation method) and biological desulfurization (Xiao et al., 2017). Compared to other methods, biological desulfurization has the advantages such as high removal rate, no chemical catalyst, low energy consumption, no two pollution, mild desulfurization condition and can generate sulfur recovery resources (Zhao et al., 2003)(Syed et al., 2006). According to Xiao et al. (2017), the development of biological desulfurization process is still not formed a certain scale of industrial application. The two main reasons for this issue; first the culture of microorganisms is restricted by the composition of biological population and environmental factors and second the biochemical control is difficult, which restricts the development of biological desulfurization technology.

Nevertheless, biological desulfurization has successful attracted many attentions because of its advantages of low energy consumption and no pollution. Therefore, in order to obtain large scale applications, it is necessary to make efforts in the fields of desulfurization bacteria, bioreactor and desulfurization process.

In Chapter 4, the physical treatment of biogas with H_2S contains ranges from 0-3% was performed in a reactor packed with sponge carrier. High removal efficiency of H_2S with almost untraceable data readings were recorded. However, the performance of biological desulfurization in treating high H_2S from biogas using the similar reactor is still undetermined. The objective of this chapter was to determine the performance of high H_2S gas concentration removal from biogas by using a biological treatment. In stead of that, a comparison between the physical treatment performance (as performed in Chapter 4) to biological treatment performance.

5.2 Material and methods

5.2.1 Experimental setup and conditions

The overall experimental laboratory set-up system used in this study is illustrated in **Figure 5.1**. The main parts of the design are at a gas generating part, an up-flow gas injected point at side port of the reactor that work counter current with the nutrients (0.06 g L^{-1} $NaHCO_3$, 0.001 g L^{-1} KH_2PO_4, 0.001 g L^{-1} K_2HPO_4, and 0.0005 g L^{-1} NH_4CL) fed flow, and gas collecting point on top of the column surface. The bioreactor is a packed bed filter that made from a cylindrical acrylic column. About 23 polyurethane foam (PUF) cubes (8 cm^3) were installed as the packing media for biomass immobilization. Prior to the start of the experimentation, PUF cubes were soaked into a diluted aerobic sludge (1:1) obtained from wastewater treatment plant treating municipal sewage intended for reactor inoculation. A mix of synthetic H_2S, CO_2 and CH_4 gases are feed by peristaltic pump to the reactor with biogas composition as in **Figure 5.1**. The overall gas feeding rate is measured and controlled by flowmeter. The details of the system properties and its operational condition are described in **Table 5.1**.

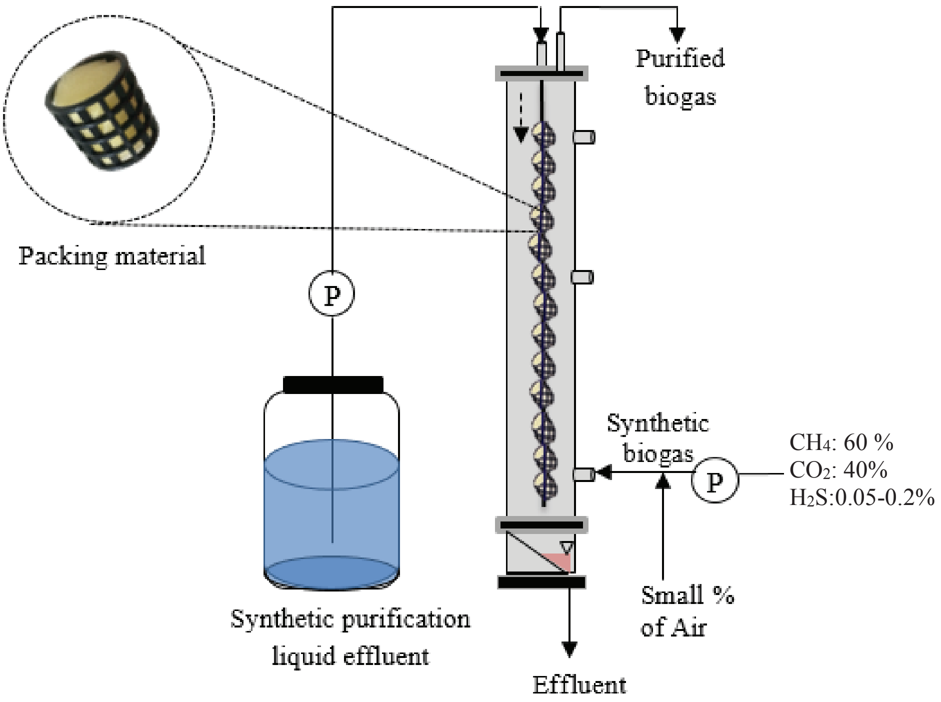

Figure 5.1: Schematic diagram of the develop treatment system

Table 5.1: Properties and operational parameter of the develop reactor system

Packing material	Polyurethane foam
Packing height (m)	1.2
Reactor inner diameter (m)	0.05
Packed volume (L)	0.425
Reactor volume (L)	1.83
Liquid flow, Q_L (L d^{-1})	0.58
Gas flow, Q_G (L d^{-1})	5.1
nutrient liquid pH	7-8
Temperature, (˚C)	5-30
O_2 loading rate, (g/m^3/h)	10-70
H_2S loading rate, (g/m^3/h)	10-70
Q_L/Q_G	0.5; 1.5
O_2/H_2S	1-7

5.2.2 Sampling and analysis

The sampling ports are located at the top, middle and bottom of the reactor for laboratory analysis. A gasbag (Smart Bag PA, GL SCIENCE/CEK 3008-97720) was used to store the gas and the CH_4, CO_2, O_2, and N_2 concentrations were measured using a gas chromatograph equipped with a thermal conductivity detector (GC-TCD, Shimadzu GC-8A). The H_2S concentration in the off gas were measured using Kitagawa detector tubes (Tube Nos. 120SM, 120SB, and 120SH). pH meter was used to measure the pH. Sulfate (SO_4^{2-}) concentration was analyzed using an HACH water quality analyzer (HACH DR4000).

5.2.3 Microbial analysis

Microbial DNA sequencing was performed for the squeezed suspended sludge collected from the reactor after 33 days of operation. The sludge samples (SS) were stored in 2-mL centrifuge tubes with a 50:50 (V/V) ratio of SS/glycerol and stored at -20°C until sequencing. DNA was isolated and extracted using the Fast DNA spin kit for soil (MP Biomedicals, Irvine, CA), as described in the manufacturer's instructions. The extracted DNA was used for amplification of bacterial 16S rRNA gene fragments with primer pairs of 341F-805R. 16S rRNA gene sequences at $\geq$ 97% similarity were grouped into the same phylogenetic clone type. The PCR products were purified using an Agencourt AMPure XP (Beckman Coulter, Brea, CA, USA) according to the manufacturer's protocols. PCR products were confirmed using a 1% (W/V) agarose gel and Qubit dsDNA Assay Kit

(Thermo Fisher Scientific). Purified DNA was sequenced using a Miseq platform with a Miseq Reagent Kit v3 (Illumina Inc., San Diego, CA, USA).

5.3 Results and discussions

5.3.1 Inoculation and start up

During the 10 days startup phase the inlet H_2S concentration was set to 5000 ppm$_v$ (91.23 g H_2S m^{-3} h^{-1}), the pH set point to 7-7.5 and the O_2/H_2S supplied ratio was 2-3. The H_2S and O_2 concentration varied significantly (**Figure 5.2a**) due to poor manual handling at the inlet gas point. The H_2S removal efficiency (RE) decreased to 55% from 64% on the second days caused by overloaded input of H_2S gas. On the first and second days the H_2S removal can be due to physical absorption of H_2S gas into the purification liquid and the biological degradation of H_2S as in equation 5.1 by sulfide oxidation bacteria (SOB) start at day three onward where 90% and above of RE were measured except for day 6 where RE suddenly drop to 49%. This happen due to insufficient of O_2 supply for the loaded H_2S concentration which corresponding to biological limitation to occur. This can be further explained with RE data on day 7 where almost similar amount of O_2 was supply but exposed to much lower H_2S concentration and the result showed 100% RE was recorded. The reactor able to achieve RE up to 99.9% or 0.07 g H_2S m^{-3} h^{-1} after 10 days of operation (**Figure 5.2b**). However, the performance was still not stable yet, with an average RE of 84.2%.

$$H_2S + CO_2 + \text{nutrient} + O_2 \longrightarrow S^0 \text{ and/or } SO_4^{2-} + H_20 \qquad (5.1)$$

Low SO_4^{2-} concentrations were observed in the liquid effluent (**Figure 5.2c**) from day 1 to 5. High SO_4^{2-} was measured after six days operation (**Figure 5.2c**) with maximum of 50 mg/l of SO_4^{2-} on day 10 at pH 3.4. Formation of SO_4^{2-} occurred when the supply of H_2S is depleted. Therefore, the energy obtained for the sulfur oxidizing bacteria (SOB) usually from further oxidation of elemental sulfur to sulfate as in equation 5.2. This proportional with gradually decreased of effluent pH reading which indicated the formation of sulfuric acid (H_2SO_4) in the liquid effluent (**Figure 5.2c**).

$$H_2S+2O_2 \longrightarrow SO_4^{2-} + 2H^+ \qquad (5.2)$$

The SOB uses inorganic carbon dioxide (CO_2) or bicarbonate ions as a food source to acquire carbon. For that, the H_2S were oxidized to obtain energy for CO_2 synthesizing process. High CO_2 removal was occurred after day two (**Figure 5.2d**). This progress indirectly showed the effective growth of SOB cultured. In conjunction, during the growth high enrichment of methane gas (CH_4) was measured with maximum of 17% with almost completely removed of H_2S gas during day 4. Nevertheless, the CH_4 enrichment starts decreasing when there is reduction in O_2 supply. This situation shows that the heterotrophic bacteria start to growth where it's utilizing the CH_4 as a food source due to oxygen limitation condition and this make the oxidation process slower. However, once suitable amount of O_2 was supplied more than 90% of H_2S removal can be achieved from the oxidation of H_2S to SO_4^{2-}.

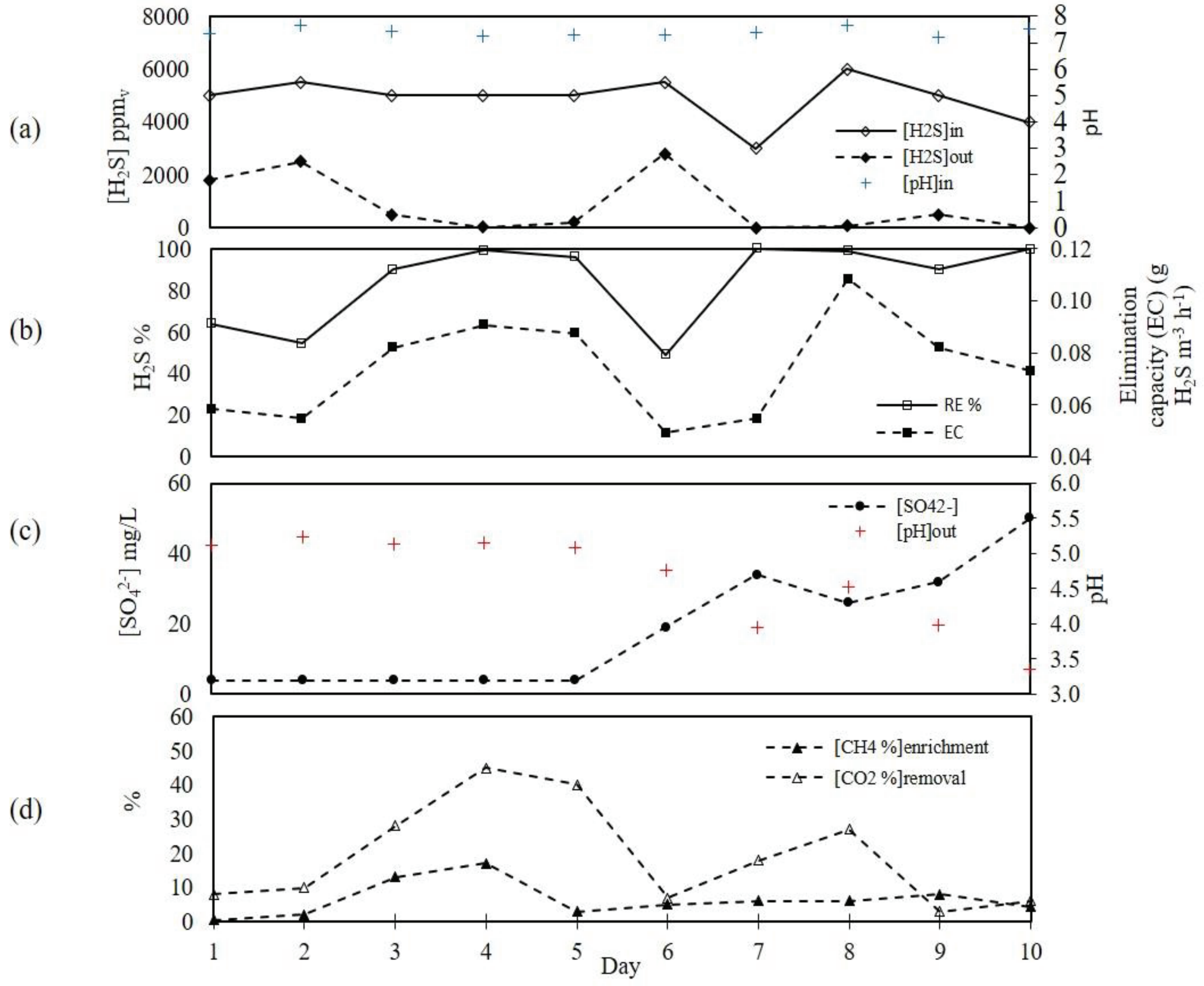

Figure 5.2: Monitoring of data during startup phase (a) H_2S inlet and out concentration and input pH profile (b) H_2S elimination capacity and removal efficiency (c) SO_4^{2-} and output pH profile (d) Percent of CH_4 enrichment and CO_2 removal.

5.3.2 Biological treatment performance

The biological purified biogas generation levels recorded in the reactor is presented in **Figure 5.3**. Q_L/Q_G ratio of 1.5 and low input concentration of hydrogen sulfide gives more CH_4 generation compared to ratio 0.5 (**Figure 5.3a**). 91% of methane gas was generate with lower oxygen supply condition and showing gradually decreased as the O_2 supply increased. However, contradict with CO_2 and H_2S gas where high concentrations were detected at low ratio of Q_L/Q_G and high input H_2S concentration (**Figures 5.3b & 5.3c**). The concentration of CO_2 gas could have reached up to 20% when the O_2 supply is increased.From biological treatment data in **Figure 5.3**, it can be concluded that gas-liquid flow ratio does give effect on the system performance. For high concentration of H_2S (>0.5%) lower gas flowrate is required to achieve high purify methane concentration. This provide high gas retention time for the bacteria to oxidize the gas components. The higher ratio of O_2/H_2S supplied for the biological treatment seem no effect on the removal of hydrogen sulfide gas. Therefore, for high water flowrate small amount of oxygen gas is sufficient for the oxidation process. Nevertheless, high concentration of hydrogen sulfide with low Q_L/Q_G might require much higher oxygen supply for the growth of SOB in the biofilm. However, higher supply of oxygen gas will reduce the purified CH_4 generation.

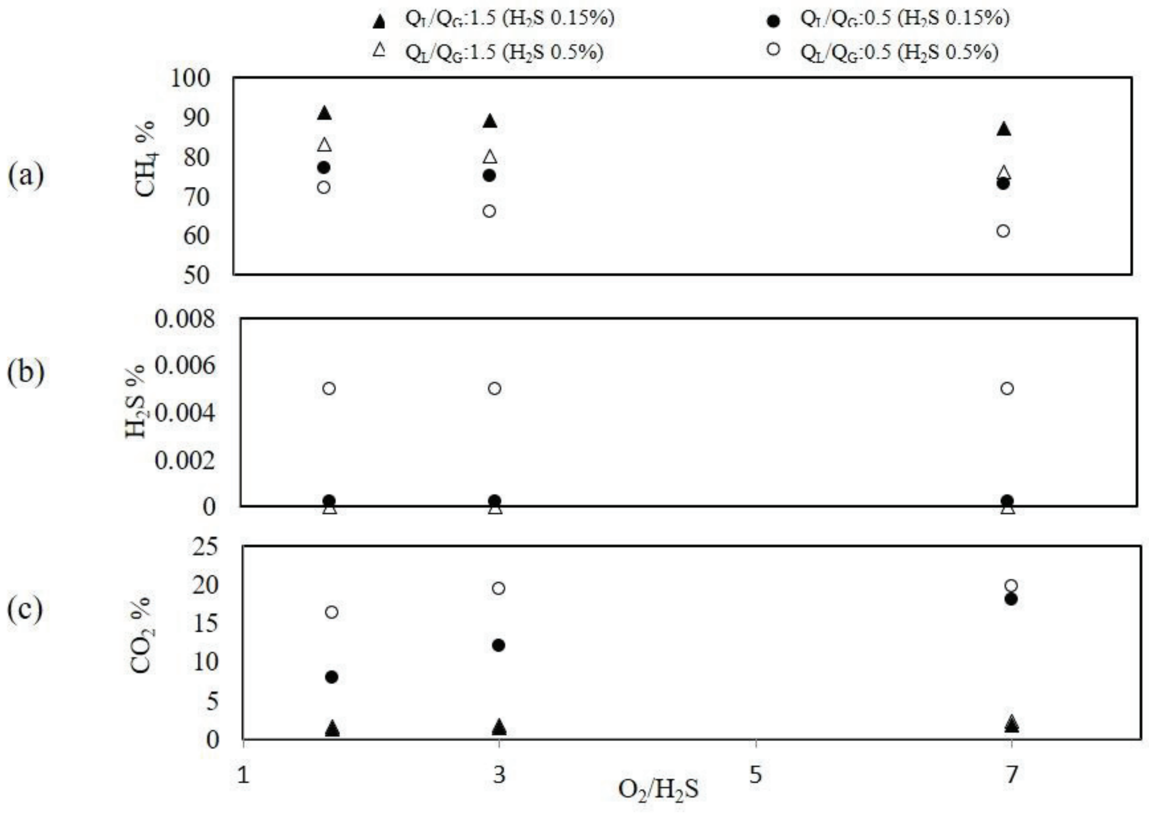

Figure 5.3: Percentage of CH_4, H_2S and CO_2 gas generation at the outlet gas point for biological treatment.

5.3.3 Comparison between physical and biological treatment

The data from physical treatment as reported in Chapter 4 were used to compare with the performance of biological treatment in treating the H_2S gas and purified the CH_4 gas. The graph plotted in **Figure 5.4** showing that good correlation in between biological and physical data for the purified methane generation.

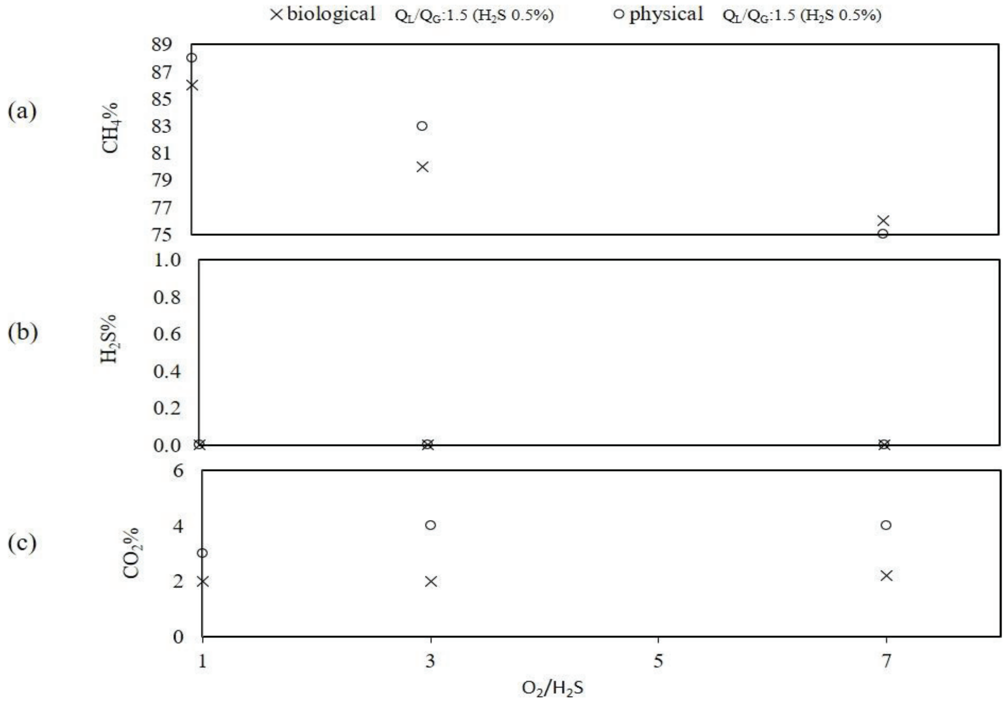

Figure 5.4: The comparison of CH_4, H_2S and CO_2 gas generation rate at the outlet gas point for biological, physical and simulation at Q_L/Q_G:1.5 and H_2S: 0.5%

Furthermore, due to almost similar amount of purified gas generated from both physical and biological, it seem that physical treatment is enough to treat for the given H_2S concentration and Q_L/Q_G without the application of biological treatment. On the contrary, for low Q_L/Q_G the physical treatment is unable to efficiently treat for biogas contain with high H_2S concentration, which is contradict with biological treatment, where it able to treat at low Q_L/Q_G with percentage of H_2S removal more than 90% as shown in **Figure 5.5**. **Figure 5.6** described the contribution of physical process in percentage in the biological treatment system in treating hydrogen sulfide gas. At low oxygen supplied biological process able to contribute higher compared to physical process and vice versa at high oxygen condition.

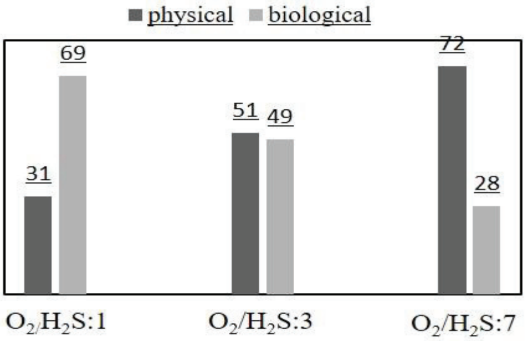

Figure 5.5: The proportions of physical and biological reaction of develop biological treatment process system in treating H_2S gas at Q_L/Q_G:1.5 and H_2S: 0.5%

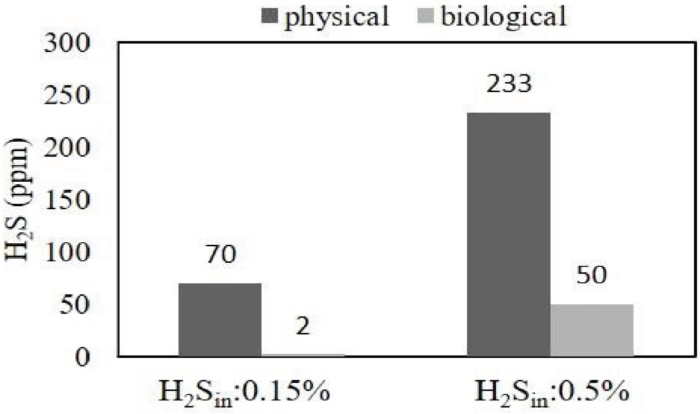

Figure 5.6: The performance of H_2S removal for physical and biological treatment at Q_L/Q_G:0.5

5.3.4 Microbial analysis

The analysis of the bacterial communities presents in the inoculum after 33 days of operation was elucidated in **Figure 5.7 & 5.8**. Bacteria belonging to the phyla *Proteobacteria, Bacteroidetes, Verrucomicrobia* and *Firmicutes* were predominant (**Figure 5.7**). The most abundance genus of sulfide oxidation bacteria (SOB) and methane oxidation bacteria (MOB) is shown in **Figure 5.8**. The SOB was dominated by Pseudomonas and Hypomicrobium. Methylobacter, Methylocaldum and Methylomicrobium were the dominance genus species of MOB present in the study.

Figure 5.7: Major phylum of bacteria

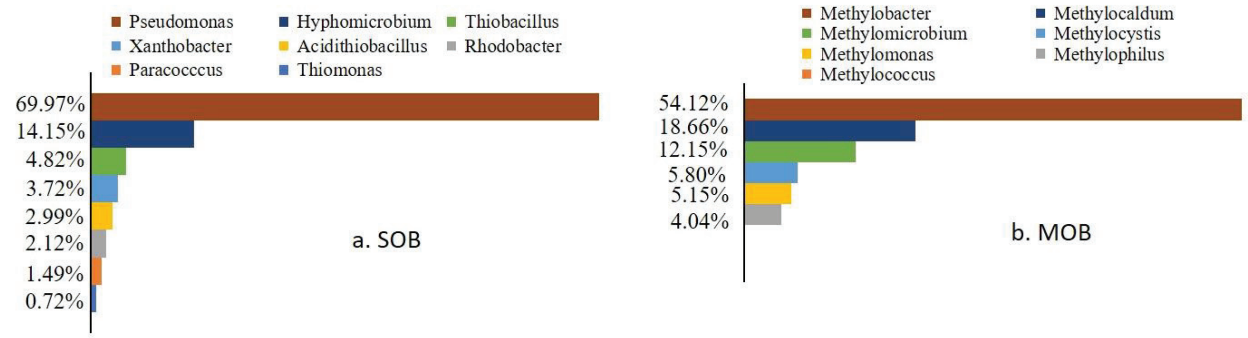

Figure 5.8: Major genus identified in inoculum. (a) sulfide oxidation bacteria (SOB) (b) Methane oxidation bacteria (MOB).

5.4 Conclusion

As a conclusion, biological treatment is no need for the treatment of biogas with high hydrogen sulfide in the develop sponge scrubber system, because physical treatment is capable to achieved high purified methane generation with almost undetectable of hydrogen sulfide gas if suitable operational conditions especially the Q_L/Q_G is implemented. The initial H_2S concentration and the ration between O_2 and H_2S also required proper controlled in ensuring high removal of H_2S gas from the system.

References

Dai, Q.J., Yi, L.I., Fang, X.J., 2008. Discussion on correlation between sulfur in sludge and hydrogen sulphide in biogas. Journal of China Water & Wastewater.

Hatamoto, M., Yamamoto, H., Kindaichi, T., Ozaki, N., Ohashi, A., 2010. Biological oxidation of dissolved methane in effluents from anaerobic reactors using a down-flow hanging sponge reactor. Water Res. 44, 1409.

Maas, Marie, F., 1987. Responses of plants to sulfur containing air pollutants (H_2S and SO_2). Journal of University of Groningen, 14(1), 61 – 62.

Pourzolfaghar, H., Mohd, H.S.I., Izhar, S., 2014. Review of H_2S sorbents at low-temperature desulfurization of biogas. International Journal of Chemical & Environmental Engineering.

Syed, M., Soreanu, G., Falletta, P., 2006. Removal of hydrogen sulfide from gas streams using biological processes -A review. Journal of Canadian Biosystems Engineering, 48(1).

Xiao, C., Ma, Y., Ji, D., Zang, L., 2017. Review of desulfurization process for biogas purification. International Global on Renewable Energy and Development, 100.

Zhao, X., Geng, B., Di, J., 2003. Study on removal of hydrogen sulphide from industrial acidic waste gas by immobilized microorganism. Journal of Speciality Petrochemicals.

CHAPTER 6

INTEGRATED BIOLOGICAL-PHYSICAK PROCESS FOR BIOGAS PURIFICATION EFFLUENT TREATMENT

TABLE OF CONTENTS

6.1 Introduction

Biogas purification is a well-established technology applied in wastewater treatment plants to produce high-purity methane (CH_4) particularly for use as vehicle fuel or for injection into the gas grid. Currently, there are several technologies for biogas purification that are available such as water scrubbing, pressure swing adsorption, membrane technology, cryogenic separation, hydrate formation, biological methods, and physical and chemical absorption (Sun et al., 2015). Among all these methods, biogas purification via water scrubbing is the most widely applied technology because it is the simplest and cheapest method (Nock et al., 2014; Karim and Fatima, 2018). In water scrubbing, water is used as the solvent to remove gaseous pollutants, especially carbon dioxide (CO_2) and hydrogen sulfide (H_2S) using absorption techniques (Heyden et al., 2016). However, during absorption, a substantial amount of CH_4 is dissolved in the water, which results in a significant loss of CH_4 (i.e., energy) in the effluent (Hartley and Lant, 2006). Besides, the presence of dissolved CH_4 also has a serious impact on global climate change and air pollution when released into the environment (Liu et al., 2014). Furthermore, CH_4 is known to have a greenhouse power 25 to 34 times higher than CO_2 gas and all halocarbons combined (Gu et al., 2017; Stocker et al., 2014). It is reported that 5% of the global CH_4 emissions is from wastewater treatment plants and most of the emissions come from dissolved CH_4 in effluents (E-Fadel and Massoud, 2001; Smith et al., 2014).

Heile et al. (2017) reported that under atmospheric conditions, the concentration of dissolved CH_4 in the anaerobic wastewater effluents could reach 35 $mgCH_4L^{-1}$ when the temperature is below 5°C and decreases following an increase in water temperature. It should be noted that if anaerobically treated effluent is going to be sent to a closed conduit, it must be degassed to a concentration of 0.14 $mgCH_4L^{-1}$ to prevent the creation of a potentially explosive environment; this is usually done with forced aerators, packed towers, and bubble columns (Cookney at al., 2016; Henares et al., 2016). There are several other techniques proposed for dissolved CH_4 removal or recovery from anaerobic wastewater effluent. These include aeration, biological oxidation, air stripping, and membrane-based recovery (Crone et al., 2016). Hatamoto et al. (2011) reported biological oxidation of dissolved CH_4 from anaerobic effluent using a highly spacious down-flow hanging sponge (DHS) reactor can remove more than 90% of CH_4. The use of DHS was extended to CH_4 recovery when two DHSs were used sequentially, in which most of the dissolved CH_4 was removed in the first stage, and the residue was then oxidized in the second stage (Matsuura et al., 2010, 2015).

In contrast with anaerobic wastewater effluent, the biogas purification effluent is usually associated with high saturation of dissolved CO_2 and H_2S. When the purification effluent becomes saturated with CO_2, it not only potentially contributes to global warming but also reduces the effluent pH as well (Summerfelt et al., 2015). In addition, the dissolution of H_2S in water makes the water corrosive, which can result in leaching of metals present in the plumbing system (Ling et al., 2011). Considering the worst possible effects of the dissolved contaminants, this effluent appears unsuitable for regeneration purposes.

To gain a better understanding of biogas purification and its effluent constituents, prior to this study, a biogas purification experiment was conducted using artificial as in Chapter 4. During this experiment, a new water scrubber packed with a sponge carrier was used to purify the biogas under atmospheric conditions, and more than 90% CH_4 with no H_2S gas was successfully obtained. It was also observed during the experiment that the purification effluent comprised of dissolved CH_4, CO_2, and H_2S, with the final effluent having a pH of 5.64 (data not published) (**Figure 6.1a**). Continuing this study was the objective behind the present chapter, in which a similar type of reactor was used to eliminate the dissolved components of CH_4, H_2S, and CO_2 through integration of biological oxidation and physical stripping processes (**Figure 6.1b**).

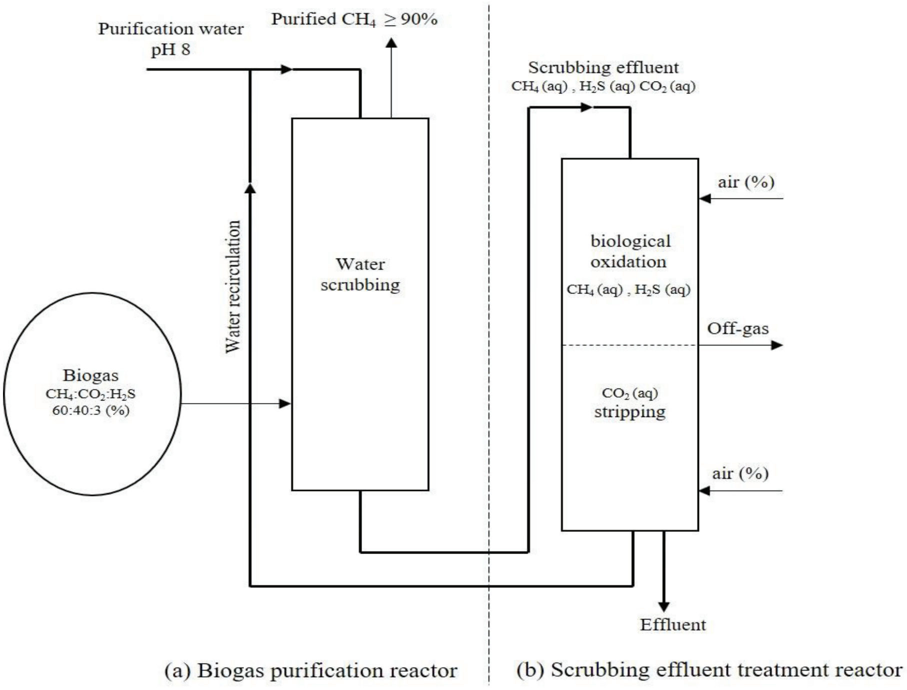

(a) Biogas purification reactor (b) Scrubbing effluent treatment reactor

Figure 6.1: Schematic of the sustainable biogas treatment. (a) Biogas purification reactor. (b) Scrubbing effluent treatment reactor.

The use of biological oxidation and physical stripping to remove dissolved CH_4, H_2S, and CO_2 from biogas purification effluents is very unusual because to the best of our knowledge, there is no study investigating the removal or recovery of dissolved components by integrating these two processes in a single reactor. Therefore, the feasibility of the proposed system remains unknown.

The goal of this chapter was to reduce greenhouse gas emissions from the biogas purification effluent whilst correcting the effluent pH for water regeneration. To reach this goal, a post-treatment system for biogas purification was developed by combining biological oxidation and physical stripping processes to remove CH_4, H_2S, and CO_2 simultaneously. Evaluations of the experimental performance of the proposed system via coupling with a mathematical model were conducted to simulate and determine the optimum performance of biological oxidation and physical stripping in removing the CH_4 and recovering the effluent pH.

6.2 Material and methods

6.2.1 Experimental setup and processes

A schematic of the system used in this study is shown in **Figure 6.2**. The system combines biological oxidation and physical stripping processes in a single reactor. The reactor was a cylindrical packed bed reactor with a packed height of 120 cm and working volume of 2.3 L. The reactor column consisted of a string with 23 packed carriers consisting of a plastic frame equipped with a polyurethane sponge connected in series, and the initial volume of each packed carrier was 18.5 cm^3. The sponge packed initially was soaked in a diluted aerobic sludge (1:1) obtained from a wastewater treatment plant treating municipal sewage intended for reactor inoculation.

A synthetic biogas purification effluent containing a mineral medium and the dissolved components of CH_4, CO_2, and H_2S was fed from the top; it flowed down onto the sponges and was finally discharged through the bottom. The composition of the mineral medium added in 1 L of the synthetic biogas purification effluent was as follows: 0.001 g KH_2PO_4, 0.001 g K_2HPO_4, and 0.0005 g NH_4CL. The alkalinity was set to 0.62 mmol L^{-1} by adding of 0.06 g L^{-1} $NaHCO_3$. The dissolved components of CH_4 and CO_2 were prepared by purging the synthetic purification effluent with a gas mixture comprising of CH_4 gas (60% [v/v]) and CO_2 (40% [v/v]) until the concentration of CH_4 and CO_2 in the gas and liquid phases reached equilibrium.

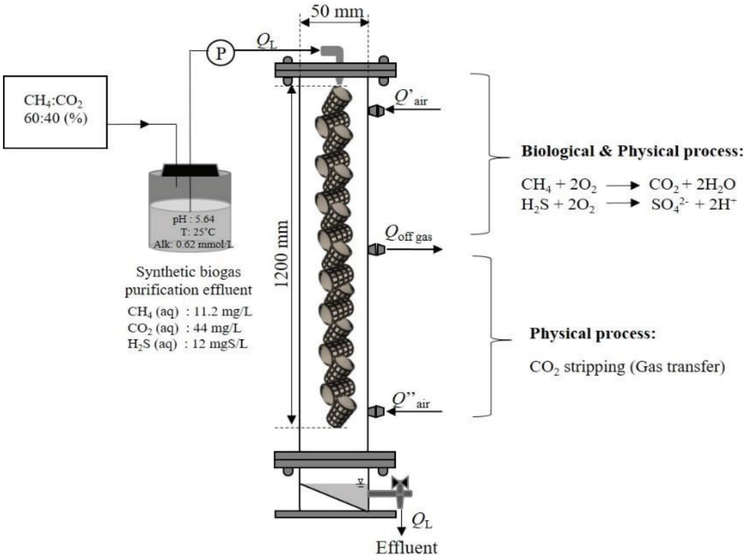

Figure 6.2: Experimental setup for scrubbing effluent treatment.

6.2.2 Operational conditions

First, biological oxidation experiments with CH_4 and H_2S were performed under hydraulic retention times (HRTs) of 2, 1.33, and 0.67 h by adjusting the volumetric flow rate of the influent liquid (Q_L) for phases 1 to 3 (**Figure 6.3**). During this experiment, a constant airflow rate (Q'_{air}) of 2.02 L dy^{-1} was used at the top of the reactor column. Next, in phases 4 to 6, with additional airflow at a supply rate of Q''_{air} from the bottom of the reactor, the experiment was continued by simultaneously conducting biological oxidation and physical stripping of CO_2. Following this experimental study, a mathematical simulation model of the process was developed and validated using the gathered experimental data. The simulation was developed to determine the effects of Q'_{air} and Q''_{air} on CH_4 removal and pH recovery, respectively.

6.2.3 Sampling and analyses

Gases in the influent and off gas were stored and collected in a gasbag (Smart Bag PA, GL SCIENCE/CEK 3008-97720) and the CH_4, CO_2, O_2, and N_2 concentrations were measured using a gas chromatograph equipped with a thermal conductivity detector (GC-TCD, Shimadzu GC-8A). Kitagawa detector tubes (Tube Nos. 120SM, 120SB, and 120SH) were used to measure the H_2S concentration in the off gas. The effluent pH was measured using a pH meter. Sulfate (SO_4^{2-}) concentration was analyzed using an HACH water quality analyzer (HACH DR4000). For measuring dissolved CH_4 (CH_4 (aq)) in the influent and effluent, the headspace measurement technique described by Hatamoto et al. (2010) was applied with Henry's Law and the Bunsen coefficient to calculate the concentration. The concentration of dissolved CO_2 (CO_2 (aq)) was measured using a Shimadzu TOC-V_{CSH} analyzer with an ASI-V autosampler.

6.2.4 Calculations

The loading and removal rates of CH_4 in terms of the gas mass per sponge volume (V_{sponge}) per unit time were calculated using equations (6.1) & (6.2). C and P are the mass concentrations of the components in the gas and liquid phases, respectively, whereas Q is the flow rate in the gas (G) and liquid (L) phases, measured at the input and output sides.

$$CH_4 \text{ loading rate} = \frac{Q_{L_{in}} C_{CH4_{in}}}{V_{sponge}} \tag{6.1}$$

$$CH_4 \text{ removal rate} = \frac{Q_{L_{in}} C_{CH4_{in}} - \left[Q_{L_{out}} C_{CH4_{out}} + Q_{G_{out}} P_{CH4_{out}}\right]}{V_{sponge}} \tag{6.2}$$

The removal efficiency for CH_4 is defined as follows:

$$CH_4\,(\%) = \frac{Q_{L_{in}} C_{CH4_{in}} - \left[Q_{L_{out}} C_{CH4_{out}} + Q_{G_{out}} P_{CH4_{out}}\right]}{Q_{L_{in}} C_{CH4_{in}}} \times 100\% \tag{6.3}$$

In this study, we did not measure the dissolved H_2S (H_2S (aq)) concentration in the effluent; only the off-gas H_2S and SO_4^{2-} concentrations were considered. Therefore, the efficiency of H_2S removal was determined according to the amount H_2S oxidized to SO_4^{2-} as follows:

$$\text{Efficiency of } H_2S \text{ oxidation to } SO_4^{2}\,(\%) = \frac{Q_{L_{in}} C_{SO_4^{2-}{}_{in}} - \left[\, Q_{L_{out}} C_{SO_4^{2-}{}_{out}} \right]}{Q_{L_{in}} C_{SO_4^{2-}{}_{in}}} \times 100\% \tag{6.4}$$

6.2.5 DNA Sequencing

Microbial DNA sequencing was performed for the squeezed suspended sludge collected from six different locations along the reactor after 79 days of operation. The sludge samples (SS) were stored in 2-mL centrifuge tubes with a 50:50 (V/V) ratio of SS/glycerol and stored at -20°C until sequencing. DNA was isolated and extracted using the Fast DNA spin kit for soil (MP Biomedicals, Irvine, CA), as described in the manufacturer's instructions. The extracted DNA was used for amplification of bacterial 16S rRNA gene fragments with primer pairs of 341F-805R. 16S rRNA gene sequences at ≥ 97% similarity were grouped into the same phylogenetic clone type. The PCR products were purified using an Agencourt AMPure XP (Beckman Coulter, Brea, CA, USA) according to the manufacturer's protocols. PCR products were confirmed using a 1% (W/V) agarose gel and Qubit dsDNA Assay Kit (Thermo Fisher Scientific). Purified DNA was sequenced using a Miseq platform with a Miseq Reagent Kit v3 (Illumina Inc., San Diego, CA, USA).

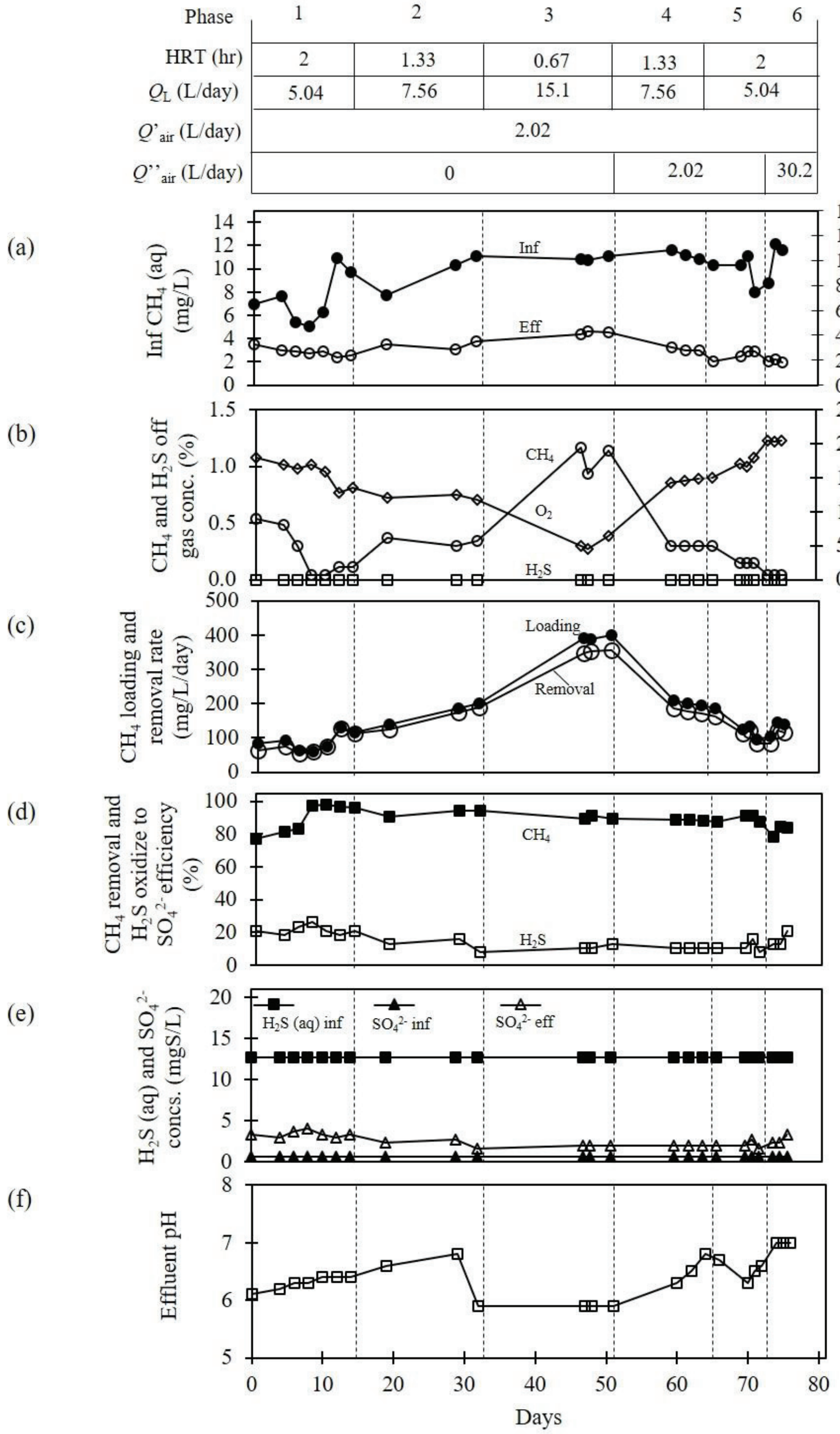

Figure 6.3: Operational conditions of biological oxidation and physical stripping performances. Time course of the (a) influent and effluent concentration of CH_4 (aq) (b)

off-gas concentration of CH_4, H_2S and O_2 (c) CH_4 loading and removal rates (d) efficiency of CH_4 removal and H_2S oxidation to SO_4^{2-} (e) H_2S (aq) and SO_4^{2-} concentration (f) effluent pH.

6.3 Model development

A mathematical model was developed based on the mass transfer of CH_4, H_2S, CO_2, O_2, and N_2 gas components in the three different phases (gas, liquid, and biofilm) with a biological reaction in the biofilm, as shown discussed in details in Chapter 3. In the system, the dissolved gas and air components were transferred by the absorption of liquid and cocurrent (at the top of the reactor) and countercurrent (at the bottom of the reactor) gas flow into the packed material. The dissolved CH_4, H_2S, and O_2 were finally utilized in the microbial oxidation that occurred at the top of the reactor. Further, the dissolved CO_2 from the supplied and produced gas during the biological process was removed from the system in the stripping process at the bottom of the reactor.

6.4 Results

6.4.1 System performance

The experiments were conducted in six different phases considering the influence of HRT and airflow rates (Q'_{air} and Q''_{air}) on the system performance, as illustrated in **Figure 6.3**. At the beginning of the experiment (Phase 1), biological oxidation of CH_4 and H_2S was performed at a Q'_{air} of 2.02 L d^{-1} (air supply at the top) without the stripping process (air supply from the bottom, Q''_{air}). A synthetic biogas purification effluent with pH 5.64 was supplied at a Q_L of 5.04 L d^{-1} and an HRT of 2 h. Under this operational condition, CH_4 (aq) and H_2S (aq) were initially fed at concentrations of 6.95 mg L^{-1} and 12.2 mgS L^{-1}, respectively (**Figures 6.3a & 6.3c**). It was observed that the CH_4 (aq) concentration was reduced to 0.003 mg L^{-1} in the effluent with the O_2 concentration in the off gas measured at 18%, indicating an O_2 consumption of 3% for the biological oxidation process (**Figures 6.3a & 6.3b**). In this study, owing to some technical difficulties, the H_2S (aq) concentration in the effluent could not be measured. However, the H_2S (aq) removal performance was determined through the measurement of the H_2S gas concentration in the off gas and during SO_4^{2-} formation. A CH_4 concentration of 0.54% with an almost undetectable H_2S gas level was observed in the off gas (**Figures 6.3e**). The off-gas H_2S reading suggested that the H_2S (aq) concentration in the effluent was negligible. The formation of SO_4^{2-} from the oxidation of H_2S (aq) was achieved at 21.5%; thus, it was apparent that the H_2S was not completely oxidized and precipitation of sulfur (S_o) or thiosulfate ($S_2O_3^{2-}$) could possibly occur in the system (**Figure 6.3d**). Meanwhile, a CH_4 removal efficiency of only 77.2% was achieved at a CH_4 removal rate of 64.7 mg L^{-1} d^{-1} (**Figures 6.3f & 6.3b**).

However, after four days of operation, the influent CH_4 (aq) concentration suddenly increased. This was because of a problem that occurred during CH_4 (aq) preparation. Despite this, the off-gas CH_4 concentration decreased to 0.49%, while the O_2 consumption and CH_4 removal efficiency increased to 4% and 81.7%, respectively. Throughout this period, off-gas H_2S concentration and the efficiency of H_2S oxidation to SO_4^{2-} were almost unchanged. In the following days, the influent CH_4 (aq) concentration reduced slightly and then increased with concentrations between 5.05 to 10.9 mg L^{-1}, but the off-gas CH_4 concentrations continuously decreased until stable readings of 0.08% were observed with an O_2 consumption of 7.50%.

It was notable that within two weeks of operation, no off-gas H_2S was detected, and a CH_4 removal efficiency greater than 95% was successfully achieved from day 8 onward, even though complete oxidation of H_2S was not achieved. Moreover, at the end of phase 1, a CH_4 removal rate of 112 mg L^{-1} d^{-1} was achieved at a CH_4 (aq) loading rate of 116 mg L^{-1} d^{-1}.

In phase 2, again under a Q'_{air} of 2.02 L d^{-1}, biological oxidation was performed without the stripping process at a higher CH_4 loading rate based on the sponge volume with a Q_L of 7.56 L d^{-1} and an HRT of 1.33 h. During this phase, the influent CH_4 (aq) was gradually fed at a concentration of 7.69 to 11.1 mg L^{-1} with no change in the H_2S (aq) influent concentration as in phase 1. The respective CH_4 (aq) effluent concentrations measured on days 19, 29, and 32 of operation were in a similar range (0.003 to 0.0035 mg L^{-1}). Meanwhile, the O_2 concentrations in the off gas gradually decreased as more O_2 was consumed for oxidation purposes. The off-gas CH_4 concentration increased to greater than 0.3% on day 19 and remained constant afterward. Regarding the performance in terms of H_2S (aq) removal, surprisingly, it was very close to that obtained in phase 1, except that the formation of elemental sulfur (S_o) was observed on day 32 in the form of white stringy bacterial filaments on the sponge carrier, as shown in **Figure 6.4**. Although a higher CH_4 loading was supplied, after 18 days of operation, a CH_4 removal efficiency of up to 94% and CH_4 removal rate of 188 mg L^{-1} d^{-1} were achieved in phase 2.

The CH_4 loading rate was further increased in phase 3, and trends practically identical to phase 2 in terms of biological oxidation performances were observed. However, the CH_4 removal efficiency was seen to decline steadily to below 90% thereafter;

although a higher O_2 uptake was observed, the off-gas CH_4 concentration measured was greater than 1%. This suggests that a higher CH_4 loading rate induces higher gasification of CH_4. In these conditions, the maximum CH_4 removal rate of 356 mg L^{-1} d^{-1} was achieved at loading rates of 400 mg L^{-1} d^{-1}.

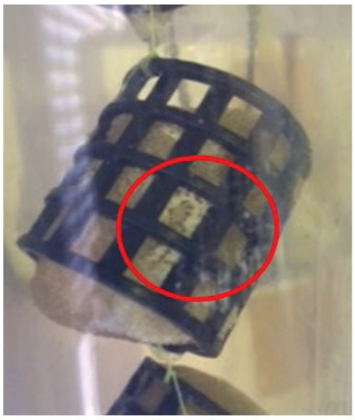

Figure 6.4 Sulfur precipitation on the frame sponge carrier

According to the experimental results obtained in phases 1 to 3, the proposed biological oxidation process of CH_4 and H_2S shows high potential for minimizing the release of CH_4 and H_2S into the atmosphere. Nevertheless, as can be seen from **Figure 4.3f**, the effluent pH after the biological treatment in phases 1, 2 and 3 was only 5.9–6.8. Therefore, correcting the effluent pH to 8 (utilized in the water scrubbing process) appears to be necessary for water regeneration. In the subsequent phases (phases 4 to 6), biological oxidation integrated with physical stripping was performed through additional airflow supply from the bottom (Q''_{air}).

The operational conditions of phase 2 were used in phase 4 with a Q''_{air} of 2.02 L^{-1} d^{-1}. The same conditions as those used in phase 2 were chosen owing to the high effluent pH compared to the other phases. Although the stripping process was performed concurrently in the reactor, interestingly, the performances during the biological oxidation of CH_4 and H_2S observed were almost identical with those of phase 2, thus indicating that the Q''_{air} did not affect the performance of the reactor during biological oxidation. Still, the effluent pH was only recovered up to pH 6.9 after the 13th day of operation.

Further analysis on the effect of Q''_{air} on biological oxidation was carried out in phase 5 at a much lower CH_4 loading rate than in phase 1. As expected, a similar trend for biological oxidation performance was observed, and on day 71 of operation, a CH_4 removal rate of 112 mg L^{-1} d^{-1} was measured for a CH_4 loading of 132 mg L^{-1} d^{-1}. However, in comparison with the performance during phase 1, the off-gas methane concentration increased to 0.15%. This suggests that the movement of air in the liquid induced turbulence during mixing with the biological oxidation effluent and coincidently forced the CH_4 gas to escape. The effluent pH showed a small increase to 6.6, thus illustrating that the Q''_{air} was not enough to recover the effluent pH to 8.

In phase 6, the Q''_{air} was further increased to 30.2 L^{-1} d^{-1}. After four days of operation, the effluent pH was increased to pH 7, thus apparently indicating that the pH could be increased by increasing the $Q''_{air.}$ The CH_4 removal efficiency was reduced to 83.9%, and this reduction occurred owing to high off-gas CH_4 detection. The excessive airflow supplied caused the dilution of the gas to an almost undetectable level. However, during this study, this did not happen, and we attributed this to instrument problems because the gas analyzer used can only detect concentrations only to a certain level. Nevertheless, the other performance parameters remained practically unchanged. Therefore, under appropriate control of the HRT and airflow rate, the proposed integrated system can not only treat the CH_4 (aq) and H_2S (aq) but also concurrently recover the effluent pH. However, to achieve the optimal performance during stripping and biological oxidation, specifically for CH_4, the most effective airflow rates (Q''_{air} and Q'_{air}) need to be determined.

6.4.2 Effect of operational conditions

6.4.2.1 Hydraulic retention time (HRT)

The HRT of the proposed system was one of the most important operation parameters affecting the system performance. The HRT affected the amount of off-gas CH_4 released from the reactor to the atmosphere. During the study, the HRT was shortened from 2 h to 0.67 h during phases 1 to 3 with a subsequent increase in Q_L from 5.04 to 15.1 L d^{-1}. As shown in **Figure 6.5**, a high off-gas CH_4 emission rate of approximately 39.6 mg L^{-1} d^{-1} was achieved with an HRT of 0.67 h, whereas a lower off-gas CH_4 emission rate of 7.89 mg L^{-1} d^{-1} was obtained for an HRT of 2 h. At short HRTs, the strong hydraulic pressure could trigger biomass washout and led to reactor failure (Pan et al., 2004). In this regard, it must be noted that a proper HRT should be judiciously selected to optimize the performance of the biological process; thus, CH_4 emission to the atmosphere could be inhibited.

6.4.2.2 Effect of upper airflow rate (Q'_{air}) on O_2 consumption of biological process

Biological oxidation of CH_4 and H_2S was performed at a constant airflow rate of 2.02 L d^{-1}, supplied from the upper side of the reactor. With an increase in the influent liquid flow rate during this fixed O_2 condition, progressive performances were recorded for CH_4 and H_2S removal; the O_2 consumption rate during CH_4 and H_2S oxidation correspondingly increased from phases 1 to 3. Using the theoretical oxygen demands of 4 g-O_2 g-CH_4^{-1} and 1.5 g-O_2 g-S^{-1} from the CH_4 removal rate and SO_4^{2-} production rate, respectively, the O_2 consumption rates were calculated based on the sponge volume and are presented in **Figure 6.6**. The experimental O_2 consumption rate was measured by distinguishing the O_2 concentration in the supply (at a constant supply of 21% O_2 cons.) from the off-gas O_2 concentration measured, as shown in **Figure 6.3b**. It is evident that the actual amount of O_2 consumed for both the oxidation processes is almost identical with the theoretically calculated O_2 consumption rate (**Figure 6.6**).

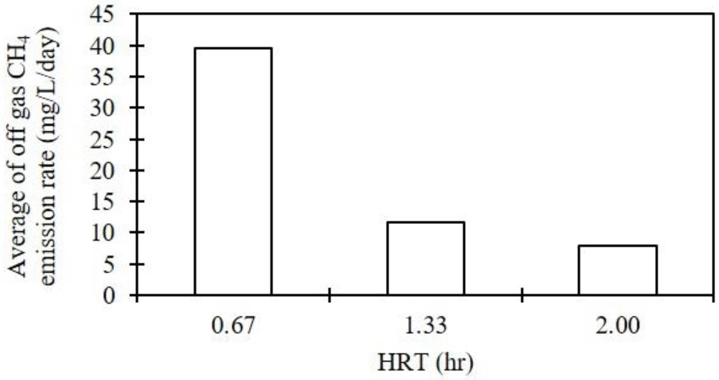

Figure 6.5 Effect of HRT on average off gas CH_4 emission rate

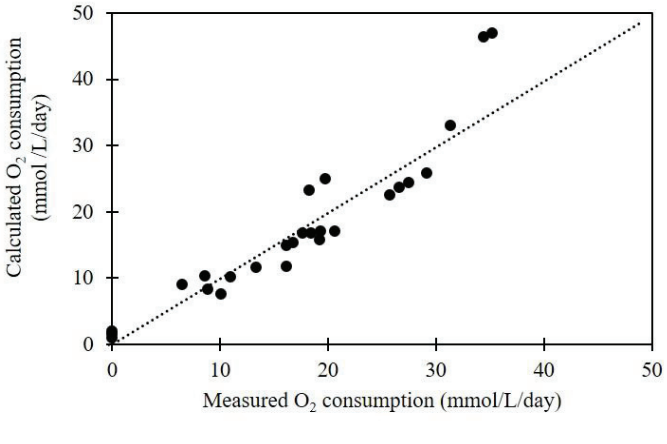

Figure 6.6 Scatter plot of O_2 consumption as determined by experimental (measured) and theoretical (calculated) method.

These results prove that the bacterial activities during biological oxidation in the system were highly effective in consuming the supplied O_2. The presence of O_2 was a significant factor influencing biological oxidation. Adequate O_2 supply proportional to the amount of CH_4 (aq) in the influent is necessary for achieving high CH_4 oxidation performance (Hatamoto et al., 2010). In this study, the maximum O_2 consumption rate corresponded to 76.2% of the supplied O_2 measured in phase 3; this could be the limit of O_2 uptake for the biological oxidation process in the proposed system.

6.4.2.3 Influence of bottom airflow rate (Q''_{air}) on effluent pH

The effect that Q''_{air} values of 2.02 and 30.2 L d^{-1} had on the effluent pH was tested during phases 4 to 6 for two influent Q_L values (5.04 and 7.56 L d^{-1}). A slight effect on effluent pH was detected when a Q''_{air} of 2.02 L d^{-1} was applied for both Q_L values. At a Q_L of 5.04 L d^{-1}, the effluent pH increased from 5.64 to 7 when a minimum Q''_{air} of 30.2 L d^{-1} was applied. This suggests that the recovery of the effluent pH corresponds to the amount of air supplied.

6.4.3 Simulation performance

6.4.3.1 Determination of Q'_{air} for high performance of biological process

Due to insufficient data, we investigate the effect of O_2 based on air supply rate during the biological oxidation using a mathematical model. The model used is a modified simulation model from our previous study (Noorain et al., 2018). By using the information gathered from the last study, we managed to determine the overall mass transfer coefficient for different liquid flowrates (data not shown) and the relation of Q'_{air} on CH_4 performance are depicted in **Figure 6.7**. In the simulation, the potential removal rate of CH_4 and H_2S of 0.02 mol L^{-1} d^{-1} and 0.0008 mol L^{-1} d^{-1} were assumed according to data gathered in experimental study. The maximum CH_4 removal efficiency of 98.7, 95.4 and 77.6 % could be achieved with airflow rate of 0.10, 0.33 and 2.01 L d^{-1} for liquid flowrate of 5.04, 7.56 and 50.4 L d^{-1}, respectively. Surprisingly, it was found that further increase of Q'_{air} only caused a small change in CH_4 removal efficiency and too low of Q'_{air} however, might contributed to reduce the CH_4 removal efficiency for both measured conditions. In order to check the validity of the simulation, the simulated performance was compared with the experimental data. As shown in **Figure 6.7**, the simulated data were in agreement with the measured values. This indicated that the constructed model is acceptable to simulating the oxidation process performance. Further, the agreement could also be illustrated from the data plotted in **Figure 6.8**, which elucidated about the off gas CH_4 concentration. Note that, minimum off gas CH_4 concentration of 0.02, 0.06 and 1.55 % could be achieved with Q'_{air} of 12.1 L d^{-1} for Q_L of 5.04, 7.56 and 50.4 L d^{-1}, respectively. Therefore, by the experimental and simulation results performance indicated that the emission of CH_4 to the atmosphere can be successfully minimize or prohibited by using the proposed operational methods under suitable Q'_{air}.

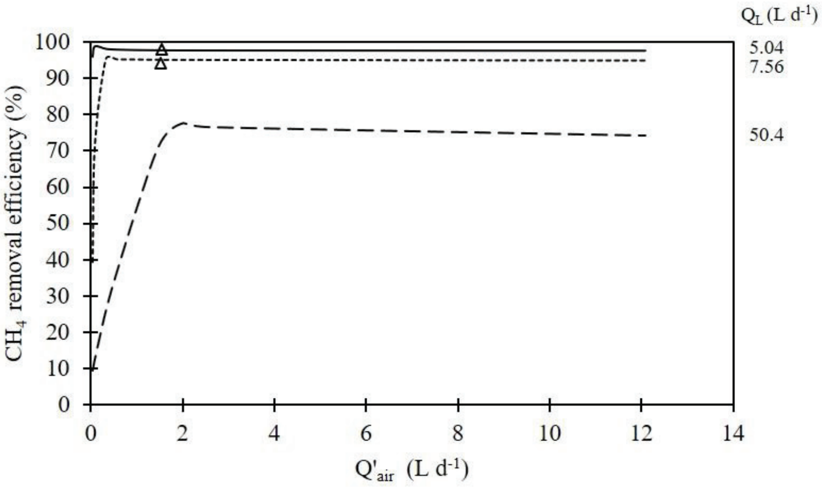

Figure 6.7: Influence of the Q'_{air} on the removal efficiencies of CH_4 gas for Q_L of 5.04, 7.56 and 50.4 L d^{-1}, respectively. The lines and shapes correspond to simulation and experimental data.

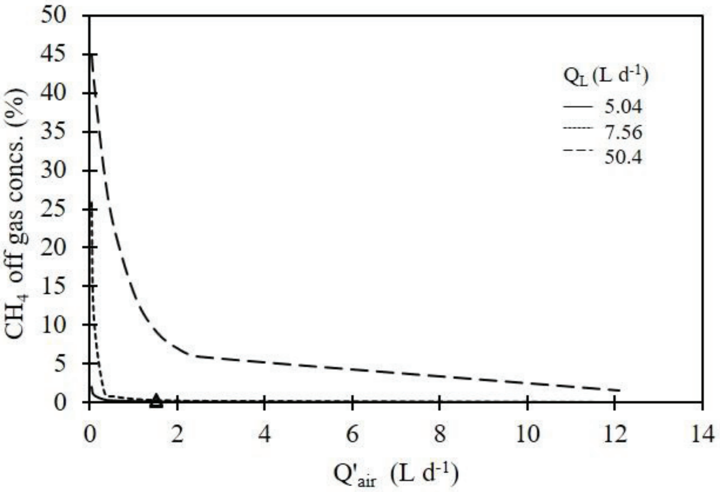

Figure 6.8: Relationship of the Q'_{air} supply of biological process with off-gas CH_4 concentration at Q_L of 5.04, 7.56 and 50.4 L d^{-1}, respectively. The lines and shapes correspond to simulation and experimental data.

6.4.3.2 Determination of Q''_{air} for effluent pH recovery

As mentioned earlier, the amount of air supplied affects pH recovery, and a high amount of air is needed for good performance. However, owing to some technical problems, we were unable to conduct the experiment at high values of Q''_{air}. Therefore, to obtain the desired solution, we used our developed mathematical model to investigate the effect of Q''_{air} on the effluent pH. The effluent pH could be recovered up to 7.3 with a minimum Q''_{air} of 50 L d^{-1} (**Figure 6.9**). Interestingly, further increasing the Q''_{air} did not have any effect on the effluent pH. This means H^+ and OH^- ions were in equilibrium, and the effluent solution reached its saturation level. From this investigation, it can be concluded that the proposed gas stripping method could recover the effluent pH from 5.64 to 7.3, and the stripping process did not significantly affect the biological process, which operated concurrently. Therefore, the results presented in this study demonstrated that dissolved CH_4, H_2S, and CO_2 could be simultaneously removed through a combined process involving biological and physical treatments.

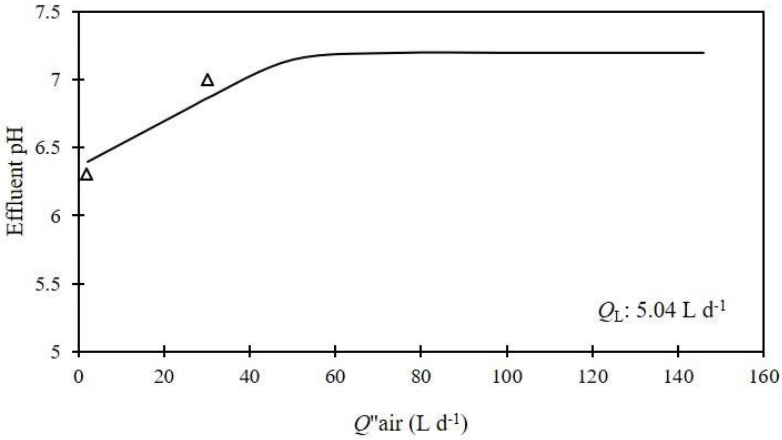

Figure 6.9: Influence of the Q''_{air} on the effluent pH recovery at constant Q_L value of 5.04 L d^{-1}. The lines and shapes correspond to simulation and experimental data, respectively.

6.4.4 Microbial analysis

Experimental results of biological oxidation process suggest that methane oxidation and sulfide oxidation processes coexist; however, there is no clear proof regarding this. To reveal whether the representative bacterial communities related to these processes were present, I constructed bacterial 16SrRNA gene clone libraries using DNA that was extracted from suspended sludge samples taken on day 79 (phase 6). The samples were taken at six different locations along the reactor height (H) and their phylogenetic affiliations are shown in **Figure 6.10**. The study found that the samples collected from all locations showed the presence of the bacteria, except for the sample from location H6, in which bacterial DNA was untraceable (**Figure 6.10a**). As expected, the result matched with the experimental findings from the physical treatment of CO_2 (aq) via gas stripping, which occurred at a location approximately corresponding to location H6. The four major phyla identified in all the inoculum samples were *Proteobacteria*, *Bacteroidetes*, *Verrucomicrobia*, and *Firmicutes* (**Figure 6.10a**). This finding agrees with those reported in the study by Dupnock and Deshusses (2017) that involved sequenced samples taken from biogas reactors. Moreover, most of the inoculum samples taken in this study were dominated by *Proteobacteria* as this is the major phylum of gram-negative bacteria that also includes methanotrophs and heterotrophs.

The proportions of methane oxidizing bacteria (MOB) and sulfide oxidizing bacteria (SOB) at every location are described in **Figure 6.10b**. There is only a small difference in the growth percentage of MOB at locations along the reactor height; a maximum of 34.76% was recorded at position H5, which is above the air inlet. However, a maximum of 1.39% SOB was detected at H4, which is near the off-gas position. This indicates that owing to few SOB near the air inlet (position H1), complete oxidation of sulfide could be difficult, thus causing the partial oxidation of sulfide to sulfur or thiosulfate to occur. The most abundant genus of MOB and SOB is shown in **Figure 6.11**. The clone libraries from locations H1 to H3 of the inoculum indicate *Hyphomicrobium* as the dominant species of SOB (**Figure 6.11a**). Within the five locations (H1–H5), other species detected in SOB were *Acidithiobacillus*, *Rhodobacter*, *Xanthobacter*, *Thiomonas*, *Thiobacillus*, *Paracocccus*, and other *Gammaproteobacteria*. Further, the methanotrophs detected were *Methylobacter*, *Methylococcus*, *Methylomonas*, *Methylocystis*, *Methylocaldum*, *Methylomicrobium*, *Methylosarcina*, and *Methylophilus*. The population of MOB gradually changed from the top to the bottom of the reactor column, showing an obvious alteration of *Methylobacter*, *Methylocaldum*, and *Methylomicrobium*, respectively (**Figure 6.11b**). At the top of the reactor (H1–H3), the MOB population was dominated by *Methylobacter* and that at the bottom (H4–H5), was mostly composed of *Methylocaldum* and *Methylomicrobium*. This indicates that the methanotrophs actively involved in the oxidation of dissolved CH_4 detected in the effluent from biological oxidation were type 1 methanotrophs.

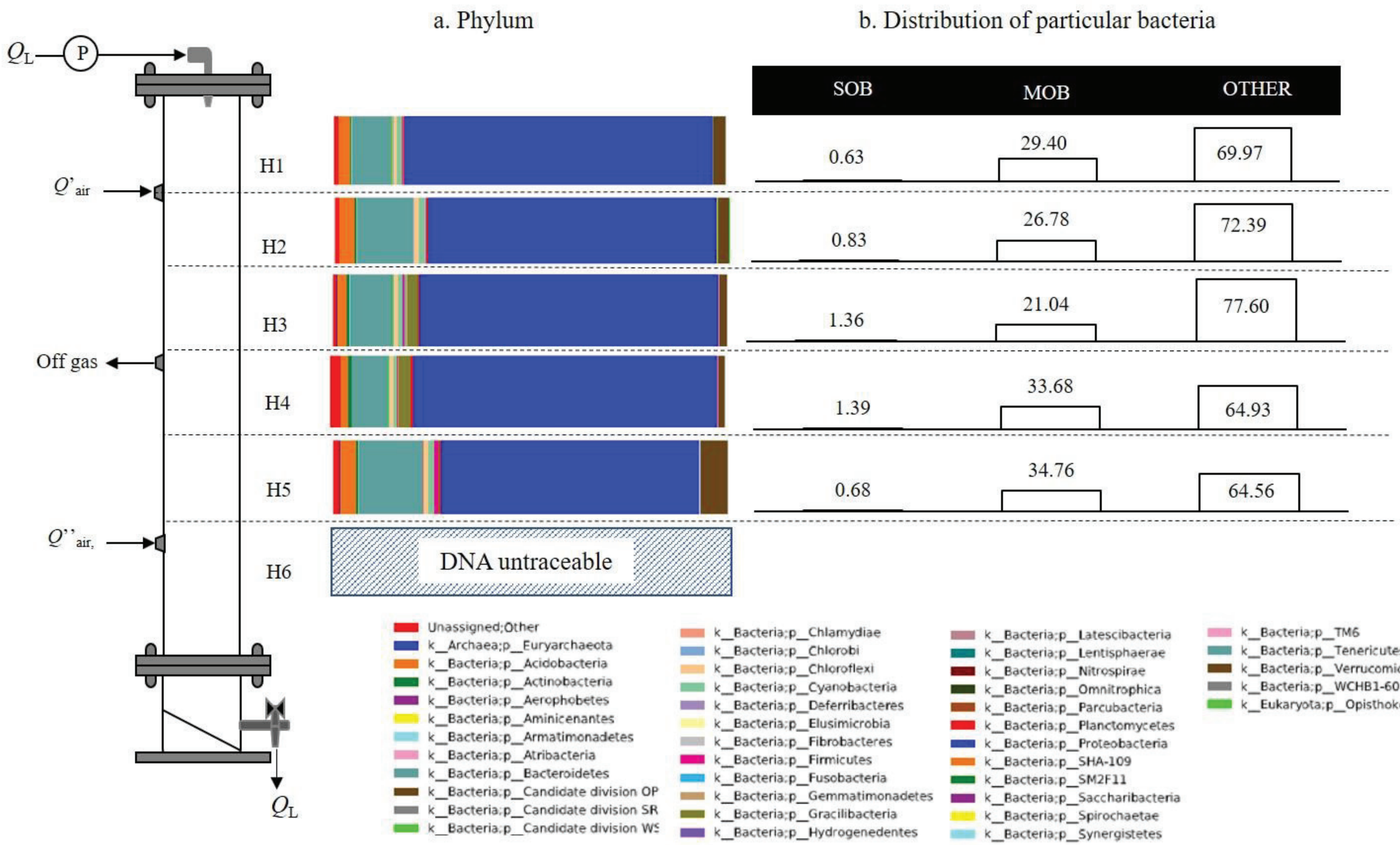

Figure 6. 10: Bacterial community identified in inoculum along reactor height (H). (a) Major phylum of bacteria (b) Distribution of sulfide (SOB) and methane (MOB) oxidation bacteria

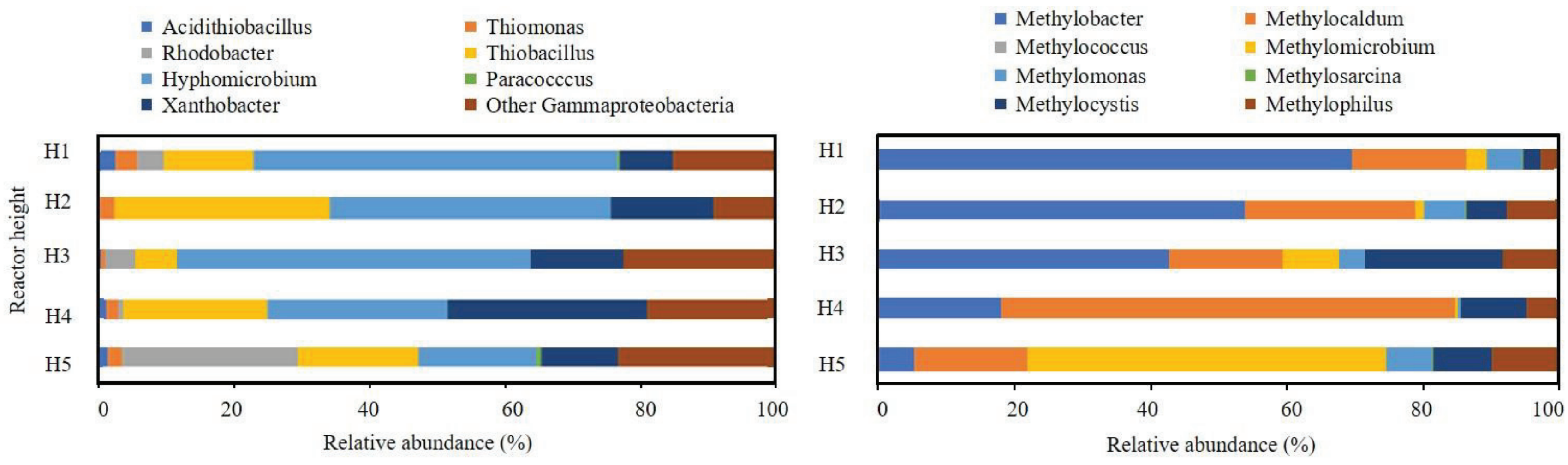

a. SOB

b. MOB

Figure 6.11: Major genus identified in inoculum at specific reactor height (H). (a) Sulfide oxidation bacteria (SOB) (b) Methane oxidation bacteria (MOB).

6.5 Discussion

6.5.1 Reducing greenhouse gas emissions

In this study, the biological oxidation process for inhibiting the emission of CH_4 and H_2S gases from the effluent of biogas purification were carried out. Liu et al. (2014) reported that approximately 0.10 to 5% of CH_4 gas was generally released from a sewer. My study, successfully proved that the emission of CH_4 from the effluent could be reduced. It was found that a minimum CH_4 gas concentration of 0.04% of with almost no trace of H_2S gas was detected in the off gas when the system was operated at a Q'_{air} of 2.02 L d^{-1}, an HRT of 2 h, and a Q_L of 5.04 L d^{-1}, leading to a 98% CH_4 removal efficiency. Furthermore, it should also be noted that in our system, although physical stripping of CO_2 was conducted simultaneously in the reactor, the biological oxidation performance was maintained.

However, using the developed mathematical model, an interesting phenomenon involving a slight deterioration in the CH_4 removal efficiency was observed after reaching the maximum value, and a similar trend was observed when a different Q_L was employed (**Figure 6.7**). The overall mass transfer coefficient (K_La) in between the liquid and gas phases of the system was generally influenced by the Q_L, and an increase in Q_L caused an increase in the mass transfer for the degasification and absorption processes to occur (Noorain et al., 2018). Furthermore, Matsunaga et al. (2012) reported that a higher liquid velocity led to a greater transfer of CH_4 (aq) to the reactor headspace and CH_4 (aq) concentrations nearer to thermodynamic equilibrium. During my study, an excessive supply of Q'_{air} appeared to promote the degassing process in the reactor. However, even at a high Q_L, the rate of degasification was below the biological oxidation process rate after achieving the maximum CH_4 removal efficiency. This indicated that the CH_4 mass transfer rate from the liquid to the gas phase was smaller than CH_4 transfer rate from the gas to the liquid phase and subsequently increased the availability of the CH_4 substrate for the biological process. At an extremely low Q'_{air}, a high off-gas CH_4 concentration was found (**Figure 6.8**), indicating that the performance efficiency of the biological oxidation process had reduced and more effusion of CH_4 to the gas phase had occurred owing to the higher liquid velocity (Pauss et al., 1990). Therefore, setting an appropriate Q'_{air} is extremely important in the biological treatment of dissolved gases, especially CH_4, to reduce greenhouse gas emissions, whilst ensuring high biological oxidation performance.

6.5.2 Potential for effluent pH recovery

The feasibility of stripping CO_2 (aq) from the biogas purification effluent to raise the pH was investigated and mathematically modeled at various bottom airflow rates ranging from 2.02 to 146 L d^{-1}, respectively. The results show that with a minimum airflow rate of 50 L d^{-1} , the pH increased from 5.64 up to a maximum of 7.3 and remained constant afterward (**Figure 6.9**). The performance of CO_2 stripping was dependent on several factors such as the characteristics of the influent, including the total alkalinity, temperature, initial CO_2 (aq) concentration, influent flow rate, and aeration rate (Fattah et al., 2008). This indicated that pH elevation using the stripping method in this study has its own limitations and that the final pH is largely dependent on the buffering capacity of the liquid solution (Cohen and Kirchmann, 2004). A similar study reported that an increase in the air supply rate had a very limited positive influence on the CO_2 stripping efficiency (Fattah et al., 2008). The buffering capacity in this study was represented by the total alkalinity and a value of 0.62 mmol L^{-1} was set as the initial concentration. In this study, it was observed that the pH was difficult to be raised. It is expected that owing to the precipitation of HS^-, S_o, and SO_4^{2-} ions from the oxidation of H_2S (aq), the liquid solution easily becomes saturated and more acidic rather than alkaline, with the pH decreasing. Therefore, to attain high efficiency in terms of pH recovery, the sponge carriers should be cleaned or changed regularly. Otherwise, some additional fresh water is needed to recover the pH from 7.3 to 8 before utilizing this water as purification water in water scrubbing.

6.5.3 SOB and MOB community analysis

The microbial community structures of dissolved CH_4 and H_2S in the biogas purification effluent at a pH of 5.64 was analyzed using DNA extraction. Microbial analysis results indicated that the SOB and MOB were dominated by *Hyphomicrobium* and the type 1 methanotroph of *Methylobacter* and *Methylocaldum*, respectively. Generally, the amount of O_2 supplied can affect the bacterial community compositions (Namgung and Song, 2015). During the experiment, the bacterial community was continuously exposed to a relatively high O_2 supply rate ranging from 2.02 to 30.2 L d^{-1}. This condition creates a favorable environment for type I methanotrophs and could lead to the dominance of *Methylobacter* and *Methylocaldum* in the bacterial community (Strong and Clarke, 2015). A similar finding was reported by Hatamato et al. (2010), who investigated the removal of CH_4 (aq) in anaerobic wastewater effluent with pH 7 using a closed DHS reactor. This study showed that the species of methanotrophs that contributed highly to the oxidation of CH_4 (aq) either in the effluent from the post-treatment process or in the anaerobic or biogas purification effluent was similar; an influent pH of 5.64 did not affect the growth of type 1 methanotrophs. Next, during a high rate of air supply, the H_2S was slightly degraded to SO_4^{2-} and the SOB strain was dominated by *Hyphomicrobium*. Zhang et al. (1991), reported that *Hyphomicrobium* was capable of removing H_2S. Moreover, according to Mohapatra et al. (2008), the genera of *Hyphomicrobium* is known for its oxidation of H_2S to elemental sulfur. Thus, a very high rate of air supply at a pH of 5.64 could foster the growth of sulfate-oxidizing communities. However, the oxidization of S_o to SO_4^{2-} occurred at a much lower rate and could eventually affect the efficiency of H_2S removal. The study revealed that an excessively high rate of air supply not only affected the type 1 methanotroph communities but also affected the sulfate-oxidizing communities.

6.6 Conclusion

The newly developed post-treatment process for biogas purification effluent using an integrated process of biological oxidation and physical stripping in a single reactor is capable of removing 98% of CH_4 (aq) with 0.04% off-gas CH_4 captured. Under a minimum bottom airflow rate of 50 L d^{-1}, the effluent pH could be raised to 7.3. The HRT and airflow rate played a crucial role in governing the performance of the biological oxidation and physical stripping processes. A mathematical simulation model of the biological oxidation process elucidated that a slight deterioration in the CH_4 removal performance occurred during a high Q'_{air} owing to the effect of gasification. Increasing Q''_{air} during the process only had a limited positive influence on the CO_2 stripping efficiency. Overall, this study provides a detailed analysis of the biological–physical treatment of dissolved gasses aimed at reducing greenhouse gas emissions with a high possibility for water regeneration.

References

Cohen, Y., Kirchmann, H., 2004. Increasing the pH of wastewater to high levels with different gases- CO_2 stripping. Water Air Soil Pollut. 159, 265.

Cookney, J., Mcleod, A., Mathioudakis, V., Ncube, P., Soares, A., Jefferson, B., McAdam, E.J., 2016. Dissolved methane recovery from anaerobic effluents using hollow fibre membrane contactors. J. Membr. Sci. 502, 141.

Crone, B.C., Garland, J.L., Sorial, G.A., Vane, L.M., 2016. Significance of dissolved methane in effluents of anaerobically treated low strength wastewater and potential for recovery as an energy product: A review. Water Res. 104, 520.

Dupnock, T.L., Deshusses, M.A., 2017. High-performance biogas upgrading using a biotrickling filter and hydrogenotrophic methanogens. Appl. Biochem. Biotechnol. 183, 488.

El-Fadel, M., Massoud, M., 2001. Methane emissions from wastewater management. Environ. Pollut. 114 (2), 177.

Fattah, K.P., Mavinic, D.S., Koch, F.A., Jacob, C., 2008. Determining the feasibility of phosphorus recovery as struvite from filter press centrate in a secondary wastewater treatment plant. J Environ. Sci. Health A Tox. Hazard Subst. Environ Eng. 43, 756.

Foust, A.S., Wenzel, L.A., Clump, C.W., Maus, L., Anderson, L. 1960. Principle of Unit Operations, John Wiley &Sons, New York.

Frank, J.M., 1986. The thermodynamics and kinetics of the hydrogen sulfide system in natural waters. Mar. Chem.18, 121.

Gu, J., Xu, G., Liu, Y., 2017. An integrated AMBBR and IFAS-SBR process for municipal wastewater treatment towards enhanced energy recovery, reduced energy consumption and sludge production. Water Res. 110, 262.

Hartley, K., Lant, P., 2006. Eliminating non-renewable CO_2 emission from sewage treatment: An anaerobic migrating bed reactor pilot plant study. Biotechnol. Bioeng. 95, 384.

Hatamoto, M., Miyauchi, T., Kindaichi, T., Ozaki, N., Ohashi, A., 2011. Dissolved methane oxidation and competition for oxygen in down-flow hanging sponge reactor for post-treatment of anaerobic wastewater treatment. Bioresour. Technol. 102 (22), 10299.

Hatamoto, M., Yamamoto, H., Kindaichi, T., Ozaki, N., Ohashi, A., 2010. Biological oxidation of dissolved methane in effluents from anaerobic reactors using a down-flow hanging sponge reactor. Water Res. 44, 1409.

Heile, S., Chernicharo, C.A.L., Brandt, E.M.F., McAdam, E.J., 2017. Dissolved gas separation for engineered anaerobic wastewater systems. Sep. Purif. Technol. 189(22), 405.

Henares, M.., Izquierdo, M.., Penarrocha, J.M., Martinez, V., 2016. Comparative study of degassing membrane modules for the removal of methane form expanded granular sludge bed anaerobic reactor effluent. Sep. Purif. Technol. 170, 22.

Heyden, C.V.D., Vanthillo, B., Pieters, J.G., Demeyer, P., Volcke, E.I.P., 2016. Mechanistic modelling of pollutant removal, temperature and evaporation in chemical air scrubbers. Chem. Eng. Technol. 39 (10), 1785.

Karim, G., Fatima, Z.B.F., 2018. Power-to-methane: A state-of-the-art review. Renew. Sust. Energ. Rev. 81, 433.

Ling, E.J., Benham, B., Wright, B., Haering, K., Scott, J.P., 2011. Virginia household water quality program: Sulfate and hydrogen sulfide in household water. Virginia Cooperative Extension Publication, 442.

Liu, Y., Sharma, K.R., Murthy, S., Johnson, I., Evans, T., Yuan, Z., 2014. On-line monitoring of methane in sewer air. Sci. Rep. 4, 6637.

Liu, Z.H., Yin, H., Dang, Z., Liu, Yu., 2014. Dissolved methane: a hurdle for anaerobic treatment of municipal wastewater. Environ. Sci. Technol. 48 (2), 889.

Matsunaga, K., Kindaichi, T., Ozaki, N., Ohashi, A., Nakahara, Y., Sasakawa, M., 2012. Development of anammox reactor equipped with a degassing membrane to improve biomass retention. Water Sci. Technol. 66 (2), 451.

Matsuura, N., Hatamoto, M., Sumino, H., Syutsubo, K., Yamaguchi, T., Ohashi, A., 2015. Recovery and biological oxidation of dissolved methane in effluent from UASB treatment of municipal sewage using a two-stage closed downflow hanging sponge system. J. Environ. Manag. 151, 200.

Matsuura, N., Hatamoto, M., Sumino, H., Syutsubo, K., Yamaguchi, T., Ohashi, A., 2010. Closed DHS system to prevent dissolved methane emissions as greenhouse gas in anaerobic wastewater treatment by its recovery and biological oxidation. Water Sci. Technol. 61 (9), 2407.

Mohapatra, B.P., Gould, W.D., Dinardo, O., Koren, D.W., 2008. An overview of the biochemical and molecular aspects of microbial oxidation of inorganic sulfur compounds. CLEAN: Soil, Air, Water 36 (10-11), 823.

Namgung, H.K., Song, J., 2015. The effect of oxygen supply on the dual growth kinetics of Acidithiobacillus thiooxidans under acidic conditions for biogas desulfurization. Int. J. Environ. Res. Public. Health 12 (2), 1368.

Nock, W.J., Walker, M., Kapoor, R., Heaven, S., 2014. Modeling the water scrubbing process and energy requirements for CO2 capture to upgrade biogas to biomethane. Ind. Eng. Chem. Res. 53 (32), 12783.

Noorain, R., Kindaichi, T., Ozaki, N., Aoi, Y., Ohashi, A., 2018. Biogas purification performance of new water scrubber packed with sponge carriers. J. Clean. Prod. (Accepted on 19 Dec 2018).

Pan, S., Tay, J.H., He, Y.X., Tay, S.T.L., 2004. The effect of hydraulic retention time on the stability of aerobically grown microbial granules. Appl. Microbiol. 38, 158.

Pauss, A., Andre, G., Perrier, M., Guiot, S.R., 1990. Liquid – to – gas mass transfer in anaerobic processes: Inevitable transfer limitations of methane and hydrogen in the biomethanation process. Appl. Environ. Microbiol. 56 (6), 1636.

Robinson, J.A., Tiedje, J.M., 1983. Nonlinear estimation of Monod growth kinetic parameters from a single substrate depletion curve. Appl. Environ. Microbiol. 45, 1453.

Smith, A.L., Stadler, L.B., Cao, L., Love, N.G., Raskin, L., Skerlos, S.J., 2014. Navigating wastewater energy recovery strategies: A life cycle comparison of anaerobic membrane bioreactor and conventional treatment systems with anaerobic digestion. Environ. Sci. Technol. 48 (10), 5972.

Stocker, F.T., et al., 2014. Climate change 2013: The physical science basis. Cambridge University Press Cambridge, UK and New York.

Strong, P.J., Clarke, W.P., 2015. Methane as a resource: can the methanotrophs add value? Environ. Sci. Technol 49, 4001.

Stumm, W., Morgan, J.J., 1981. An introduction emphasizing chemical equilibrium in natural waters, second ed. John Wiley & Sons, New York.

Summerfelt, S.T., Zuhlke, A., Kolarevic, J., Reiten, B.K.M., Selset, R., Gutierrez, X., Terjesen, B.F., 2015. Effects of alkalinity on ammonia removal, carbon dioxide stripping and system pH in semi-commercial scale water recirculating aquaculture systems operated with moving bed bioreactors. Aquacult. Eng. 65, 46.

Sun, Q., Li, H., Yan, J., Liu, L., Yu, Z., Yu, X., 2015. Selection of appropriate biogas upgrading technology-a review of biogas cleaning, upgrading and utilization. Renew. Sust. Energy Rev. 51, 521.

Zhang, L., Hirai, M., Shoda, M., 1991. Removal characteristics of dimethyl sulfide, methanethiol and hydrogen sulfide by *Hyphomicrobium* sp. 155 isolated from peat biofilter. J. Ferment. Bioeng. 72, 392.

CHAPTER 7

SUMMARY

TABLE OF CONTENTS

7.1 Conclusion

The experimental outcomes and conclusions drawback from this study are briefly described as follows:

7.1.1 Biogas purification performance of new water scrubber packed with sponge carrier

In **Chapter 4** the potential of a new water scrubber packed with sponge carrier for biogas purification was investigated under atmospheric condition and a mathematical model to describe the purification phenomena was constructed. During the study successful purification performance was demonstrated and a maximum average of 90-93% of output methane gas with untraceable output H_2S gas concentration were produced. Practically no influence of input H_2S concentration, HRT and pH (7 to 8) were observed whereas changed in temperature and Q_L/Q_G showing fluctuation of CH_4 contents. Through the develop simulation, the methods found an interesting finding that proper control of Q_L/Q_G is necessary in producing high methane concentration. Under high temperature condition, by using high scrubber column low Q_L/Q_G is enough to produce more than 90% of output methane. However, imposing with too low of Q_L/Q_G ratio condition, high purification performance is impossible to achieve although a very high column is installed. Here, the approaching method by installing framed sponge with proper controlled of Q_L/Q_G ratio compensated for the lack of pressurizing equipment under specified conditions.

7.1.2 Biological desulfurization of high H_2S from biogas

In **Chapter 5** the biological treatment of high H_2S concentration ranging from 0.05-0.2% from biogas was showing a good performance with almost undetectable of output H_2S gas. Three parameters (initial H_2S concentration, Q_L/Q_G and O_2/H_2S ratios) were observed during the study. The efficiency of H_2S biological oxidation to SO_4^{2-} not only rely on the amount of O_2 supply but also depending on H_2S loaded concentration. Where, when high concentration of H_2S is supplied more than 0.1%, a minimum 2% of O_2 supply is required to achieve more than 90% of H_2S removal efficiency. In comparison between the physical treatment and biological treatment performance it be observed that the physical treatment was capable to treat the H2S gas as performed by biological treatment. This indicated that from the develop system the physical treatment is enough to give high purified CH4 generation, which mean the operational time can be reduce compared to biological treatment.

7.1.3 Integrated biological-physical process for biogas purification effluent treatment

In **Chapter 6** a new post treatment method for the biogas purification effluent that is able to simultaneously remove the dissolved methane, hydrogen sulphide and carbon dioxide by biological oxidation and physical stripping process in a single reactor. A mathematical model was constructed, and simulations were conducted to explain on the effect of airflow rate supply on the biological and physical stripping process for high performance. The result demonstrated high performance with up to 98% of CH_4 was removed and effluent pH was successfully raised from 5.64 to 7.3. It was found that although physical stripping of carbon dioxide gas was conducted simultaneously in the reactor, the biological performance was maintained. This indicated that the integration of biological and physical process in a reactor is not only feasible but also providing with high treatment performance in removing dissolved gasses and regenerating the effluent water.

7.2 Applications

Considerable attention has been given to the issue of biogas limitations as a transport vehicle fuel due to lower calorific value of CH_4 produce, thus resulting to the tardy expansion of biofuel production far from clear. High pressure water scrubbing technology are in common use today, but the application of the technology is mostly focused on large scale biogas production sites (Abatzoglou and Boivin, 2009). Due to the installation of pressurize equipment coupled with the effluent treatment system, the energy and maintenance cost for the whole system become higher (Kapoor et al., 2017). The availability of high purified methane by water scrubbing under low pressure case has remained the question. To the best of my knowledge, nobody has ever succeeded in generating (>90 % (v/v)) of purified methane at any temperatures and column heights under low pressure conditions. In this research a novel approach for the said problems is proposed. The technology proposed is applicable for all industry scales and it function not only limit to enhance the biogas performance but also could be used as bad odor treatment system. Furthermore, the installation of biogas effluent treatment system to the water scrubbing gives a value added such as preventing greenhouse gas emission and reducing the water usage. With more than 90% of output methane generation the technology is suitable to be applied for energy production in transportation and gas grid injection.

7.3 Future work recommendations

The implementation of low-pressure water scrubbing packed with sponge carrier on full-scale is the next, for the culmination of the research presented in this thesis. The findings obtained on laboratory scale must be tested on a larger scale. The sponge packed water scrubber couple with is a promising technology for biogas treatment. A preliminary assessment in this study highlights that this novel system can fulfil all the desirable characteristics of an biogas upgrading reactors for contaminant removal from gas and liquid phase: simple configuration, no clogging problems, low oxygen demand, high capability to transform sulphide into sulfate, easy recovery of the generated elemental Sulphur, reduce water need, and robustness to fluctuations in operational conditions. Nonetheless, its design and operating conditions must be still optimised in order to evaluate its maximum removal capacity and the optimum criteria for scale-up. Obviously, although the effluent Ph in this study is capable to be increased to 7.3, however Ph 8 is required for high water scrubbing performance. For this purpose, strategic air flow adjustment for physical stripping of carbon dioxide still needs to be determined for future work.

References

Abatzoglou, N., Boivin, S., 2009. A review of gas purification processes. Biofuels Bioprod. Biorefin. 3, 42-71.

Kapoor, R., Subbarao, P.M.V., Vijay, V.K., Shah, G., Sahota, S., Singh, D., Verma, M., 2017. Factor affecting methane loss from a water scrubbing based biogas upgrading system. Appl Energy.